https://www.mdc-berlin.de/de/veroeffentlichungstypen/clinical-journal-club

Als gemeinsame Einrichtung von MDC und Charité fördert das Experimental and Clinical Research Center die Zusammenarbeit zwischen Grundlagenwissenschaftlern und klinischen Forschern. Hier werden neue Ansätze für Diagnose, Prävention und Therapie von Herz-Kreislauf- und Stoffwechselerkrankungen, Krebs sowie neurologischen Erkrankungen entwickelt und zeitnah am Patienten eingesetzt. Sie sind eingeladen, uns beizutreten. Bewerben Sie sich!

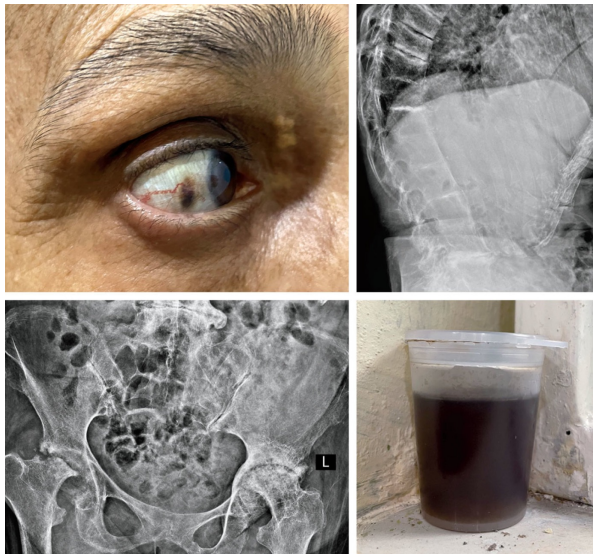

A 64-year-old woman with no known medical history presented to clinic with a 4-year history of worsening low back pain and difficulty walking. Exam was notable for a finding in the eyes, kyphosis, and a Trendelenburg gait. Radiographs of the lumbosacral spine and pelvis are shown. A urine sample turned black after being left at room temperature overnight. Which of the following is the most likely diagnosis?

Alkaptonuria

Ankylosing spondylitis

Hemochromatosis

Metastatic melanoma

Porphyria

Urine levels of homogentisic acid were elevated, confirming alkaptonuria. Alkaptonuria is an autosomal recessive disorder of tyrosine metabolism that results in high levels of homogentisic acid that subsequently polymerizes to form a pigment. The condition manifests in childhood with darkening of urine after oxidization by air (which this patient recalled noting) and in adulthood with pigmentation of connective tissues (known as ochronosis) and early-onset, severe osteoarthropathy (known as ochronotic arthropathy).

Der **Alkaptonurie** liegt ein Defekt des Enzyms **Homogentisat-1,2-Dioxygenase (HGD)** zugrunde. Dieses Enzym ist normalerweise für den Abbau der Aminosäuren Phenylalanin und Tyrosin (Bausteine von Nahrungseiweiß) zuständig.

Durch den Enzymdefekt kann ein Zwischenprodukt, die **Homogentisinsäure (HGA)**, nicht weiter abgebaut werden und reichert sich im Körper an.

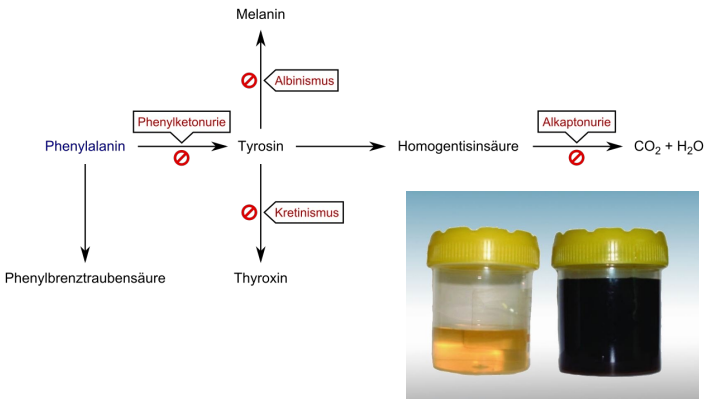

Typische Symptome und Verlauf

- **Dunkelfärbung des Urins:** Das auffälligste Frühsymptom zeigt sich oft schon im Säuglingsalter an dunklen Flecken in der Windel. Der Urin verfärbt sich dunkelbraun bis tiefschwarz, sobald er mit Luftsauerstoff in Kontakt kommt und oxidiert.

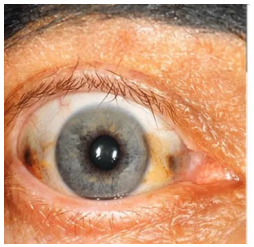

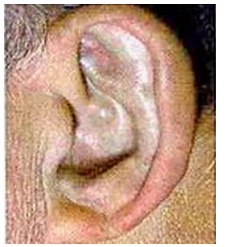

- **Ochronose:** Ab dem mittleren Erwachsenenalter (meist ab dem 30. Lebensjahr) lagern sich die Abbauprodukte als bläulich-schwarze Pigmente im Gewebe ab. Besonders sichtbar wird dies am **Ohrknorpel** und an den **Skleren (Lederhaut) der Augen**.

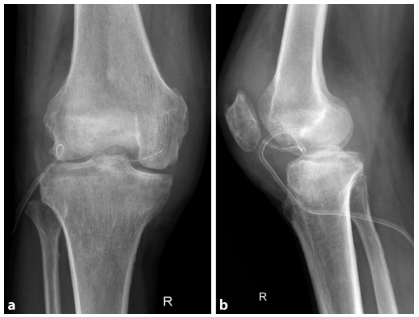

- **Gelenk- und Wirbelsäulenbeschwerden:** Die Ablagerungen im Knorpelgewebe führen zu einer schweren, fortschreitenden Zerstörung der großen Gelenke (Hüfte, Knie, Schultern) und der Wirbelsäule (**ochronotische Arthropathie**), die oft einer schweren Arthrose ähnelt.

Trikuspidalinsuffizienz

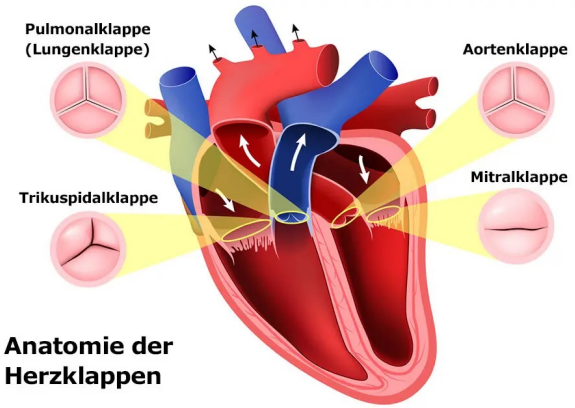

Anatomie der Herzklappen

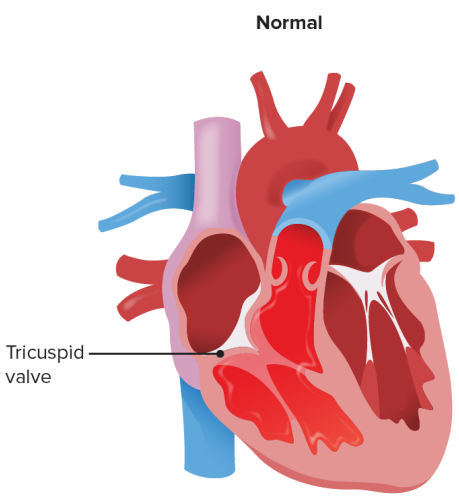

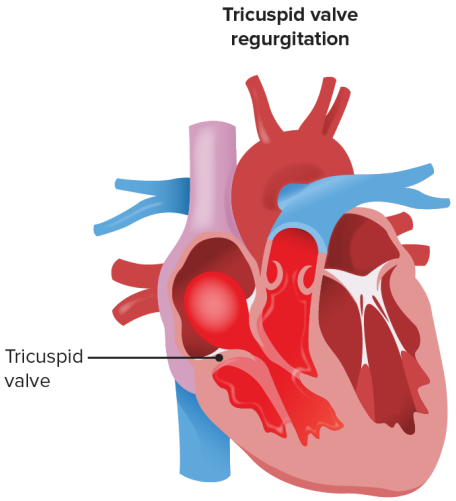

Die **Trikuspidalinsuffizienz (TI)** – die Undichtigkeit der Herzklappe zwischen rechtem Vorhof und rechter Herzkammer – galt lange als „vergessene Klappe“. Heutzutage unterscheidet die moderne Kardiologie präzise zwischen verschiedenen Ursachen, wobei die sekundäre (funktionelle) Trikuspidalinsuffizienz mit über 90 % der Fälle die mit Abstand häufigste Form im klinischen Alltag darstellt.

Hier ist die Übersicht der heutigen Hauptursachen, aufgeteilt nach ihrer Entstehung:

1. Sekundäre (funktionelle) Trikuspidalinsuffizienz (> 90 % der Fälle)

Hierbei ist die Herzklappe selbst anatomisch intakt. Sie wird jedoch undicht, weil sich der rechte Ventrikel (Herzkammer) oder der rechte Vorhof stark erweitert (dilatiert), wodurch der Klappenring auseinandergezogen wird.

- **Linksherzerkrankungen (Ventrikuläre sekundäre TI):** Dies ist der klassische Auslöser. Durch Erkrankungen des linken Herzens – wie eine Mitralklappeninsuffizienz, eine Aortenklappenstenose oder eine allgemeine Linksherzschwäche (Herzinsuffizienz) – staut sich das Blut chronisch über die Lunge zurück in die rechte Herzkammer.
- **Lungenhochdruck (Pulmonale Hypertonie):** Ein erhöhter Druck in den Lungengefäßen (z. B. durch chronische Lungenerkrankungen wie COPD oder wiederkehrende Lungenembolien) zwingt die rechte Herzkammer zu massiver Mehrarbeit, woraufhin sie sich erweitert.
- **Vorhofflimmern (Atriale sekundäre TI):** Diese Ursache hat in den letzten Jahren enorm an Bedeutung gewonnen. Chronisches Vorhofflimmern führt zu einer starken Vergrößerung des *rechten Vorhofs*. Dadurch dehnt sich der Klappenring direkt aus, ohne dass die Herzkammer primär vergrößert sein muss (isolierte TI).

Tricuspid-Valve Intervention in Heart Failure

The effect of transcatheter tricuspid-valve repair on clinical outcomes, including death and hospitalization for heart failure, in patients with severe tricuspid regurgitation remains uncertain. We randomly assigned patients with symptomatic severe tricuspid regurgitation and an increased risk of future heart-failure events in a 2:1 ratio to tricuspid-valve repair plus medical therapy (tricuspid-repair group) or medical therapy alone (medical-therapy group). The first primary end point was a hierarchical composite of death from any cause, hospitalization for heart failure, and quality-of-life improvement at 1 year, assessed by win ratio. If the between-group difference was significant, a second primary end point would be tested: a composite of death from any cause or hospitalization for heart failure through 3 years.

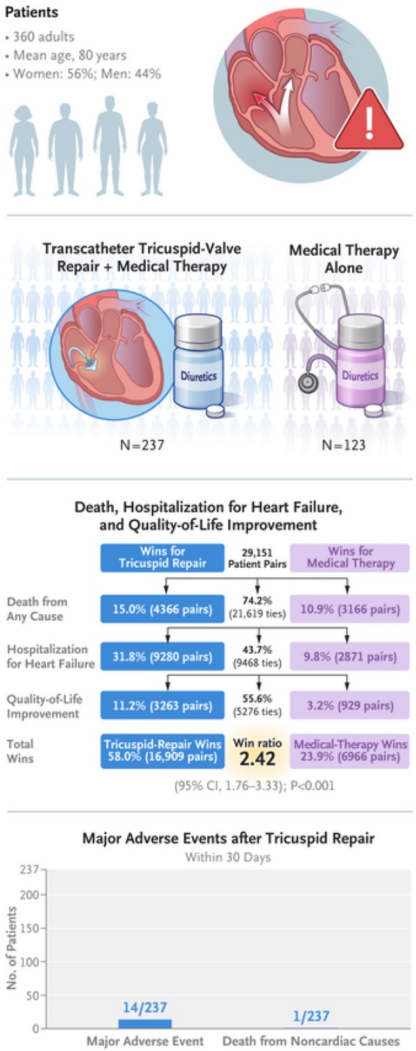

Tricuspid regurgitation is associated with increased morbidity and mortality. Options for medical therapy remain limited, and isolated tricuspid-valve surgery is rarely performed owing to increased operative risk. Transcatheter tricuspid-valve interventions have emerged as an alternative to surgery. Among these, tricuspid edge-to-edge repair is the most widely adopted and is associated with high procedural success and a favorable safety profile. The Tricuspid Intervention in Heart Failure (TRIC-I-HF) trial was designed to evaluate whether a strategy of transcatheter tricuspid-valve repair plus medical therapy would result in a lower risk of death and hospitalization for heart failure than medical therapy alone among patients with severe tricuspid regurgitation who are at increased risk for future heart-failure events.

Patient Selection

Patient selection and enrollment was at the discretion of the local heart team, without need for approval by a central eligibility committee or screening for baseline medical treatment. Patients who were eligible for enrollment had at least severe tricuspid regurgitation on a five-grade scale (mild, moderate, severe, massive, and torrential), despite medical therapy including diuretic therapy adjusted to the individual optimal dose for at least 30 days.

Strategy for Transcatheter Tricuspid-Valve Repair

The local heart-valve team selected from devices that have received a European Certificate of Conformity (known as the CE mark) for transcatheter tricuspid-valve repair suitable for the individual patient. The commercially available CE-marked devices included the PASCAL system and the Cardioband system (both Edwards Lifesciences) and the TriClip system (Abbott Cardiovascular).

End Points

The first primary end point was a hierarchical composite of death from any cause, hospitalization for heart failure, and quality-of-life improvement at 12 months, as assessed by means of the Kansas City Cardiomyopathy Questionnaire (KCCQ), with a clinically meaningful improvement defined as an increase of at least 15 points; scores on the KCCQ range from 0 to 100, with higher scores indicating better health status.

Characteristic	Tricuspid Repair (N=237)	Medical Therapy (N=123)
Age — yr	80.6±5.9	80.2±6.6
Female sex — no. (%)	134 (56.5)	69 (56.1)
Race or ethnic group — no. (%)†		
White	195 (82.3)	101 (82.1)
Other	13 (5.5)	6 (4.9)
Missing data	29 (12.2)	16 (13.0)
Body-mass index‡	26.1±5.3	25.9±5.0
Median EuroSCORE II score (IQR) — %§	4.3 (2.9–6.2)	4.2 (2.8–7.9)
Median TRI-SCORE (IQR) — points¶	4.0 (3.0–6.0)	5.0 (4.0–6.0)
NYHA class III or IV heart failure — no. (%)	181 (76.4)	89 (72.4)
Atrial fibrillation or flutter — no. (%)	218 (92.0)	120 (97.6)
Diabetes mellitus — no. (%)	60 (25.3)	32 (26.0)
Arterial hypertension — no. (%)	188 (79.3)	101 (82.1)
Dyslipidemia — no. (%)	100 (42.2)	54 (43.9)
Coronary artery disease — no. (%)	110 (46.4)	68 (55.3)
Previous myocardial infarction — no. (%)	14 (5.9)	16 (13.0)
Previous CABG — no. (%)	18 (7.6)	14 (11.4)
Previous stroke or TIA — no. (%)	22 (9.3)	17 (13.8)
COPD — no. (%)	23 (9.7)	15 (12.2)
CIED with right ventricular lead — no. (%)	49 (20.7)	25 (20.3)
Hospitalization for heart failure in previous 12 mo — no. (%)	135 (57.0)	63 (51.2)
Cardiorenal syndrome — no. (%)‖	194 (81.9)	100 (81.3)
Estimated GFR — ml/min/1.73 m²	46.0±17.5	43.7±16.3
Cardiohepatic syndrome — no./total no. (%)**	80/181 (44.2)	46/92 (50.0)
Bilirubin — mg/dl	0.9±0.5	0.9±0.5
Median γ-glutamyltransferase (IQR) — U/liter	84 (41–155)	79 (43–138)
Alkaline phosphatase — U/liter	113.5±54.4	115.7±53.0
Hemoglobin — mg/dl	12.3±2.3	12.4±2.3
Median NT-proBNP (IQR) — pg/ml	2022 (1229–3283)	2076 (1195–4066)
KCCQ score††	51.9±22.3	52.4±23.5
6-Min walk distance — m‡‡	240.1±128.4	233.4±117.8
Tricuspid regurgitation at baseline — no. (%)		
Moderate	12 (5.1)	5 (4.1)
Severe	119 (50.2)	64 (52.0)
Massive	81 (34.2)	42 (34.1)
Torrential	25 (10.5)	12 (9.8)
Median tricuspid annular plane systolic excursion (IQR) — mm§§	19.1 (16.5–22.0)	18.0 (15.2–20.8)
Median right ventricular fractional area change (IQR) — %¶¶	37.1 (31.6–44.3)	36.4 (31.2–40.7)

Primary and Secondary End Points.

End Point	Tricuspid Repair (N=237)	Medical Therapy (N=123)	Effect Size (95% CI)
Primary			
Win-ratio analysis for death from any cause, hospitalization for heart failure, and quality-of-life improvement at 1 yr — wins/pairs (%)*	16,909/29,151 (58.0)	6966/29,151 (23.9)	2.42 (1.76 to 3.33)†
Kaplan–Meier estimate of freedom from death or hospitalization for heart failure at 3 yr (95% CI) — % of patients	52.4 (43.2 to 63.6)	21.0 (12.7 to 34.6)	0.40 (0.29 to 0.55)‡
No. of deaths or hospitalizations for heart failure (% of patients)	79 (33.3)	76 (61.8)	
Secondary§			
Kaplan–Meier estimate of survival at 1 yr (95% CI) — % of patients	86.5 (82.3 to 91.1)	82.5 (75.8 to 89.8)	0.74 (0.42 to 1.29)‡
No. of deaths (% of patients)	31 (13.1)	20 (16.3)	
Kaplan–Meier estimate of survival at 3 yr (95% CI) — % of patients	72.3 (64.1 to 81.6)	53.9 (41.5 to 70.0)	0.62 (0.40 to 0.96)‡
No. of deaths (% of patients)	45 (19.0)	34 (27.6)	
Kaplan–Meier estimate of freedom from hospitalization for heart failure at 1 yr (95% CI) — % of patients	79.6 (74.5 to 85.1)	51.3 (42.7 to 61.5)	0.35 (0.25 to 0.51)‡
No. of hospitalizations for heart failure (% of patients)	46 (19.4)	54 (43.9)	
Kaplan–Meier estimate of freedom from hospitalization for heart failure at 3 yr (95% CI) — % of patients	62.4 (52.8 to 73.6)	31.0 (21.4 to 44.8)	0.35 (0.25 to 0.50)‡
No. of hospitalizations for heart failure (% of patients)	59 (24.9)	66 (53.7)	
Mean change in KCCQ score from baseline to 1 yr — points	11.20±21.93	4.31±24.94	6.89 (1.76 to 12.02)¶
NYHA functional class of I or II heart failure at 1 yr — no./total no. (%)	138/187 (73.8)	49/86 (57.0)	2.13 (1.24 to 3.64)‖
Mean change in distance on 6-min walk test from baseline to 1 yr — m	40±90	20±95	20 (–0.1 to 40.1)¶
Mean change in body weight from baseline to 1 yr — kg	0.13±5.59	–0.65±6.93	0.78 (–0.79 to 2.35)¶
Peripheral edema of grade 2+ or higher at 1 yr — no./total no. (%)	21/175 (12.0)	14/80 (17.5)	0.64 (0.31 to 1.34)‖

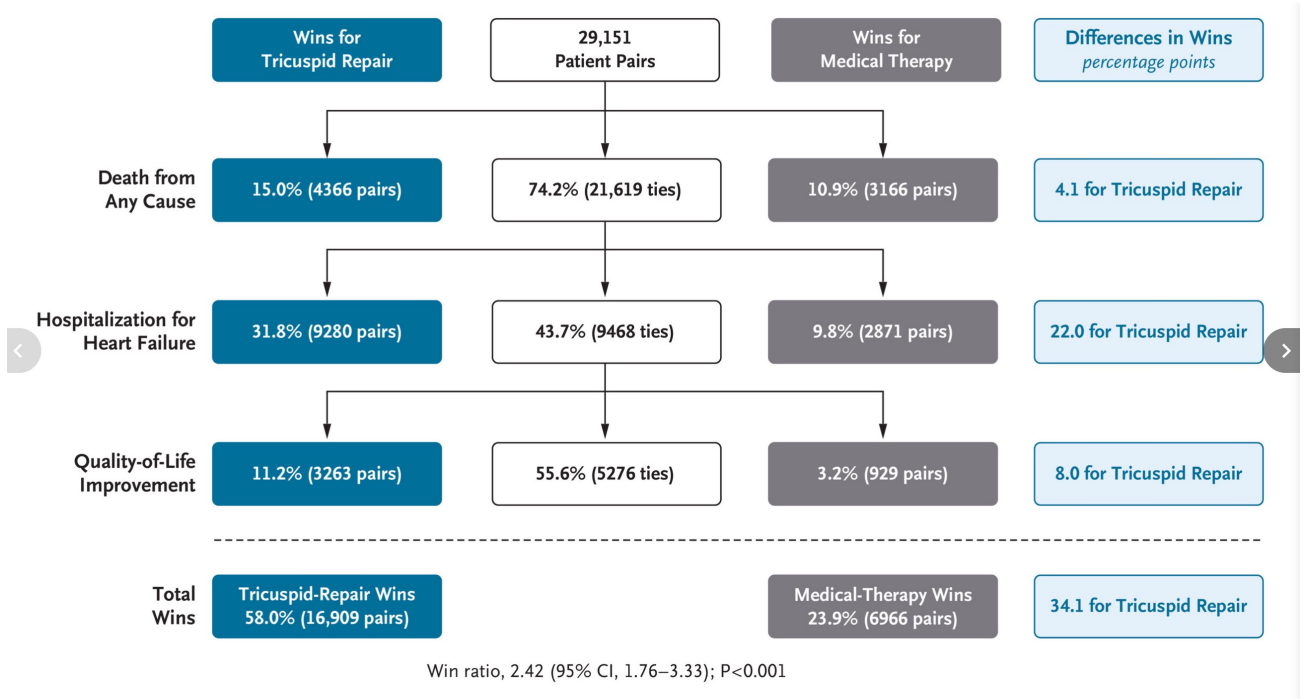

Win-Ratio Analysis for Death, Hospitalization for Heart Failure, and Quality-of-Life Improvement (First Coprimary End Point).

Shown are the components of the win-ratio calculation in the tricuspid-repair group as compared with the medical-therapy group. The win ratio was determined from the analysis of the hierarchical composite primary end point by systematically comparing all possible patient pairs, starting with the first event in the hierarchy. The win ratio was calculated by dividing the number of wins in the tricuspid-repair group by the number of wins in the medical-therapy group. Values are reported as percentages and numbers of pairs. The results for this composite primary end point were calculated after the last patient had reached the 12-month follow-up. Included in the medical-therapy group are patients who crossed over to receive tricuspid repair within the 1-year visit window. Quality-of-life improvement was assessed by the Kansas City Cardiomyopathy Questionnaire (KCCQ), with a clinically meaningful improvement defined as an increase of at least 15 points; scores on the KCCQ range from 0 to 100, with higher scores indicating better health status. Details on the imputation strategy for missing KCCQ data are provided in the Supplementary Appendix, including Table S15.

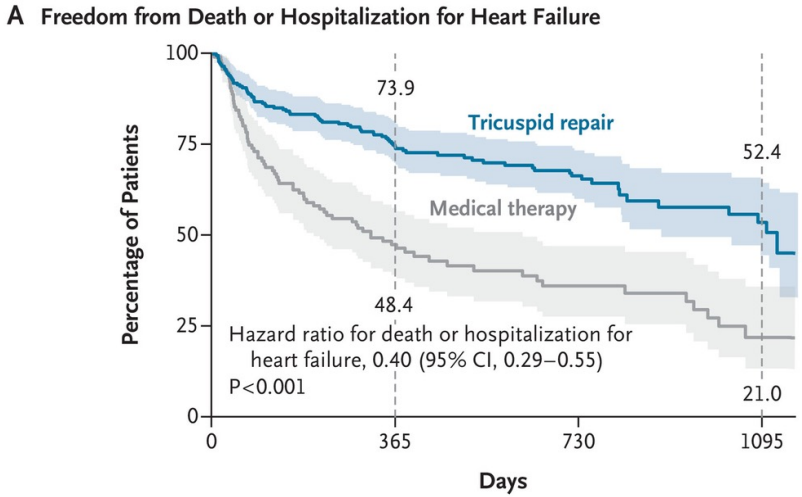

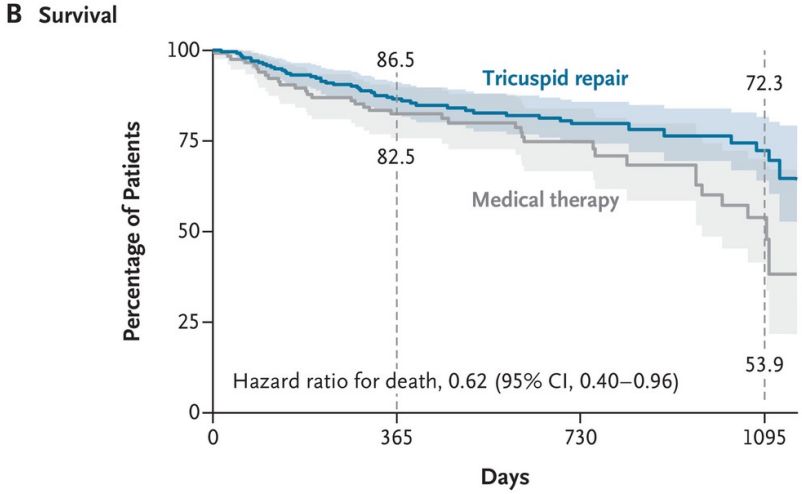

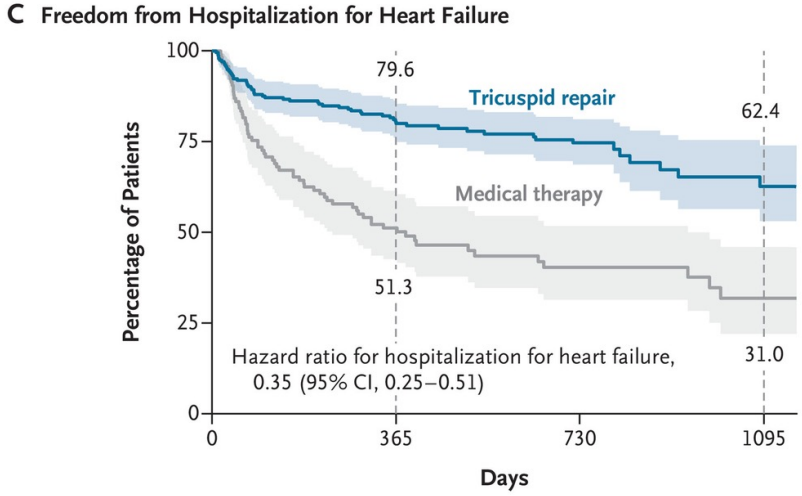

Kaplan–Meier Estimates of Adjudicated Clinical Events at 3 Years.

Shown are Kaplan–Meier estimates for prespecified events as adjudicated by the clinical-events committee at 3 years. Panel A shows freedom from death from any cause or hospitalization for heart failure (second coprimary end point), Panel B survival, and Panel C freedom from hospitalization for heart failure. Shaded areas indicate 95% confidence intervals. For the individual end points of survival and freedom from hospitalization for heart failure, the widths of the confidence intervals have not been adjusted for multiplicity and should not be used to infer treatment effects.

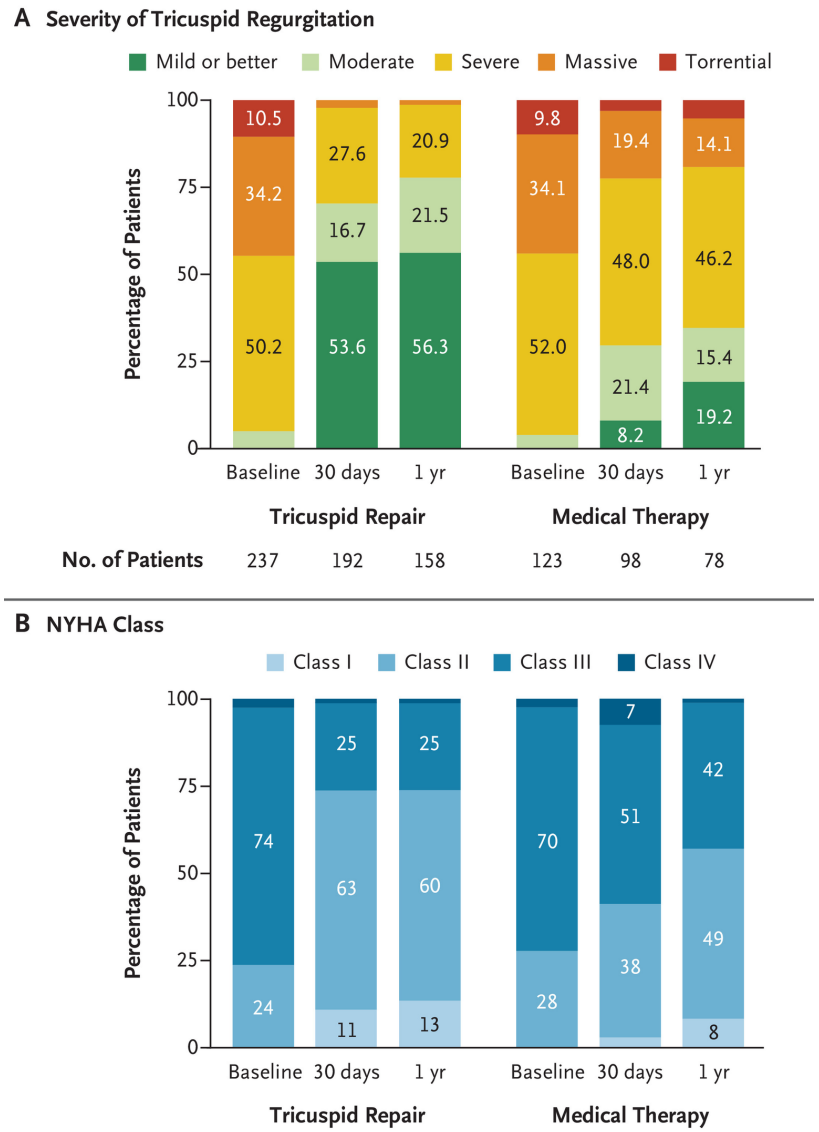

Severity of Tricuspid Regurgitation and NYHA Class.

The bar graphs summarize the severity of tricuspid regurgitation as adjudicated by the echocardiographic core laboratory (Panel A) and the severity of heart failure as defined by the New York Heart Association (NYHA) functional class (Panel B) at baseline, 30 days, and 1 year in both trial groups.

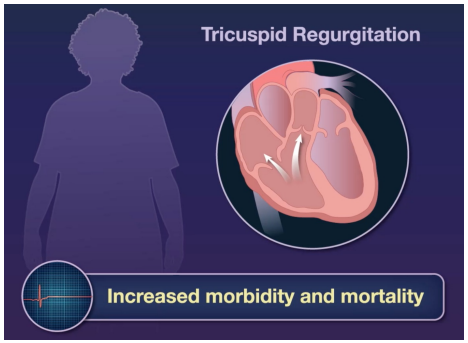
Tricuspid Regurgitation
Increased morbidity and mortality

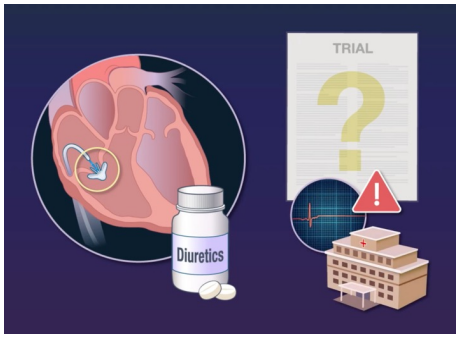
TRIAL
Diuretics

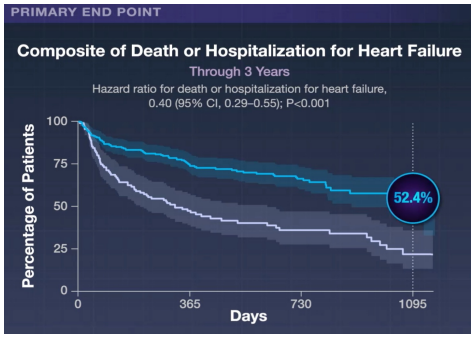
PRIMARY END POINT
Composite of Death or Hospitalization for Heart Failure
Through 3 Years
Hazard ratio for death or hospitalization for heart failure,
0.40 (95% CI, 0.29–0.55); P<0.001
Percentage of Patients
100
75
50
25
0
0
365
730
1095
Days
52.4%

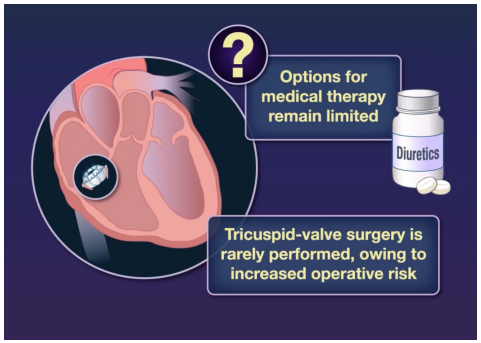
Options for medical therapy remain limited
Diuretics
Tricuspid-valve surgery is rarely performed, owing to increased operative risk

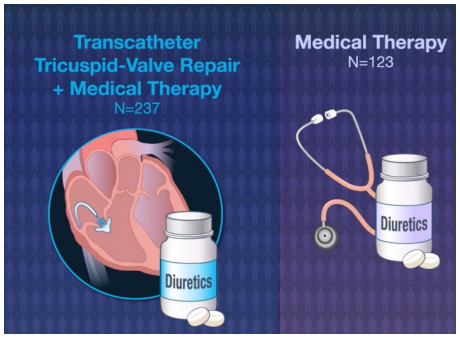
Transcatheter Tricuspid-Valve Repair + Medical Therapy
N=237
Medical Therapy
N=123
Diuretics
Diuretics

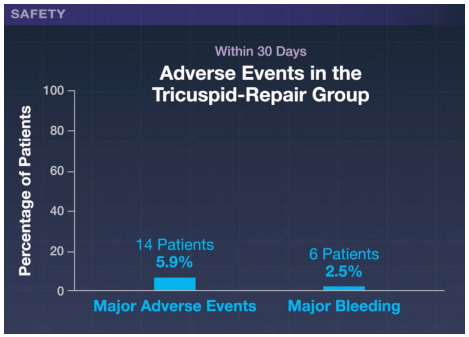
SAFETY
Within 30 Days
Adverse Events in the Tricuspid-Repair Group
Percentage of Patients
100
80
60
40
20
0
14 Patients
5.9%
6 Patients
2.5%
Major Adverse Events
Major Bleeding

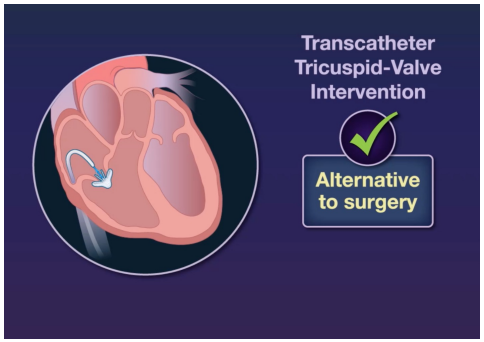
Transcatheter Tricuspid-Valve Intervention
Alternative to surgery

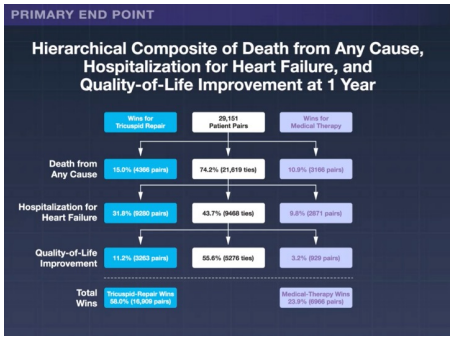
PRIMARY END POINT
Hierarchical Composite of Death from Any Cause, Hospitalization for Heart Failure, and Quality-of-Life Improvement at 1 Year
Wins for Tricuspid Repair
25,151 Patient Pairs
Wins for Medical Therapy
Death from Any Cause
15.0% (4366 pairs)
74.2% (21,619 ties)
10.9% (3166 pairs)
Hospitalization for Heart Failure
31.6% (9260 pairs)
43.7% (9468 ties)
9.6% (2871 pairs)
Quality-of-Life Improvement
11.2% (3263 pairs)
55.6% (5276 ties)
3.2% (929 pairs)
Total Wins
Tricuspid-Repair Wins
56.0% (16,909 pairs)
Medical-Therapy Wins
23.9% (6906 pairs)

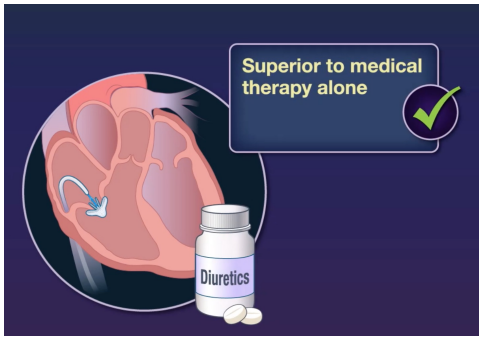
Superior to medical therapy alone
Diuretics

Multikrebs-Früherkennungstests (**MCED-Tests**, *Multi-Cancer Early Detection*)

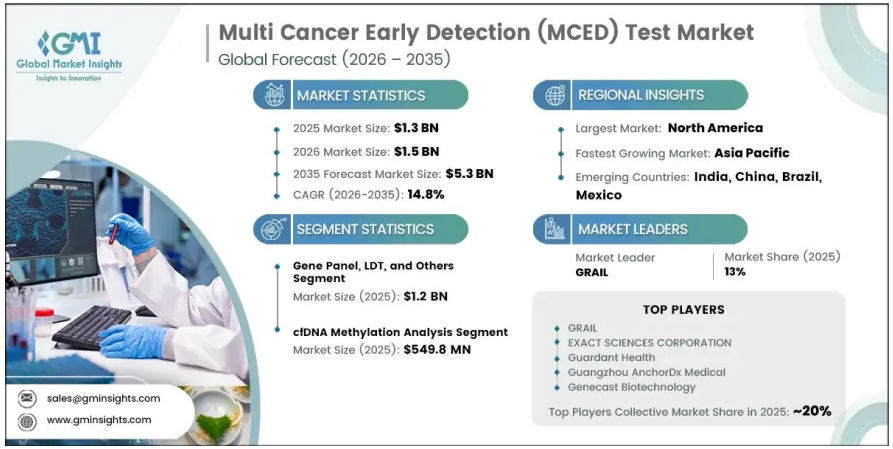

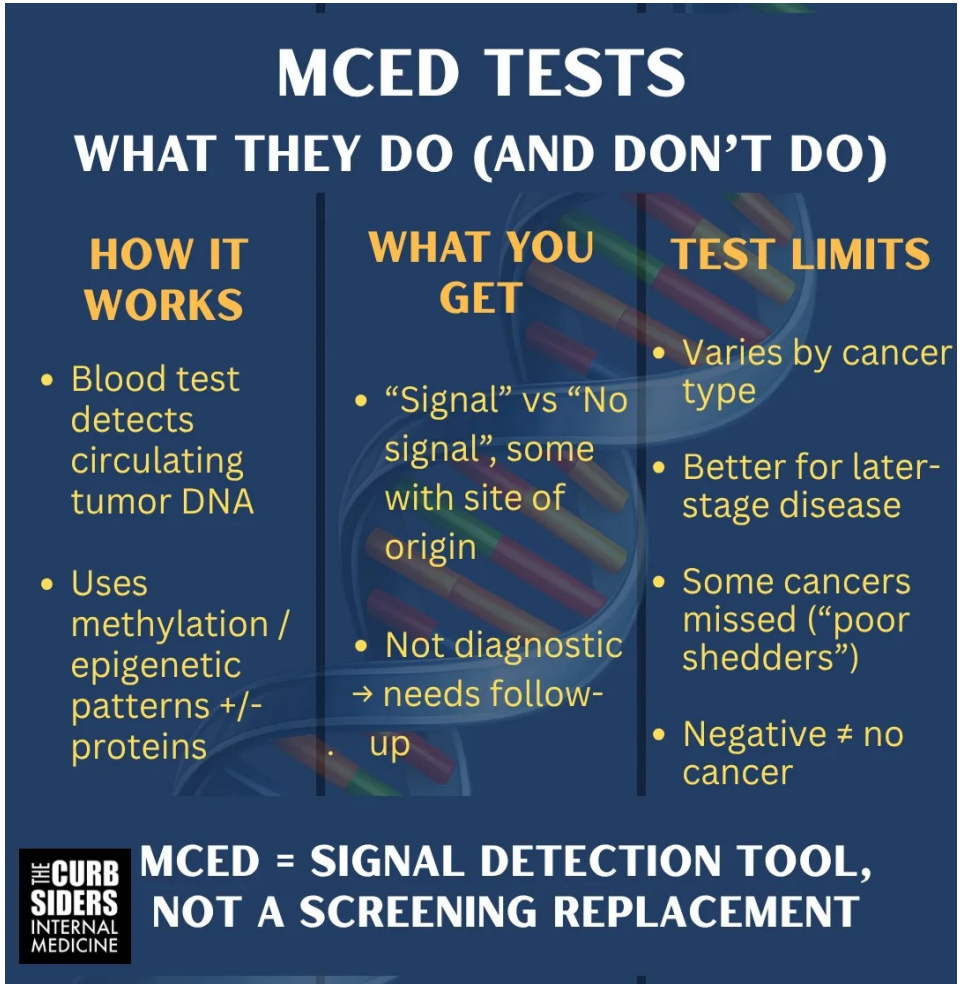

Multikrebs-Früherkennungstests (**MCED-Tests**, *Multi-Cancer Early Detection*) sind innovative blutbasierte Untersuchungen, die darauf abzielen, Dutzende verschiedene Krebsarten anhand von zellfreier DNA (cfDNA) oder Biomarkern im Blut nachzuweisen, noch bevor Symptome auftreten.

Funktionsweise

- **Flüssigbiopsie (Liquid Biopsy):** Die Tests analysieren zellfreie DNA-Fragmente (cfDNA) oder Immunzellen (wie Fresszellen bei bestimmten Verfahren) aus einer normalen Blutprobe.
- **Signalerkennung:** Sie suchen nach tumorspezifischen Veränderungen, wie etwa DNA-Methylierungsmustern oder Krebsenzymen.
- **Ursprungsvorhersage:** Fortgeschrittene Tests können oft auch angeben, aus welchem Gewebe oder Körperbereich das Krebssignal vermutlich stammt.

Bekannte Beispiele

- **Galleri-Test:** Ein US-Test von GRAIL, der über Methylierungsmuster der cfDNA mehr als 50 Krebsarten erkennen soll (in den USA und im Rahmen von Studien bekannt, in der EU meist nicht regulär im Alltag verfügbar).
- **PanTum Detect®:** Ein in Deutschland entwickelter und im August 2026 nach der EU-In-vitro-Diagnostika-Verordnung (IVDR) zertifizierter Bluttest der Zyagnum AG, der über das Immunsystem (Fresszellen und EDIM-Technologie) Hinweise auf veränderte Zellprozesse liefert

Effect of Screening with Multicancer Early-Detection Test on Late-Stage Cancer Diagnosis

Whether screening with blood-based early-detection tests for multiple cancers in addition to usual care has clinical utility is unknown. In a randomized, controlled trial conducted in England, we obtained peripheral blood from persons 50 to 77 years of age at up to three annual visits. After baseline blood collection, participants were randomly assigned in a 1:1 ratio to the intervention group (participants whose blood was tested) or the control group (participants whose blood was stored). Participants and trial personnel were initially unaware of the group assignments. The primary end point was stage III or IV cancer among 12 prespecified types of cancer, and a key secondary end point was stage IV cancer among the 12 prespecified types. The differences between the groups in the incidence rate (the number of first eligible events divided by person-years at risk) were measured after three screening rounds and at least 12 months of follow-up after the last participant's third visit.

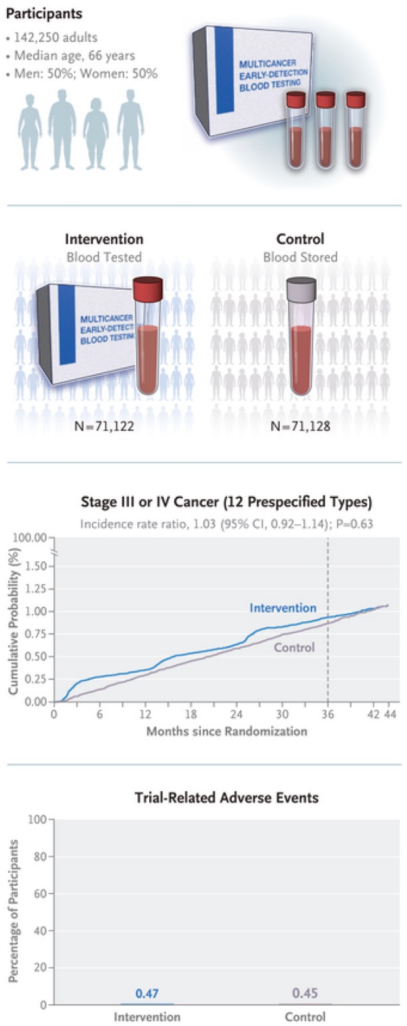

The survival advantage associated with detection of cancer at earlier stages reflects broader eligibility for curative treatment and lower disease burden. Standard-of-care screening contributes to earlier diagnosis and improved survival, yet the recommended single-cancer screening accounts for less than 7% of all cancer diagnoses in England and less than 15% in the United States. Multicancer early-detection testing offers a different approach by simultaneously screening for multiple cancer types in a biologic specimen (e.g., blood). One multicancer early-detection test that analyzes methylation patterns in cell-free DNA (cfDNA) to detect a cancer signal and predict the associated tissue type or organ (cancer signal origin) has shown the ability to detect cancer across a broad range of cancer types. The test has shown strong performance in case–control studies and in prospective clinical studies, as well as in real-world experience.

Here, we report the primary results from the NHS-Galleri trial, a randomized, controlled trial.

Procedures

Initial appointments were conducted in mobile phlebotomy clinics. After participants provided written informed consent, a baseline peripheral blood sample was obtained by routine venipuncture, and participants were then randomly assigned in a 1:1 ratio to the intervention or control group.

All participants, except those for whom the trial team had received death notification, were invited to provide a blood sample at two further annual (12 months, with a window of ±6 weeks) visits; participants missing the second visit could return for the third. Participants who had received treatment for cancer in the preceding year were advised to contact the trial team, because they may not have needed to attend the next screening visit. All participants and trial staff were initially unaware of the group assignments; participants in the intervention group who had a positive result on a multicancer early-detection test (i.e., a cancer signal was detected) received the results in communications from trial nurses who became aware of the group assignment. Only statisticians who were aware of the group assignments reviewed unblinded safety data and presented results to the independent data monitoring committee in closed meetings conducted every 6 months.

Blood samples from participants in the intervention group were analyzed with the multicancer early-detection test.

Blood samples from participants in the intervention group were analyzed with the multicancer early-detection test. The trial team facilitated referral for diagnostic testing of participants who received a positive result through established NHS urgent cancer referral pathways that followed existing guidelines for anatomical site–specific suspected cancer based on the cancer-signal origin predicted by the multicancer early-detection test. All blood samples from participants in the control group and remaining plasma samples from the participants in the intervention group (kept in case of a processing error) were stored for future testing with the consent of the participants.

Cancer outcomes were obtained through linked national health care datasets. Participants were passively followed for cancer diagnoses and death until they emigrated or withdrew consent.

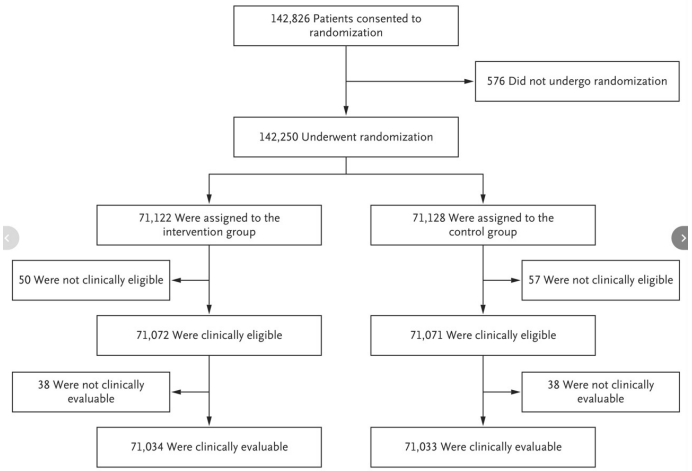

Randomization and Follow-up.

Participants were considered to be clinically eligible if they met inclusion criteria and did not meet exclusion criteria and underwent randomization. Participants were considered to be clinically evaluable if their data were successfully linked in the routine datasets used in this trial.

An overview of the NHS-Galleri trial.[4]

MCED, multi-cancer early detection; NHS, National Health Service.

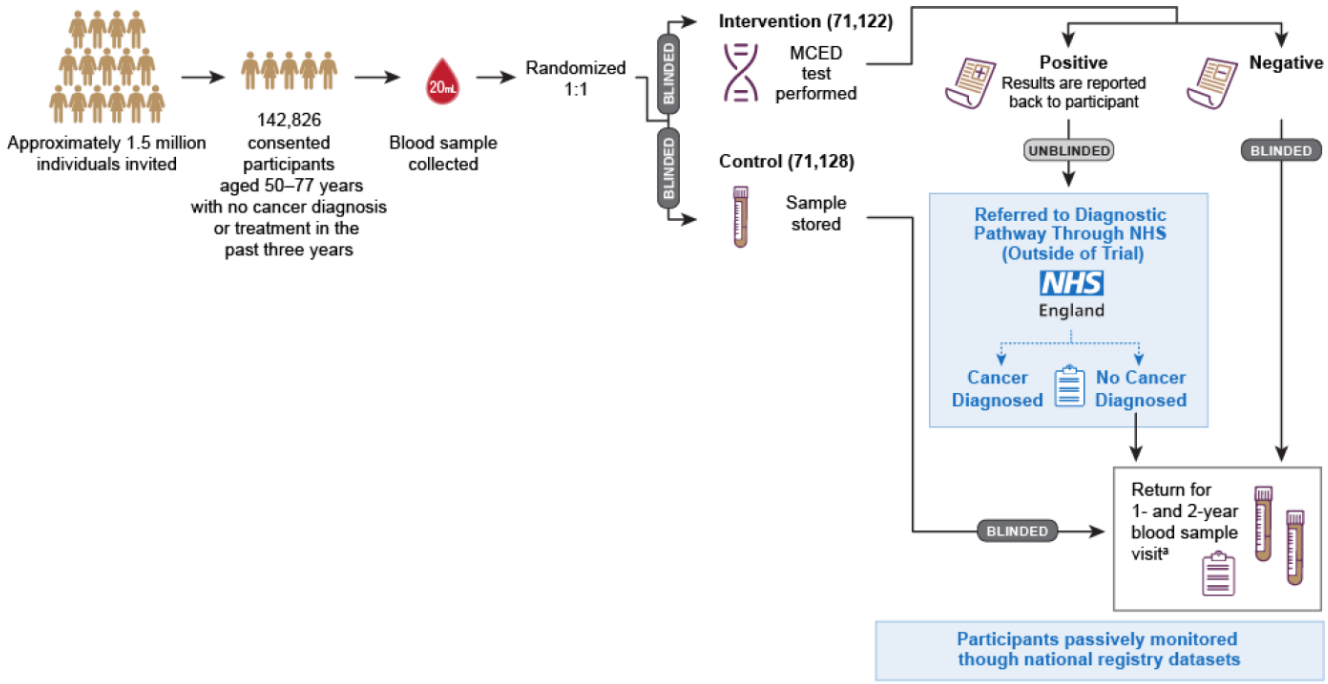

[a]Participants who were diagnosed with cancer were not required to return for blood sample collection.

Demographic and Clinical Characteristics of the Participants at Baseline.

Characteristic	Intervention (N = 71,122)	Control (N = 71,128)	Total (N = 142,250)
Median age (IQR) — yr	66 (59–71)	66 (59–71)	66 (59–71)
Age group — no. (%)†			
50–59 years	18,791 (26.4)	18,889 (26.6)	37,680 (26.5)
60–69 years	28,596 (40.2)	28,792 (40.5)	57,388 (40.3)
70–79 years	23,734 (33.4)	23,447 (33.0)	47,181 (33.2)
Sex — no. (%)			
Female	35,723 (50.2)	35,739 (50.2)	71,462 (50.2)
Male	35,399 (49.8)	35,389 (49.8)	70,788 (49.8)
Race or ethnic group — no. (%)‡			
Asian or Asian British	2,360 (3.3)	2,365 (3.3)	4,725 (3.3)
Black, Black British, Caribbean, or African	1,016 (1.4)	1,038 (1.5)	2,054 (1.4)
White	66,552 (93.6)	66,566 (93.6)	133,118 (93.6)
Mixed	776 (1.1)	768 (1.1)	1,544 (1.1)
Other	318 (0.4)	309 (0.4)	627 (0.4)
Data missing	100 (0.1)	82 (0.1)	182 (0.1)
IMD quintile — no. (%)§			
1	16,071 (22.6)	16,062 (22.6)	32,133 (22.6)
2	13,942 (19.6)	13,980 (19.7)	27,922 (19.6)
3	15,034 (21.1)	14,956 (21.0)	29,990 (21.1)
4	14,372 (20.2)	14,476 (20.4)	28,848 (20.3)
5	11,469 (16.1)	11,414 (16.0)	22,883 (16.1)
Data missing	234 (0.3)	240 (0.3)	474 (0.3)
Previous history of cancer — no. (%)	5,328 (7.5)	5,355 (7.5)	10,683 (7.5)
Median time since previous cancer diagnosis (IQR) — yr¶	10.2 (6.7–15.0)	10.2 (6.7–14.8)	10.2 (6.7–14.9)
Participant-reported screening participation — no./total no. (%)			
Never heard of cancer screening	2,056/71,019 (2.9)	2,108/71,039 (3.0)	4,164/142,058 (2.9)
Heard of cancer screening but never been invited	13,955/71,019 (19.6)	13,871/71,039 (19.5)	27,826/142,058 (19.6)
Invited for cancer screening but never done it	861/71,019 (1.2)	883/71,039 (1.2)	1,744/142,058 (1.2)
Invited for cancer screening, but did not participate every time	2,428/71,019 (3.4)	2,361/71,039 (3.3)	4,789/142,058 (3.4)
Invited for cancer screening and participated every time	51,013/71,019 (71.8)	51,150/71,039 (72.0)	102,163/142,058 (71.9)
Don't know	655/71,019 (0.9)	608/71,039 (0.9)	1,263/142,058 (0.9)
Decline to answer	51/71,019 (0.1)	58/71,039 (0.1)	109/142,058 (0.1)
Data missing	103/71,019 (0.1)	89/71,039 (0.1)	192/142,058 (0.1)
Smoking history — no. (%)			
Current smoker	4,744 (6.7)	4,708 (6.6)	9,452 (6.6)
Former smoker	27,272 (38.3)	27,148 (38.2)	54,420 (38.3)
Never smoked	39,004 (54.8)	39,187 (55.1)	78,191 (55.0)
Data missing	102 (0.1)	85 (0.1)	187 (0.1)
BMI — no. (%)‖			
<25	23,058 (32.4)	23,203 (32.6)	46,261 (32.5)
25 to <30	28,009 (39.4)	27,925 (39.3)	55,934 (39.3)
≥30	19,739 (27.8)	19,706 (27.7)	39,445 (27.7)
Data missing	316 (0.4)	294 (0.4)	610 (0.4)
History of selected medical diagnoses — no. (%)			
Barrett's esophagus	811 (1.1)	810 (1.1)	1,621 (1.1)
Chronic bowel disease	1,660 (2.3)	1,632 (2.3)	3,292 (2.3)
Chronic liver disease	1,167 (1.6)	1,056 (1.5)	2,223 (1.6)
Diabetes	7,091 (10.0)	7,129 (10.0)	14,220 (10.0)
Chronic pancreas disease	304 (0.4)	298 (0.4)	602 (0.4)
Systemic lupus erythematosus	129 (0.2)	140 (0.2)	269 (0.2)
Education level — no. (%)			
School up to 15 years of age	12,672 (17.8)	12,887 (18.1)	25,559 (18.0)
Completion of secondary education, e.g., CSEs, O-levels, or equivalent**	19,262 (27.1)	19,260 (27.1)	38,522 (27.1)
A-levels or equivalent††	6,517 (9.2)	6,509 (9.2)	13,026 (9.2)
Further education without a degree	14,776 (20.8)	14,570 (20.5)	29,346 (20.6)
Bachelor's degree or equivalent	11,953 (16.8)	11,970 (16.8)	23,923 (16.8)
Further degree, e.g., Masters or Ph.D.	5,842 (8.2)	5,850 (8.2)	11,692 (8.2)
Data missing	100 (0.1)	82 (0.1)	182 (0.1)

Table continues

IMD quintiles divide areas in England into five equal groups (or 20% bands) based on the Index of Multiple Deprivation (IMD), which measures relative neighborhood deprivation

Stage III or IV and Stage IV Cancer Outcomes after Three Annual Screening Rounds.

Outcome	12 Prespecified Cancers†		All Routinely Staged Cancers Except Prostate Cancer		All Routinely Staged Cancers	
	Intervention (N=71,122)	Control (N=71,128)	Intervention (N=71,122)	Control (N=71,128)	Intervention (N=71,122)	Control (N=71,128)
Stage III or IV Cancer						
No. of participants (%)	706 (1.0)	688 (1.0)	903 (1.3)	848 (1.2)	1266 (1.8)	1208 (1.7)
Person-years of follow-up	234,959	235,249	234,667	235,044	234,062	234,495
Incidence rate per 100,000 person-years (95% CI)	300.5 (278.7–323.5)	292.5 (271.0–315.1)	384.8 (360.1–410.7)	360.8 (336.9–385.9)	540.9 (511.5–571.5)	515.1 (486.5–545.0)
Incidence rate difference (95% CI)	8.0 (–23.1 to 39.2)		24.0 (–10.9 to 59.0)		25.7 (–15.9 to 67.4)	
Incidence rate ratio (95% CI)	1.03 (0.92–1.14)‡		1.07 (0.97–1.17)		1.05 (0.97–1.14)	
Stage IV Cancer						
No. of participants (%)	342 (0.5)	397 (0.6)	412 (0.6)	467 (0.7)	503 (0.7)	563 (0.8)
Person-years of follow-up	235,584	235,662	235,501	235,585	235,347	235,434
Incidence rate per 100,000 person-years (95% CI)	145.2 (130.2–161.4)	168.5 (152.3–185.9)	174.9 (158.5–192.7)	198.2 (180.7–217.1)	213.7 (195.5–233.2)	239.1 (219.8–259.7)
Incidence rate difference (95% CI)	–23.3 (–46.0 to –0.7)		–23.3 (–48.0 to 1.4)		–25.4 (–52.6 to 1.8)	
Incidence rate ratio (95% CI)	0.86 (0.74–1.00)		0.88 (0.77–1.01)		0.89 (0.79–1.01)	

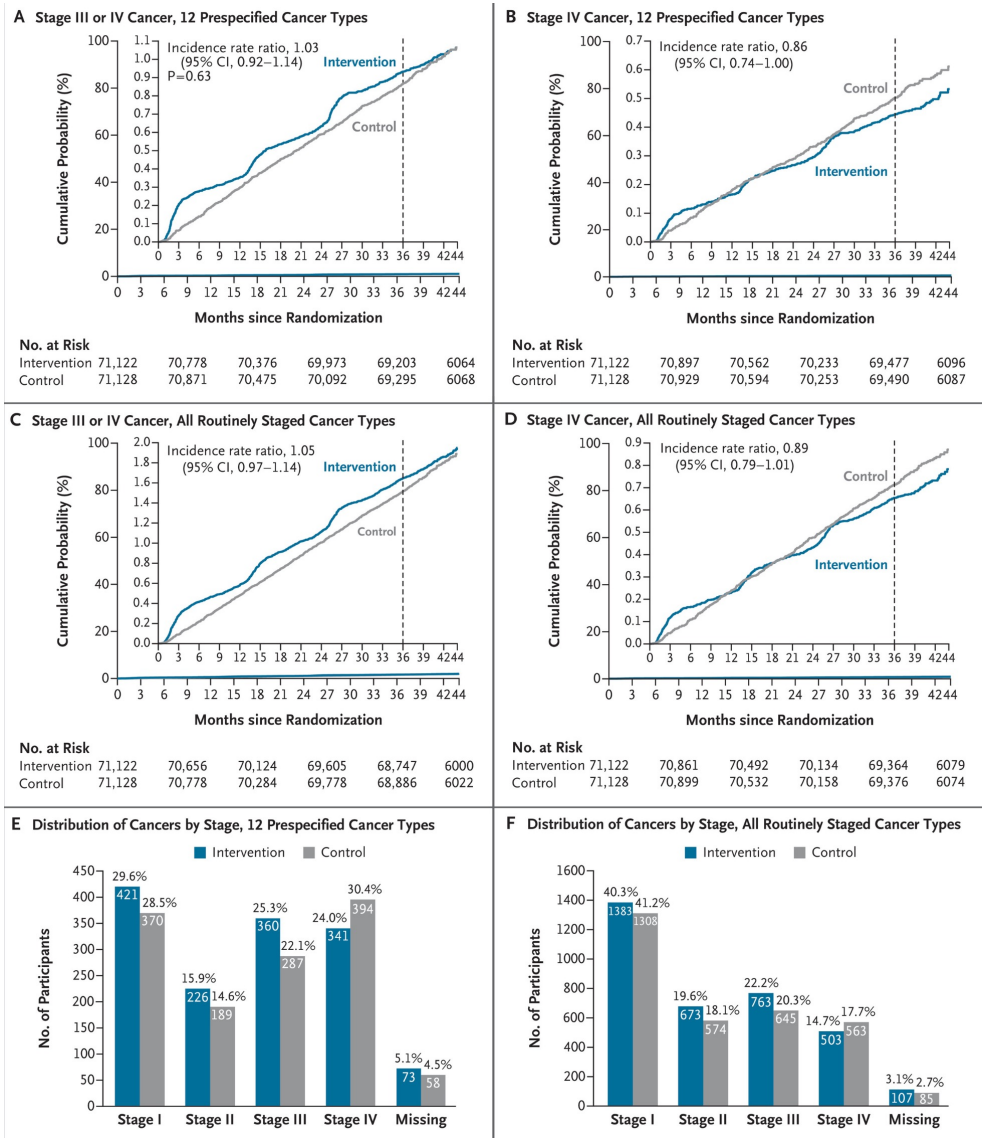

Cumulative Probability of Stage III or IV Cancers and Stage IV Cancers According to Trial Group after Three Annual Screening Rounds.

Cumulative probability based on Kaplan–Meier estimates is shown for the risk of diagnosis of stage III or IV cancer among the 12 prespecified cancer types (Panel A), of stage IV among the 12 prespecified cancer types (Panel B); of stage III or IV among all routinely staged cancer types (Panel C), and of stage IV among all routinely staged cancer types (Panel D); these cumulative-probability displays were generated post hoc, whereas the corresponding incidence-rate analyses of these end points were prespecified. The inset in each panel shows the same data on an expanded y axis. Distribution of cancers according to stage and trial group are shown for the 12 prespecified cancer types (Panel E) (post hoc analysis) and for all routinely staged cancer types (Panel F). There were two participants with stage 0 cancer in each of the intervention and control groups; all these were Paget's disease, which is invasive at stage 0. Participant-level counts in Panels E and F were determined by assigning one cancer type and stage per participant on the basis of the cancer at the highest stage and, if tied, the earliest diagnosis; counts may therefore differ from those shown in Table 2, which shows the counts determined by the first qualifying cancer event. The 12 prespecified cancer types were lung, head and neck, colon or rectum, pancreas, myeloma or plasma cell neoplasm, liver or bile duct, stomach, esophagus, anus, lymphoma, ovary, and bladder.

Participant Group Sizes

- **Intervention group:** 71,122 participants (received blood testing with the cell-free DNA multicancer early-detection test plus usual care).
- **Control group:** 71,128 participants (received usual care with blood stored but not tested).

Stage III or IV Cancer (Primary Endpoint)

- There was **no significant difference** in the incidence rate of stage III or IV cancer across 12 prespecified cancer types between the intervention and control groups.
- **Incidence Rate Ratio (IRR):** 1.03 (95% CI: 0.92 to 1.14, P = 0.63).

Stage IV Cancer (Key Secondary Endpoint)

- The incidence rate of stage IV cancer specifically was **lower** in the intervention group compared to the control group:
  - **Intervention group:** 145.2 per 100,000 person-years
  - **Control group:** 168.5 per 100,000 person-years
- **Incidence Rate Ratio (IRR):** 0.86 (95% CI: 0.74 to 1.00).

Anus, Bladder, Colorectal, Esophagus, Head & Neck, Liver/Bile Duct, Lung, Lymphoma, Myeloma/Plasma Cell Neoplasm, Ovary, Pancreas, and Stomach.

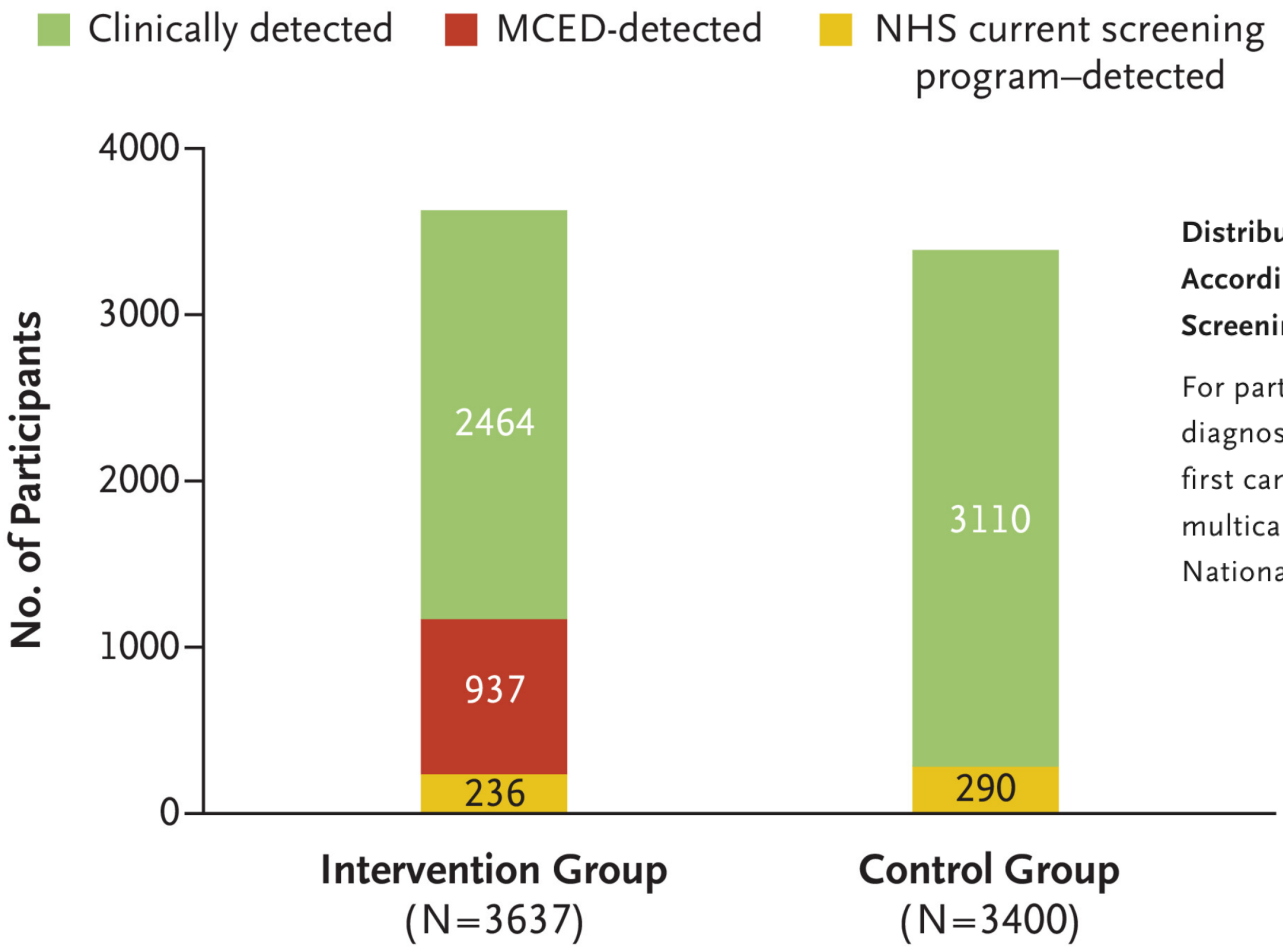

Distribution of the Route to Cancer Diagnosis According to Trial Group after Three Annual Screening Rounds.

For participants with multiple cancers diagnosed, only the route to diagnosis of the first cancer is included. MCED denotes multicancer early-detection test, and NHS the National Health Service.

Discussion

NHS-Galleri is a randomized, controlled trial that evaluated the clinical utility of a multicancer early-detection test for population screening. After three annual multicancer early-detection screening rounds with 12 months of follow-up after the last participant's third visit, we did not observe a lower incidence rate in the intervention group than in the control group of stage III or IV cancers among the 12 prespecified cancer types (the primary end point). Although the prespecified hierarchical plan to adjust for multiple testing precluded any formal testing of secondary end points, the results suggested the possibility that the intervention was associated with fewer stage IV cancer diagnoses in the second and third screening rounds, in which observed trends would be expected to reflect those of a stable screening program with a routinely screened population. Stage IV cancer reduction is clinically important since stage IV disease confers worse survival than earlier-stage disease.

In this large, randomized, controlled trial, annual multicancer early-detection testing added to usual care was not associated with a significantly lower incidence rate of stage III or IV cancer across 12 prespecified types after three screening rounds and at least 12 months of follow-up. Further follow-up is warranted to assess the way findings for stage III or IV cancers and the observed difference in stage IV cancers translate to clinical benefit over time.

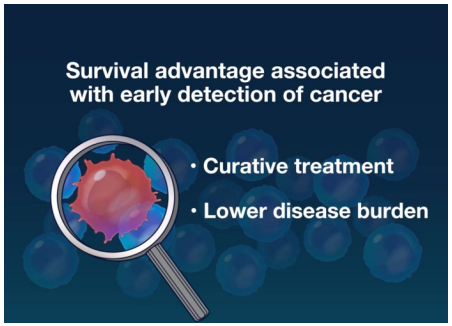

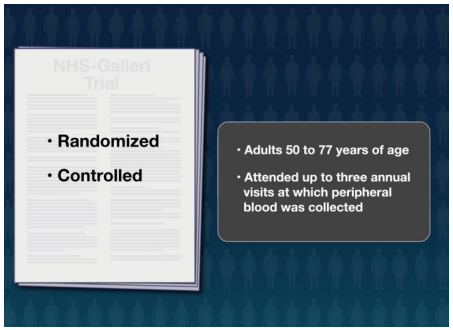

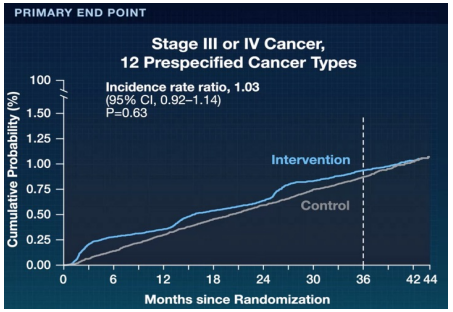

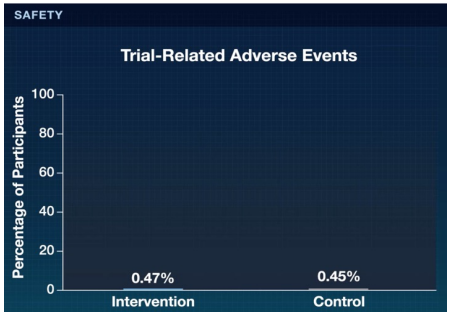

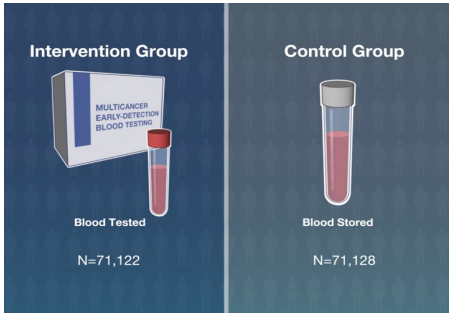

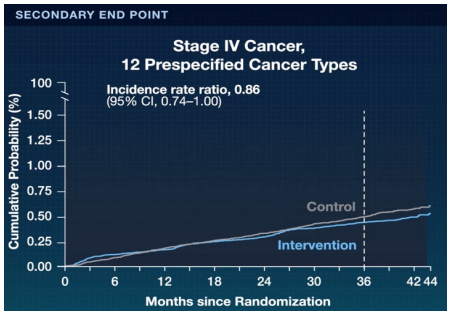

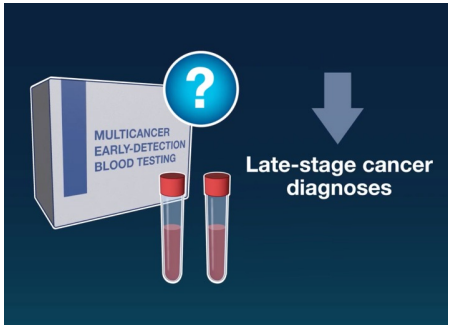

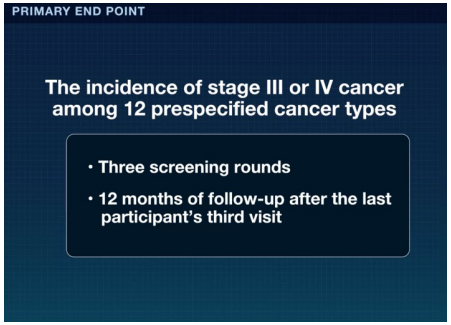

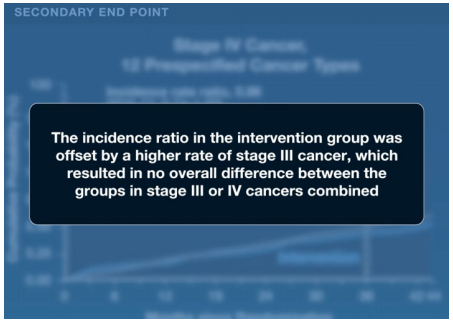

Thus, whether screening with blood-based early-detection tests for multiple cancers in addition to usual care has clinical utility, could not be shown.

Ein septischer Schock entwickelt sich meist aus einer fortschreitenden Sepsis („Blutvergiftung“). Typische Warnsignale sind:

- **Extremer Blutdruckabfall:** Der Kreislauf bricht zusammen, was zu Schwindel oder Ohnmacht führt.
- **Massives Herzrasen & schnelle Atmung:** Der Körper versucht verzweifelt, den Sauerstoffmangel auszugleichen.
- **Verwirrtheit & Wesensveränderung:** Akute Desorientierung oder extreme Schläfrigkeit (Sepsis-Enzephalopathie).
- **Hautveränderungen:** Die Haut ist oft feuchtkalt, blass oder zeigt eine fleckige Marmorierung (besonders an Knien, Händen und Füßen).
- **Nie gekanntes Krankheitsgefühl:** Betroffene klagen oft über extreme Schmerzen oder äußern Todesangst.
- **Fieber oder Untertemperatur:** Häufig tritt hoher Schüttelfrost auf, aber auch eine gefährlich niedrige Körpertemperatur (< 36 °C) ist möglich

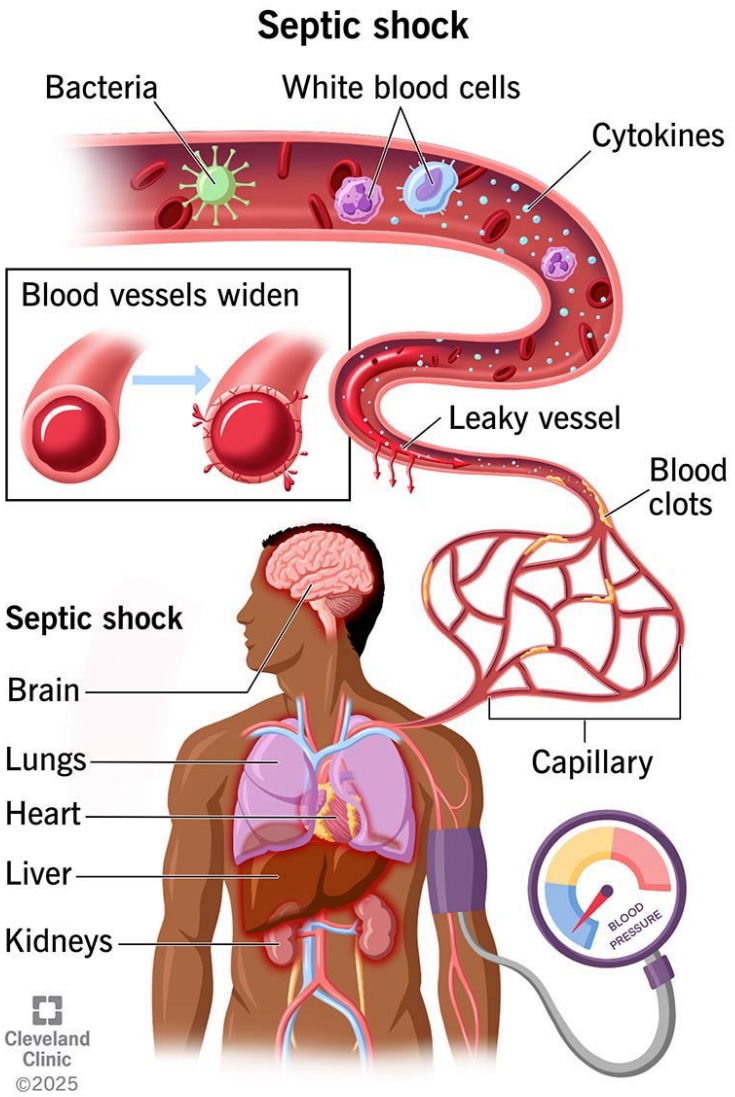

Vasopressors or Fluids in Early Septic Shock

The optimal approach to early resuscitation in septic shock is unknown. Equipoise exists between the use of larger volumes of intravenous fluids to restore perfusion and the use of early vasopressor therapy along with smaller volumes of fluids to minimize potential harm from excess fluid. We randomly assigned adult patients who presented to the emergency department with septic shock to receive either fluids at restricted volumes and early vasopressor therapy (vasopressor group) or higher volumes of fluids and later vasopressor therapy (fluids group) for at least 6 hours and up to 24 hours. The primary outcome was days alive and out of the hospital from randomization to day 90.

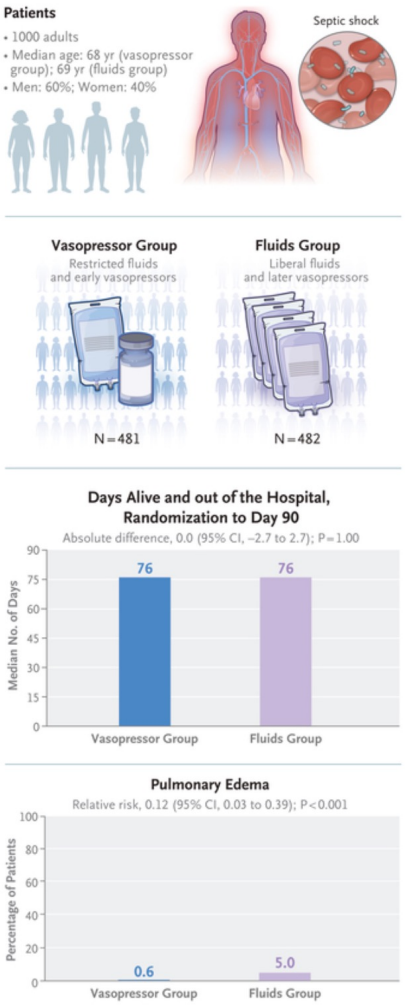

The optimal approach to intravenous fluid volume and timing of vasopressor initiation in patients with early septic shock is unknown. In patients with sepsis-induced hypotension, the Surviving Sepsis Campaign guidelines provide a weak recommendation for intravenous fluids administered at a dose of at least 30 ml per kilogram of body weight within the first 3 hours after recognition of the hypotension. The European Society of Intensive Care Medicine guidelines make a similar recommendation and call for randomized trials to assess the initial fluid dose and subsequent administration during the optimization phase (typically the first 24 hours). Neither guideline makes specific recommendations regarding the timing of vasopressor initiation. Vasopressors are typically administered in the intensive care unit (ICU), and the use of these agents to support a restricted fluid strategy may increase demand for beds and contribute to inequities when ICU resources are constrained. Limited evidence to guide early resuscitation contributes to practice variation in the management of septic shock. Clinical uncertainty is compounded by reports of potential adverse effects that occur with excess fluid administration. The largest randomized trial to evaluate a restrictive fluid strategy for early septic shock was stopped for futility and showed no benefit with regard to mortality

We conducted the Australasian Resuscitation in Sepsis Evaluation: Fluid or Vasopressors in Emergency Department Sepsis (ARISE FLUIDS) trial to test whether a strategy of restricted fluid volume and early vasopressors, as compared with a strategy of greater fluid volume and later vasopressors, would increase the number of days alive and out of the hospital at day 90 among adult patients who presented to the emergency department with early septic shock.

Patients

Adults with a clinically suspected infection were eligible if they had systolic blood pressure of less than 90 mm Hg or mean arterial pressure of less than 65 mm Hg despite receiving at least 1000 ml of fluid in the form of bolus doses (including fluids administered before hospital presentation; a bolus dose was defined as 500 to 1000 ml of fluid administered over a period of 60 minutes or less), had a blood lactate level higher than 2.0 mmol per liter, and had begun receiving treatment with an intravenous antimicrobial agent.

For patients in the vasopressor group, intravenous fluid resuscitation ceased after randomization and vasopressor therapy commenced. Vasopressor type, route, dose adjustment, and target mean arterial pressure were according to clinician preference. Fluid boluses of 250 ml were permitted if indicated, including for refractory hypotension, persistent hypoperfusion (e.g., delayed capillary refill time), a lactate level higher than 4 mmol per liter or rising from the previous level despite resuscitation for 2 hours or more, persistent tachycardia, and oliguria marked by a urine output of less than 0.5 ml per kilogram of body weight per hour for 2 hours or more. Maintenance fluids were discouraged.

For patients in the fluids group, an initial intravenous fluid bolus of up to 1000 ml infused within 60 minutes was administered after randomization. Additional 500-ml boluses were administered for persistent hypotension or hypoperfusion. Unless contraindicated, administration of fluids at a dose of 30 ml per kilogram within 3 hours after presentation to the emergency department was recommended. Fluid type, methods of assessing fluid responsiveness, maintenance fluids, and target mean arterial pressure were determined according to clinician preference.

Outcomes

The primary outcome was days alive and out of the hospital from randomization to follow-up at day 90.

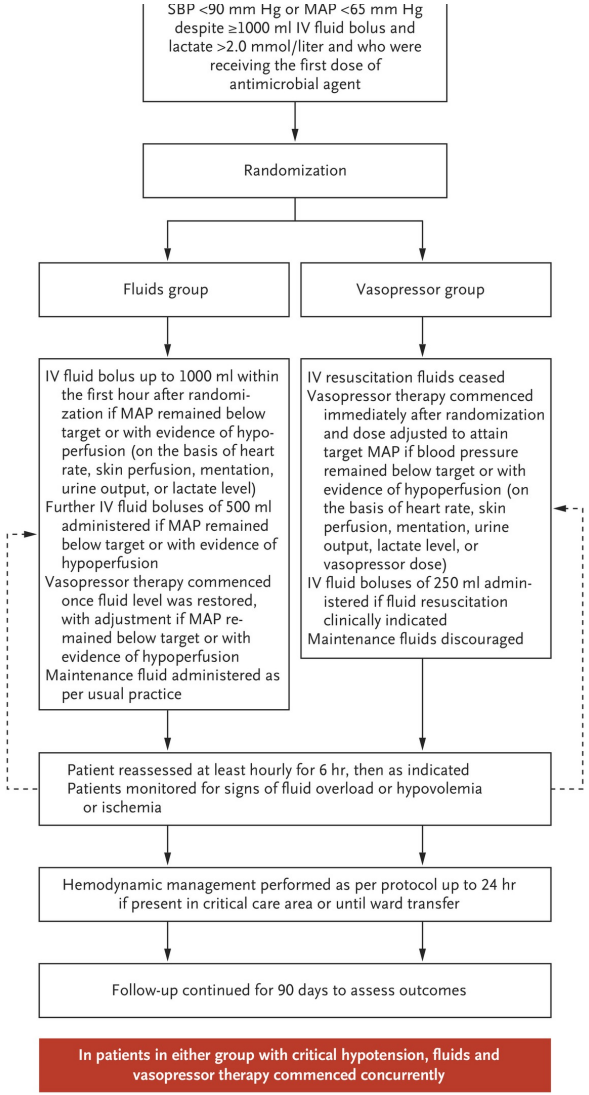

Trial Algorithm.

Patients with suspected septic shock who met eligibility criteria were randomly assigned to receive restricted fluids and early vasopressors or more liberal fluids and later vasopressors, as needed. The intervention was delivered for at least 6 hours and up to 24 hours while the patient remained in a critical care area (emergency department or intensive care unit). The target mean arterial pressure (MAP) was at the treating clinician's discretion for patients in both the fluids group and the vasopressor group. For patients in the vasopressor group, 250-ml fluid boluses were permitted if indicated, including for refractory hypotension, persistent hypoperfusion (e.g., delayed capillary refill time), a lactate level that was greater than 4 mmol per liter or that was increasing from the previous level despite resuscitation for at least 2 hours, persistent tachycardia, and urine output of less than 0.5 ml per kilogram of body weight per hour for at least 2 hours (oliguria). For patients in the fluids group who were receiving a vasopressor infusion at the time of randomization, protocolized discontinuation was not mandated and vasopressor doses were adjusted on the basis of clinician judgment. Additional details of the trial intervention are provided in the Supplementary Appendix. IV denotes intravenous and SBP systolic blood pressure.

Baseline

Characteristic or Therapy	Vasopressor Group (N=481)	Fluids Group (N=482)
Median age (IQR) — yr	68 (58–77)	69 (56–77)
Male sex — no. (%)	281 (58.4)	302 (62.7)
Median weight — kg†	79 (65–95)	78 (66–94)
Usual residence — no. (%)		
Home	465 (96.7)	452 (93.8)
Long-term care facility‡	16 (3.3)	30 (6.2)
Median Charlson Comorbidity Index score (IQR)§	1 (0–3)	1 (0–3)
Median APACHE II score (IQR)¶	18 (15–23)	18 (14–22)
Median modified SOFA score (IQR)‖	4 (3–6)	4 (3–6)
Median systolic blood pressure (IQR) — mm Hg	85 (79–92)	86 (80–91)
Median lactate level (IQR) — mmol/liter	3.3 (2.5–4.7)	3.2 (2.4–4.5)
Median total IV fluid administered (IQR)**		
Volume — ml	1500 (1000–1750)	1500 (1000–1850)
Volume by body weight — ml/kg	18 (13–23)	18 (13–23)
Invasive mechanical ventilation — no. (%)	3 (0.6)	2 (0.4)
Vasopressor infusion††		
Initiated before randomization — no. (%)	57 (11.9)	41 (8.5)
Median time from emergency department presentation to start of infusion (IQR) — hr	2.57 (1.66–4.01)	3.7 (2.12–5.63)
Median time from emergency department presentation to randomization (IQR) — hr	2.10 (1.30–3.20)	2.10 (1.30–3.40)
Median time from confirmation of inclusion criteria to randomization (IQR) — hr‡‡	0.30 (0.10–0.60)	0.30 (0.10–0.60)
Primary site of infection — no. (%)		
Pulmonary	144 (29.9)	156 (32.4)
Urinary tract	112 (23.3)	121 (25.1)
Intraabdominal	66 (13.7)	71 (14.7)
Skin and soft tissue	64 (13.3)	67 (13.9)
Primary bloodstream	11 (2.3)	5 (1.0)
Other§§	16 (3.3)	6 (1.2)
Unknown	68 (14.1)	56 (11.6)
Median time from emergency department presentation to administration of first dose of antimicrobial agent (IQR) — hr	0.97 (0.57–1.53)	0.85 (0.52–1.52)

Fluid and Vasopressor Administration (24-Hour Intervention Period).

Variable	Vasopressor Group (N=481)	Fluids Group (N=482)	Difference (95% CI)*
Median volume of IV fluid administered (IQR) — ml†			
0 to 1 hr	185 (0 to 500)	1000 (500 to 1080)	−800 (−930 to −670)
0 to 6 hr	500 (250 to 1000)	1500 (1000 to 2091)	−1000 (−1088 to −884)
6 to 24 hr	480 (0 to 1100)	600 (0 to 1256)	−120 (−437 to 0)
0 to 24 hr	1140 (500 to 2120)	2248 (1500 to 3332)	−1108 (−1395 to −850)
Median volume of IV fluid administered (IQR) — ml/kg†			
0 to 1 hr	2 (0 to 6)	10 (5 to 16)	−9 (−10 to −7)
0 to 6 hr	7 (3 to 14)	20 (13 to 27)	−13 (−15 to −12)
6 to 24 hr	5 (0 to 14)	8 (0 to 17)	−3 (−5 to −1)
0 to 24 hr	14 (6 to 27)	29 (18 to 43)	−15 (−18 to −12)
Vasopressor initiation, 0 to 24 hr			
Patients — no. (%)‡	416 (86.5)	326 (67.6)	18.9 (13.3 to 24.5)
Median time to vasopressor initiation (IQR) — hr§	0.4 (0.2 to 0.9)	1.4 (0.4 to 3.1)	−1.0 (−1.2 to −0.9)
Vasopressor administration by peripheral venous catheter — no. (%)	346 (71.9)	267 (55.4)	16.5 (10.5 to 22.4)
Duration of vasopressor administration by peripheral venous catheter — hr	6.2 (3.4 to 14.9)	5.7 (3.0 to 18.7)	0.5 (−1.1 to 1.7)
Central venous catheter in situ — no. (%)¶	188 (39.1)	180 (37.3)	1.7 (−4.6 to 8.1)
Vasopressor infusion by central venous catheter — no. (%)	179 (37.2)	159 (33.0)	4.2 (−1.8 to 10.2)

Outcomes

Outcome	Vasopressor Group (N=481)	Fluids Group (N=482)	Effect Estimate (95% CI)*
Primary outcome†			
Median no. of days alive and out of the hospital from randomization to day 90 (IQR)	76 (55 to 83)	76 (55 to 82)	0.0 (–2.7 to 2.7)
Days alive and out of the hospital to day 90, adjusted analysis‡	—	—	1.3 (–0.8 to 3.3)
Secondary outcomes			
Death by day 28 — no. (%)	62 (12.9)	48 (10.0)	1.29 (0.91 to 1.85)§
Death by day 90 — no./total no. (%)	79/481 (16.4)	69/479 (14.4)	1.14 (0.85 to 1.54)§
Time between randomization and death	—	—	1.17 (0.85 to 1.62)¶
Median no. of days alive and at home at day 90 (IQR)‖	76 (46 to 83)	76 (46 to 82)	0.8 (–1.9 to 3.5)**
No. of days free of organ support at day 28 (IQR)†††‡‡			
Vasopressor support	27 (26 to 28)	27 (26 to 28)	–0.2 (–0.5 to –0.1)**
Invasive ventilation	28 (28 to 28)	28 (28 to 28)	0.6 (–0.1 to 1.4)**
Renal replacement therapy	28 (28 to 28)	28 (28 to 28)	0.2 (–0.5 to 0.9)**
Tertiary outcomes			
Death in an intensive care unit — no./total no. (%)	32/370 (8.6)	28/333 (8.4)	
Death in a hospital, censored at 90 days — no./total no. (%)	60 (12.5)	46 (9.5)	1.31 (0.91 to 1.88)§
Use of organ support — no. (%)†††‡‡			
Vasopressor support	416 (86.5)	331 (68.7)	1.26 (1.18 to 1.35)§
Invasive ventilation	74 (15.4)	73 (15.1)	1.02 (0.76 to 1.37)§
Renal replacement therapy	30 (6.2)	25 (5.2)	1.20 (0.72 to 2.01)§
Time-to-event outcomes from randomization (IQR)§§			
First cessation of vasopressors — hr	22.4 (9.5 to 42.2)	30.1 (11.9 to 51.1)	1.25 (1.12 to 1.41)¶¶
First cessation of invasive ventilation — hr	45.4 (15.9 to 188.8)	67.9 (22.1 to 185.9)	1.14 (0.85 to 1.53)¶¶
First cessation of renal replacement therapy — hr	114.0 (45.2 to 274.0)	138.8 (80.5 to 302.3)	1.13 (0.69 to 1.87)¶¶
Time to emergency department discharge — hr	4.0 (2.4 to 6.5)	4.7 (2.9 to 8.2)	1.15 (0.99 to 1.34)¶¶
Time to intensive care unit discharge — hr	59.3 (35.3 to 94.2)	69.0 (42.0 to 117.4)	1.23 (1.06 to 1.43)¶¶
Time to hospital discharge — days	6.8 (3.7 to 12.9)	7.1 (4.1 to 13.9)	1.02 (0.89 to 1.18)¶¶

A Days Alive and out of the Hospital from Randomization to Day 90

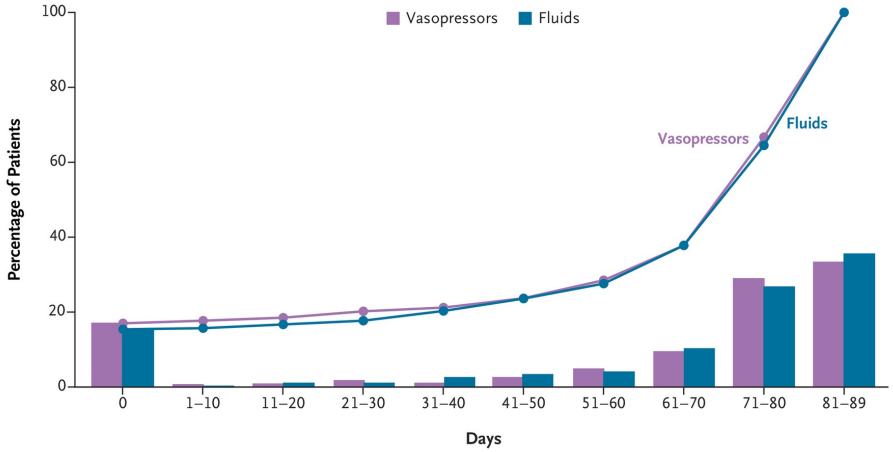

B Subgroup Analyses

Subgroup	Vasopressors	Fluids	Median Difference (95% CI)
	no. of patients with event/total no.		
All patients	481/481	479/482	–0.00 (–2.67 to 2.67)
Age			
<65 yr	207/481	201/479	–0.95 (–3.81 to 1.91)
≥65 yr	274/481	278/479	1.49 (–2.09 to 5.00)
Sex			
Male	281/481	300/479	0.26 (–3.99 to 4.52)
Female	200/481	179/479	–1.00 (–4.02 to 4.00)
Lactate			
<3 mmol/liter	196/481	211/479	1.13 (–1.69 to 3.94)
≥3 mmol/liter	285/481	268/479	–2.00 (–6.88 to 1.63)
Apache II			
<15	119/481	144/479	2.61 (–1.03 to 6.25)
≥15	362/481	335/479	–1.06 (–5.07 to 1.92)
IV fluids before randomization			
<1500 ml	240/481	236/479	0.06 (–3.08 to 3.21)
≥1500 ml	241/481	243/479	0.00 (–3.30 to 3.45)
Source of sepsis			
Respiratory	144/481	154/479	–1.60 (–8.32 to 4.05)
Urinary	112/481	121/479	0.71 (–2.00 to 4.22)
Other	225/481	204/479	0.85 (–3.08 to 5.85)

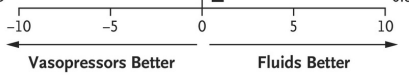

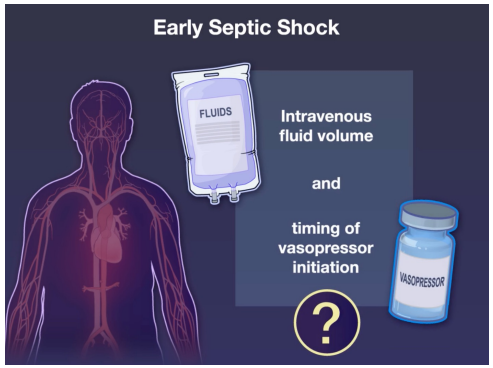

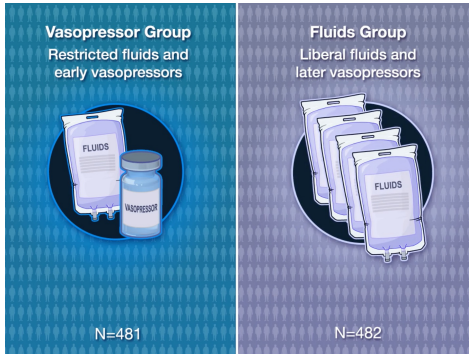

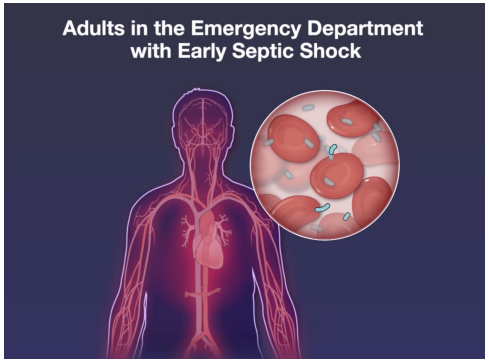

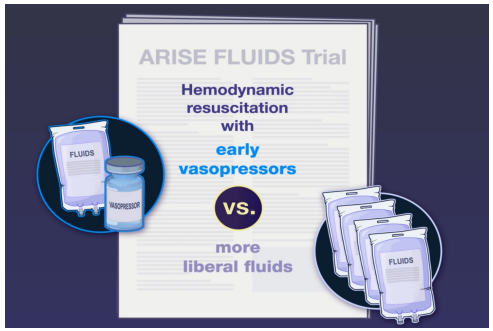

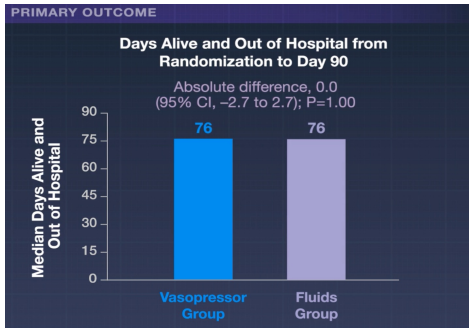

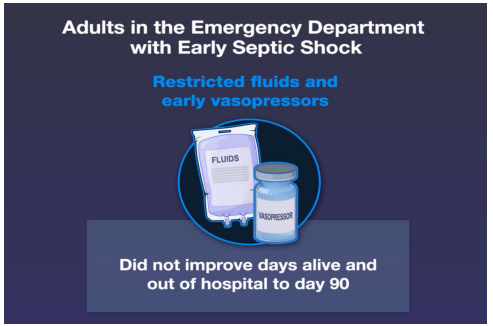

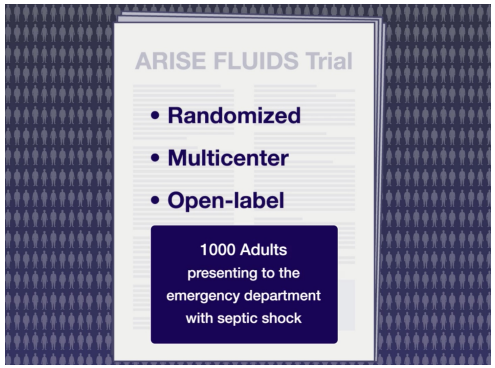

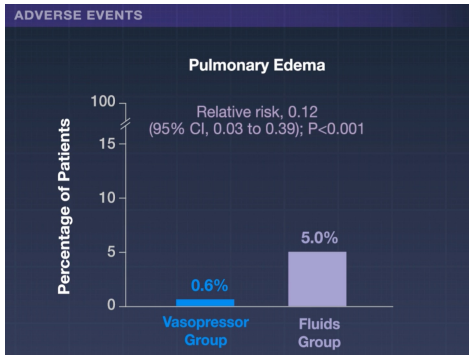

Albeit, the pulmonary edema rate was substantially reduced

Wie funktioniert Optogenetik?

Das Verfahren verbindet Methoden der Genetik und der Optik:

1. **Genetische Modifikation:** Forschende schleusen Fremdgene in bestimmte Zielzellen ein. Diese Gene stammen häufig von Mikroorganismen oder Algen (wie der Grünalge *Chlamydomonas reinhardtii*).

2. **Lichtempfindliche Proteine:** Die modifizierten Zellen bilden daraufhin lichtsensitive Ionenkanäle oder Pumpen (sogenannte Opsine) in ihrer Membran aus.

3. **Lichtsteuerung:**

    1. Bestrahlt man diese Zellen mit **blauem Licht**, öffnet sich beispielsweise das Protein *Channelrhodopsin-2*. Ionen strömen ein, und die Nervenzelle wird **aktiviert**.

    2. Andere Proteine wie *Halorhodopsin* reagieren auf **gelb-oranges Licht** und schleusen negative Ionen ein, was die Zelle **hemmt** bzw. ausschaltet.

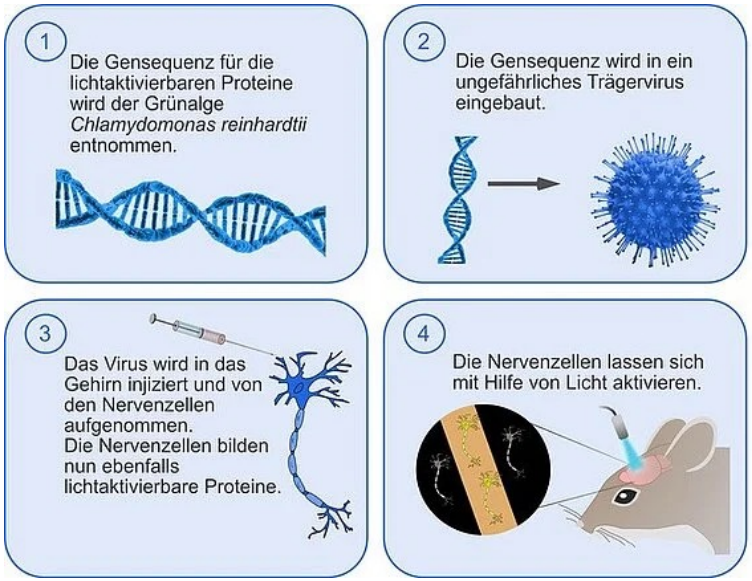

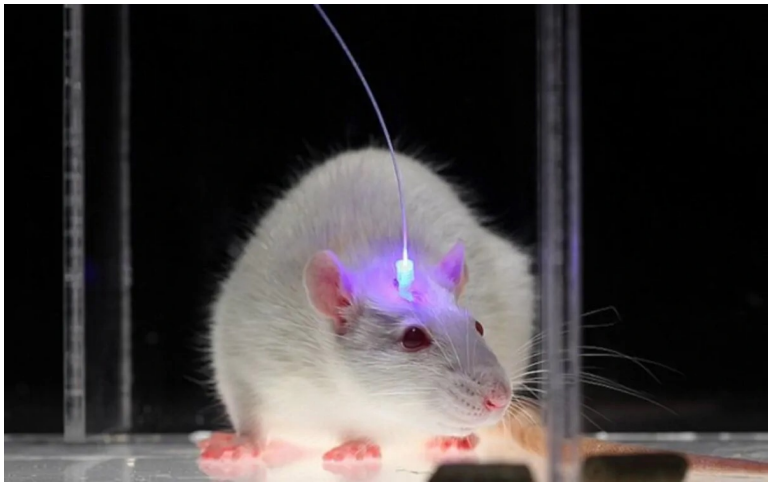

Optogenetics

Optogenetics, the precise control of genetically targeted cellular activity with light, has guided the investigation of cellular roles in living systems for more than two decades. In this approach, specific cells (e.g., specific types of neurons) are controlled (activated or inhibited) by inducing them to express a gene encoding a light-sensitive protein; this genetic targeting enables broad light exposure (e.g., to the whole tissue or organ) to exert specific direct effects on the targeted cells. The gene (for most discoveries so far) encodes a microbial light-gated ion channel called a channelrhodopsin that, as a single protein, offers versatile targeting across cells and species and is therefore useful in general for testing hypotheses in diverse biologic systems. Refinement of optogenetic specificity beyond generalizable genetic targeting strategies has resulted from increasing the precision of light delivery (the spatiotemporal shaping of light) through fiber optics, digital micromirrors, holographic spatial light modulators, and other strategies. Subsequent methods for genetically modifying cellular activity, such as with sound waves (sonogenetics) or pharmacology (chemogenetics), are based on the same principle as optogenetics: introduce a triggerable receptor to a specific type of cell, enabling more broad delivery of the trigger to exert cell-specific direct effects.

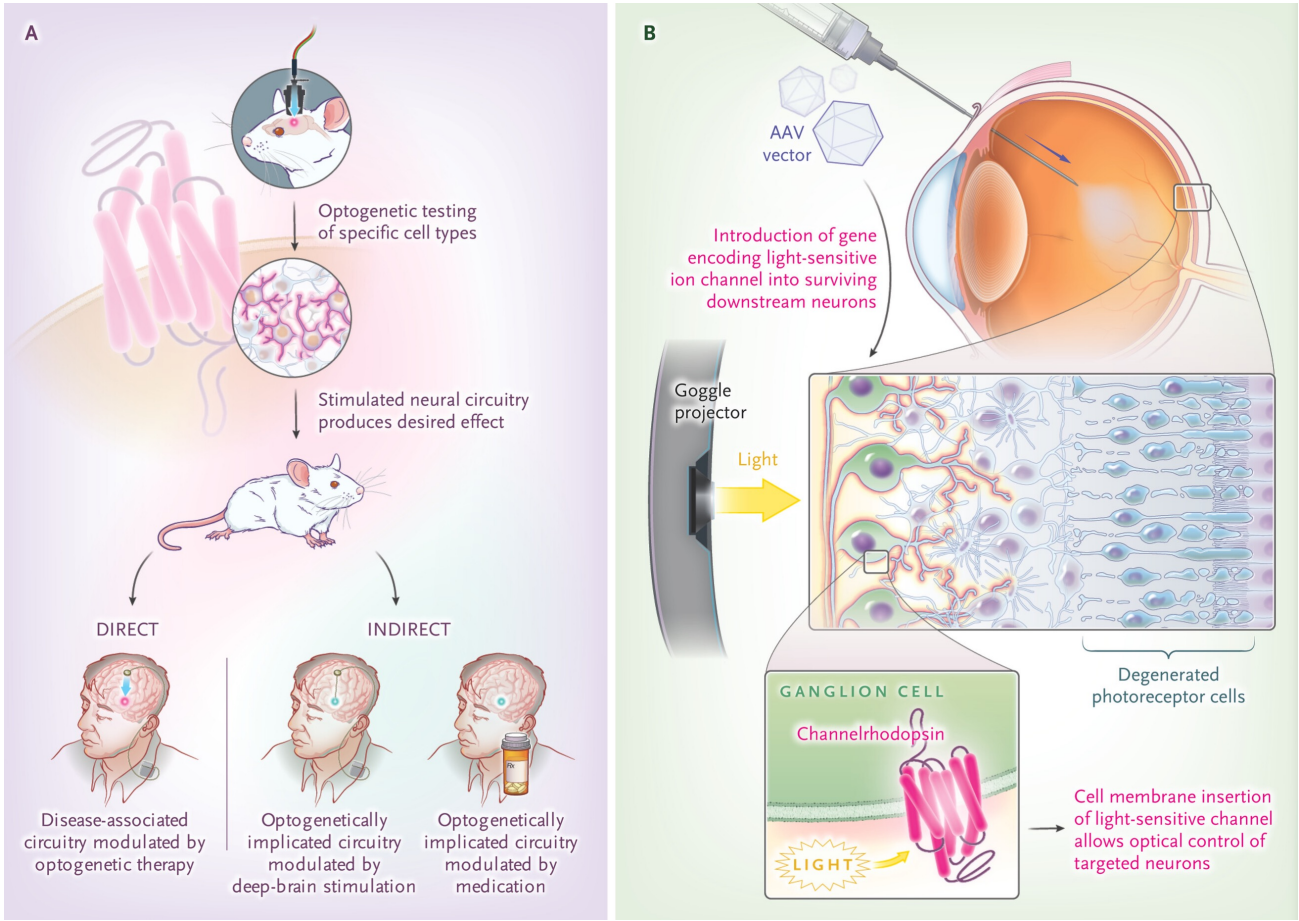

Direct and Indirect Translational Optogenetics Pathways.

Three translational optogenetics pathways are shown. Precise identification of causal cells and circuits allows principled targeting (Panel A), whether through direct (left), indirect neuromodulatory (middle), or indirect medicinal (right) approaches. Components of direct optogenetics for retinitis pigmentosa are shown (Panel B), including the adeno-associated virus (AAV) (top), the light-projecting goggles (middle), and the channelrhodopsin protein (bottom). Adapted from Lüscher et al.[7]

Optogenetics for Retinitis Pigmentosa?

The term retinitis pigmentosa describes a group of largely monogenic neurodegenerative diseases that progress to irreversible blindness owing to the loss of photoreceptor cells in the retina. Although a gene therapy for one form of retinitis pigmentosa (caused by loss-of-function variants in *RPE65*) has shown clinical benefit, more than 100 genes have been implicated as causal (when variant) of retinitis pigmentosa in the broader human population, and so the replacement (or editing) of a single gene would not help most persons with retinitis pigmentosa. Direct therapy with a single-component microbial opsin could offer a universal solution by providing targeted retinal light responsivity to surviving neurons that are downstream of the degenerating photoreceptors.

The high speed (millisecond scale) of channelrhodopsin gating is suitable for representing dynamic changes in visual input. However, the optogenetic approach bypasses the amplification and adaptation mechanisms operative in the early stages of retinal processing that normally allow robust human vision across light intensities that vary enormously — by orders of magnitude — in typical outdoor and indoor settings. Therefore, Sahel et al. replaced ambient light with a medical device: custom goggles that detect the natural visual scene and project a corresponding 595-nm light stimulus onto the target retina.

Optogenetic Therapy for Restoring Aspects of Visual Function

Background
Retinitis pigmentosa is an inherited degenerative retinal disease that can lead to irreversible blindness. Optogenetic therapy has shown potential for restoring visual function at late stages of the disease.
Methods
In this open-label study, we evaluated the safety of ganglion cell–directed optogenetic therapy in 10 participants with blindness due to advanced retinitis pigmentosa. Each participant received a single intravitreal injection of an adeno-associated viral (AAV) vector encoding the red-shifted channelrhodopsin ChrimsonR in the worse-seeing eye. The primary outcome was safety. Secondary outcomes included changes in light sensitivity as measured by full-field stimulus threshold (FST) testing conducted with the untreated eye patched and with the use of light-stimulating goggles designed to activate ChrimsonR. The definition of a clinically meaningful improvement in the FST (based on evidence from the literature and not prespecified in the protocol) was a decrease of at least 0.6 log units (i.e., an increase in light sensitivity by a factor of approximately 4).
Conclusions
Within the limits of this small study, intravitreal administration of a ChrimsonR-expressing AAV vector targeting retinal ganglion cells combined with use of light-stimulating goggles was safe. Additional research is needed to further assess safety and efficacy.

Retinitis pigmentosa is a clinically and genetically heterogeneous group of inherited, mostly monogenic, degenerative retinal diseases characterized by progressive photoreceptor loss that can lead to irreversible blindness. Variants in more than 100 genes result in retinitis pigmentosa, collectively affecting more than 1.5 million persons worldwide. Gene-augmentation therapy for an early-onset retinitis pigmentosa caused by variants in *RPE65* has shown clinical benefit. However, there is no approved treatment for most persons with retinitis pigmentosa.

Optogenetic vision restoration aims to restore retinal responsiveness to light in persons with blindness by introducing genes encoding light-sensitive proteins into surviving neurons. The effectiveness of this treatment should therefore be independent of the specific genetic cause.

One such approach involves the intravitreal delivery of an adeno-associated viral (AAV) vector (serotype AAV2.7m8) that expresses ChrimsonR–tdTomato (GS030-Drug Product [GS030-DP]) under the control of the CAG promoter. The red-shifted channelrhodopsin ChrimsonR is a light-sensitive nonselective cation channel, with peak activation at approximately 590 nm (amber light). The protein tdTomato is added as a fusion protein to enhance the membrane localization of ChrimsonR.

A first-in-human proof-of-concept study of this optogenetic system showed partial recovery of vision in a single participant with end-stage retinitis pigmentosa.[11] Here, we report results of the multicenter, open-label, dose-escalation PIONEER study (Dose-Escalation Study to Evaluate the Safety and Tolerability of GS030 in Subjects with Retinitis Pigmentosa), in which 10 participants with legal blindness due to retinitis pigmentosa received an injection of the optogenetic vector GS030-DP in their worse-seeing eye and underwent vision testing with GS030-MD light-stimulating goggles before and after the injection.

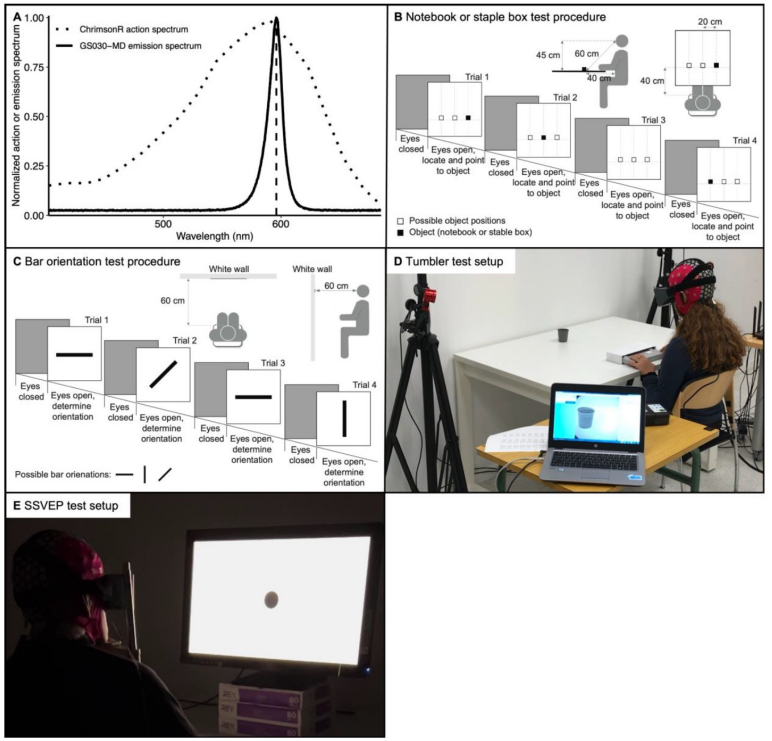

Panel A: Action spectrum of ChrimsonR (according to Klapoetke et al. 201410) and emission spectrum of the GS030-MD light-stimulating goggles. Panel B: The procedure for performing the notebook or staple box test. Panel C: The procedure for performing the bar orientation test. Panel D: EEG recording during the tumbler detection task. Panel E: EEG recording during the SSVEP test.

Baseline characteristics

Participant	Dose Group	Sex	Age at Diagnosis	Age at Injection	Inheritance of Retinitis Pigmentosa	Treated Eye	Baseline BCVA	No. of Training Sessions
			years					
L1	Low dose	M	18	58	Autosomal recessive	Right	Light perception	36
L2	Low dose	M	7	52	Autosomal dominant	Right	Light perception	12
L3	Low dose	F	18	61	X-linked	Right	Light perception	14
M1	Medium dose	F	39	68	Autosomal recessive (Bardet–Biedl syndrome)	Right	Light perception	57
M2	Medium dose	F	31	50	Not identified	Left	No light perception	22
M3	Medium dose	M	15	44	X-linked	Right	Light perception	0
H1	High dose	F	23	40	Autosomal recessive, autosomal dominant, autosomal recessive cone–rod dystrophy	Right	Light perception	24
H2	High dose	F	17	42	Autosomal recessive	Right	Light perception	35
H3	High dose	M	33	73	X-linked	Left	No light perception	18
H4	High dose	F	32	60	Autosomal recessive	Right	Hand motion	13

Safety Assessments.

Panel A shows intraocular pressure over the course of the study. Panel B shows slit-lamp findings. For anterior chamber (AC) cells and vitreous cells, higher grades indicate higher numbers of visible inflammatory cells; for AC flare, higher grades indicate greater amounts of protein due to inflammation. Grades range from 0 to 4+. Panel C shows central field thickness of the macula as measured by optical coherence tomography (OCT). Panel D shows cellular reactivity to AAV2.7m8 (AAV2), ChrimsonR (ChR), and tdTomato (tdT) as measured in enzyme-linked immunospot (ELISpot) assays. Participants L1 through L3 received 5.0×10^{10} vector genomes per eye, Participants M1 through M3 1.5×10^{11} vector genomes per eye, and Participants H1 through H4 5.0×10^{11} vector genomes per eye.

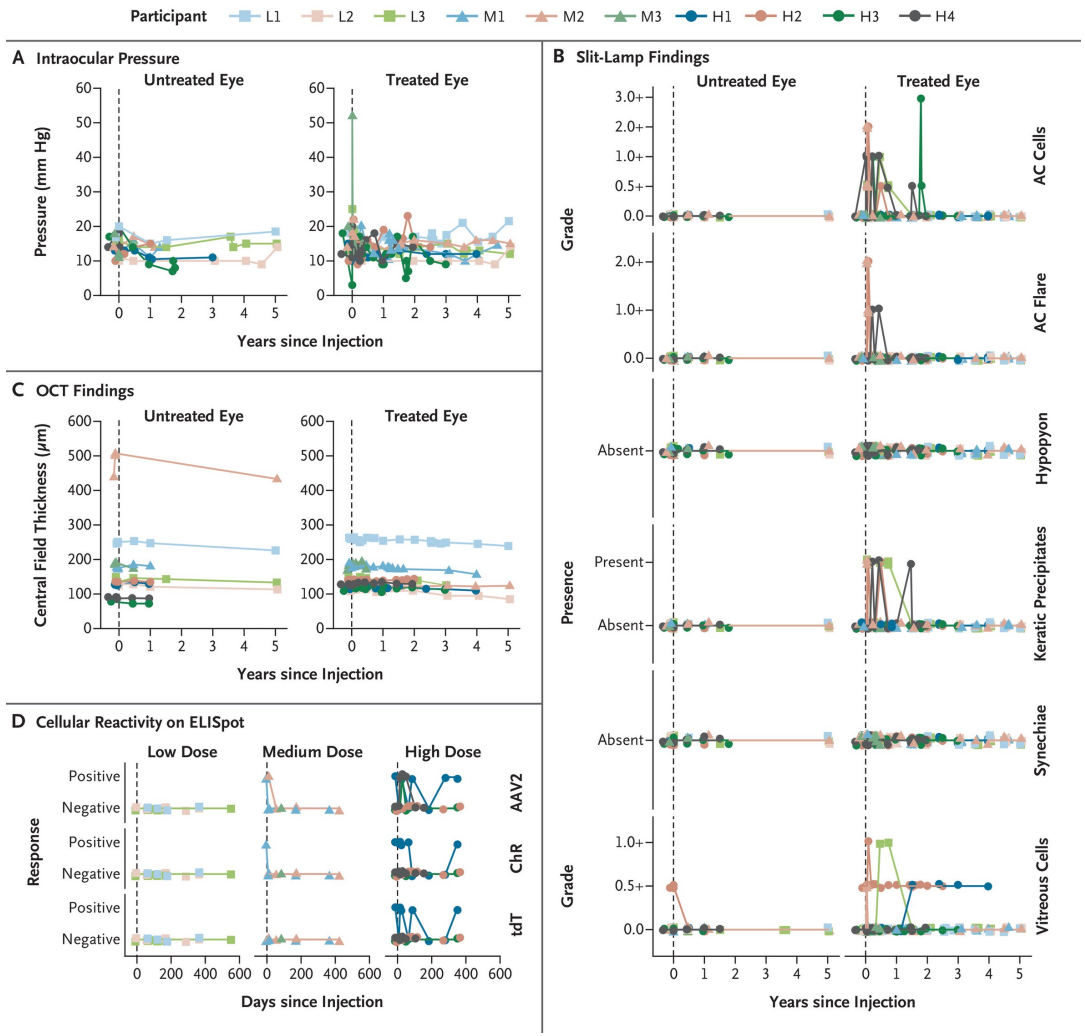

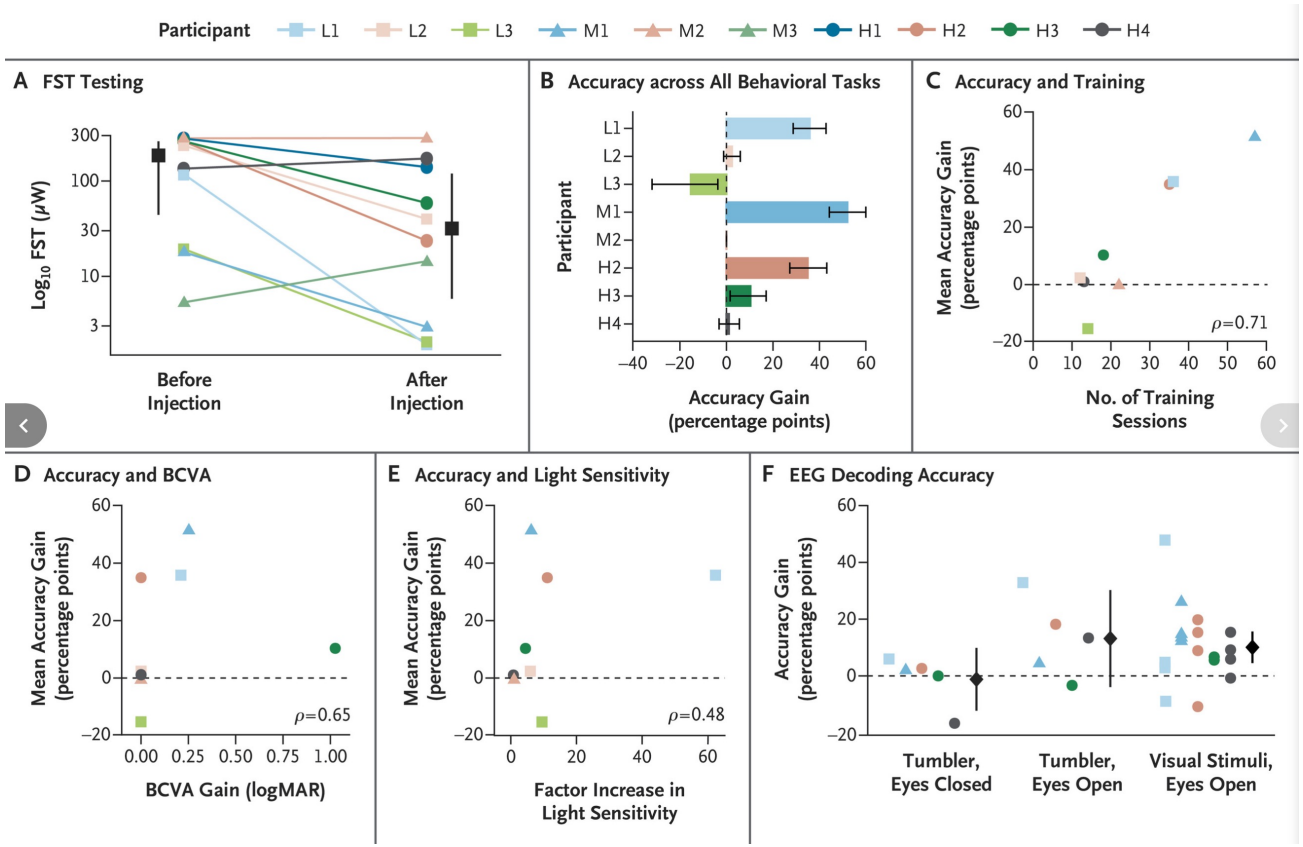

Patients treated with optogenetic therapy for retinitis pigmentosa in the New England Journal of Medicine trial do not experience traditional high-resolution sight, but they perceive more than random light flashes. Instead, they detect functional visual boundaries, shapes, and high-contrast outlines that enable real-world object localization.

Visual Function Assessments.

Panel A shows minimum $\log_{10}$-transformed goggle-based full-field stimulus threshold (FST) values before and after vector administration; colored data points are participant-level medians before and after injection. Group-level medians and interquartile ranges are indicated by black squares with vertical error bars. A decrease in the FST reflects an increase in light sensitivity. Panel B shows mean changes in accuracy across all behavioral tasks (notebook, staple box, and bar) for each participant; error bars indicate bootstrapped 95% confidence intervals. Panels C, D, and E show Spearman's coefficients (ρ) for the correlation between mean changes in behavioral accuracy and selected variables: the number of training sessions completed (Panel C), the change in best corrected visual acuity (BCVA; converted to logMAR [logarithm of the minimum angle of resolution]) without goggles after treatment (Panel D), and the factor increase in light sensitivity (Panel E). A clinically meaningful improvement in the FST was defined as a decrease of at least 0.6 log units (i.e., an increase in light sensitivity by a factor of approximately 4). Panel F shows changes in electroencephalographic (EEG) decoding accuracy, including detection of object presence (tumbler) with eyes open or closed and decoding of visual stimuli during steady-state visually evoked potential (SSVEP) testing; group results are shown as mean differences with 95% confidence intervals (black diamonds with error bars). All results are descriptive; confidence intervals have not been adjusted for multiplicity and cannot be used to infer treatment effects.

Discussion

Within the limits of this small study, intravitreal administration of a ChrimsonR-expressing AAV vector targeting retinal ganglion cells in combination with the use of light-stimulating goggles was safe. Intraocular inflammation occurred in 7 of 10 participants, was more common in the high-dose group, and manifested primarily as inflammation in the anterior chamber. The inflammatory events resolved with standard treatment and without sequelae and were consistent with such events in previous studies of intravitreal AAV administration.

Four of the participants who underwent visual behavioral testing had partial restoration of visual function, including the participant in our previous report (Participant L1). In vivo visualization of ChrimsonR–tdTomato expression for mapping transduced regions and optimizing device alignment was not achievable with currently approved clinical imaging devices, which are insufficiently sensitive to detect tdTomato in the retina. However, the changes in light sensitivity in the treated eyes of 7 of the 10 participants were consistent with the expression of the optogenetic sensor in the retinas of these 7 participants.

Brustkrebs

Advances in Systemic Treatment of Breast Cancer

Summary

Systemic therapy for breast cancer has evolved rapidly since 2020, driven by the expansion of targeted therapies, antibody–drug conjugates, and immunotherapy across biologic subtypes. The integration of tumor molecular profiling and germline testing has enabled increasingly personalized, biomarker-guided treatment strategies. In hormone-receptor–(ER)positive, human epidermal growth factor receptor 2 (HER2)–negative disease, cyclin-dependent kinase 4 and 6 inhibitors remain foundational, whereas phosphatidylinositol 3-kinase pathway inhibitors, oral selective estrogen-receptor degraders, and antibody–drug conjugates have transformed disease management after endocrine resistance. In HER2-positive disease, antibody–drug conjugates — particularly trastuzumab deruxtecan — have improved outcomes and are being used in earlier lines of therapy, a development that is reshaping treatment paradigms. In triple-negative breast cancer, immune checkpoint inhibitors have improved outcomes in both metastatic and early-stage disease. Across subtypes, advances in curative therapy increasingly emphasize risk-adapted escalation and de-escalation of treatment. Ongoing challenges include improving treatment sequencing, identifying predictive biomarkers, integrating emerging tools such as analysis of circulating tumor DNA, and ensuring equitable access to high-cost therapies.

The management of breast cancer — the most commonly diagnosed cancer and the second leading cause of cancer-related death among women in the United States annually — has changed substantially during the past two decades, with improved survival largely attributed to advances in systemic treatment. Since 2020, a total of 17 targeted therapies have been approved or granted additional indications, including one monoclonal antibody, three antibody–drug conjugates, one immune checkpoint inhibitor, three phosphatidylinositol 3-kinase (PI3K)–AKT–mammalian target of rapamycin (mTOR) pathway inhibitors, four oral selective estrogen-receptor degraders (SERDs), one human epidermal growth factor receptor 2 (HER2)–selective tyrosine kinase inhibitor, one poly(ADP-ribose) polymerase (PARP) inhibitor, and three cyclin-dependent kinase 4 and 6 (CDK4/6) inhibitors. In parallel, diagnostic and prognostic evaluation has become increasingly integrated into treatment decision making. Tumor molecular profiling now routinely extends beyond determining hormone-receptor (HR) and HER2 status and is complemented by broader germline genetic testing, which enables biomarker-guided, personalized treatment strategies. Efforts are increasingly focused on tailoring therapy to individual patients without compromising outcomes. Against this backdrop, this review summarizes advances in systemic therapy for breast cancer since 2020 and is organized according to the three major clinical subtypes, which are defined by HR expression and HER2 status.

Drug and Approval Date	Type of Therapy	Indication	Supporting Trial
Margetuximab	HER2 MAb		
December 2020		HER2-positive metastatic breast cancer, in combination with chemotherapy during third line or later	SOPHIA[3]
Trastuzumab deruxtecan	HER2 ADC		
December 2019†		HER2-positive metastatic breast cancer, third line or later	DESTINY-Breast01[4]
May 2022		HER2-positive metastatic breast cancer, second line or later	DESTINY-Breast03[5]
August 2022		HER2-low metastatic breast cancer	DESTINY-Breast04[6]
January 2025		HR-positive, HER2-low or HER2–ultra-low metastatic breast cancer	DESTINY-Breast06[7]
December 2025		HER2-positive metastatic breast cancer, first line	DESTINY-Breast09[8]
June 2026		HER2-positive stage II or III breast cancer, neoadjuvant for four cycles followed by taxane, trastuzumab, and pertuzumab	DESTINY-Breast11[9]
June 2026		HER2-positive residual disease after neoadjuvant treatment with trastuzumab (with or without pertuzumab) and taxane-based therapy	DESTINY-Breast05[10]
Sacituzumab govitecan	Trop-2 ADC		
April 2020†		TNBC after 2 systemic therapies, at least 1 line for metastatic breast cancer	ASCENT[11]
February 2023		HR-positive, HER2-negative after endocrine therapy and ≥2 lines	TROPiCS-02[12]
June 2026		Metastatic TNBC, first line when not a candidate for immune checkpoint inhibitor	ASCENT-03[13]
June 2026		Metastatic TNBC, first-line, PD-L1 (CPS ≥10) in combination with pembrolizumab	ASCENT-04/KEYNOTE-D19[14]
Datopotamab deruxtecan	Trop-2 ADC		
January 2025		HR-positive, HER2-negative after endocrine therapy and chemotherapy for metastatic breast cancer	TROPION-Breast01[15]
May 2026		Metastatic TNBC, first line when not a candidate for immune checkpoint inhibitor	TROPION-Breast02[16]
Pembrolizumab	PD-1 ICI		
November 2020†		Metastatic TNBC, PD-L1 (CPS ≥10), first line, in combination with chemotherapy	KEYNOTE-355[17]
July 2021		High-risk TNBC, neoadjuvant with chemotherapy, then adjuvant single agent	KEYNOTE-522[18,19]
Capivasertib	AKT inhibitor		
November 2023		In combination with fulvestrant for HR-positive, HER2-negative disease with *PIK3CA*, *AKT1*, or *PTEN* alteration	CAPItello-291[20]
Inavolisib	PI3Kα inhibitor		
October 2024		In combination with fulvestrant and palbociclib in *PIK3CA*-mutated, HR-positive, HER2-negative metastatic breast cancer, first line, endocrine resistant after adjuvant endocrine therapy	INAVO120[21]
Elacestrant	Oral SERD		
January 2023		HR-positive, HER2-negative *ESR1*-mutated metastatic breast cancer after ≥1 line of endocrine therapy	EMERALD[22]
Imlunestrant	Oral SERD		
September 2025		HR-positive, HER2-negative *ESR1*-mutated metastatic breast cancer after ≥1 line of endocrine therapy	EMBER-3[23]
Tucatinib	HER2 TKI		
April 2020		In combination with trastuzumab and capecitabine for HER2-positive metastatic breast cancer after >1 line of anti-HER2 therapies	HER2CLIMB[24]
Abemaciclib	CDK4/6 inhibitor		
October 2021‡		In combination with endocrine therapy for adjuvant HR-positive, HER2-negative, node-positive, early, high-risk disease	monarchE[25]
Ribociclib	CDK4/6 inhibitor		
September 2024‡		In combination with an aromatase inhibitor as adjuvant therapy for HR-positive, HER2-negative, high-risk, stage II or III breast cancer	NATALEE[26]
Olaparib	PARP inhibitor		
March 2022‡		High-risk, early-stage, HER2-negative breast cancer with deleterious germline *BRCA1* or *BRCA2* after chemotherapy	OlympiA[27]
Vepdegestrant	Oral SERD		
May 2026		HR-positive, HER2-negative, *ESR1*-mutated metastatic breast cancer after ≥1 line of endocrine therapy	VERITAC-2[28]
Camizestrant			
September 2026†	Oral SERD	HR-positive, HER2-negative, in combination with CDK4/6 inhibitor on detection of *ESR1* mutation during aromatase inhibitor and CDK4/6 inhibitor therapy	SERENA-6[29]
Gedatolisib	Inhibitor of 4 class I isoforms of PI3K, mTORC1, and mTORC2		
July 2026		HR-positive, HER2-negative metastatic breast cancer without a *PIK3CA* mutation; in combination with fulvestrant with or without palbociclib after ≥1 line of endocrine therapy in metastatic disease	VIKTORIA-1[30]
Palbociclib	CDK4/6 inhibitor		
June 2026		HER2-positive, HR-positive metastatic breast cancer in combination with trastuzumab, with or without pertuzumab, and endocrine therapy as maintenance treatment after induction treatment	PATINA[31]

Biomarker-Guided Treatment Options for Breast Cancer Independent of HR and HER2 Expression.

Biomarker Target	Variant or Mutation	Frequency of Biomarker Expression or Mutation	Drug Mechanism of Action	Available Drug or Drugs and Indication
PD-1 expression	Somatic	40%†	Antibody immune checkpoint inhibitor	Pembrolizumab (IV, combined with chemotherapy): metastatic, triple-negative, PD-L1–positive
PIK3CA activating mutation	Somatic	Approximately 30–40%	PI3K inhibitor	Alpelisib (oral, combined with fulvestrant): metastatic, HR-positive and HER2-negative, *PIK3CA* mutation Inavolisib (oral, combined with fulvestrant, palbociclib): metastatic, HR-positive and HER2-negative, *PIK3CA* mutation
PIK3CA activating mutation, *AKT1* activating mutation, or *PTEN* inactivating mutation or deletion	Somatic	Approximately 40%	AKT inhibitor	Capivasertib (oral, combined with fulvestrant): metastatic, HR-positive and HER2-negative, PI3K pathway alteration
ESR1 mutation	Somatic	40%‡	Selective estrogen-receptor degrader	Camizestrant (oral): HR-positive and HER2-negative, in combination with CDK4/6 inhibitor on detection of *ESR1* mutation during aromatase inhibitor and CDK4/6 inhibitor therapy Elacestrant (oral), imlunestrant (oral), and vepdegestrant (oral): metastatic, HR-positive and HER2-negative, *ESR1* mutation
BRCA1 or *BRCA2* mutation	Germline	Approximately 10%	PARP inhibitor	Olaparib (oral): metastatic or adjuvant high-risk, HER2-negative, *BRCA1* or *BRCA2* mutation Talazoparib (oral): metastatic, HER2-negative, *BRCA1 or BRCA2* mutation
PALB2 mutation	Germline	<5%	PARP inhibitor	Olaparib (oral, not approved): metastatic[33]
BRCA1 or *BRCA2* mutation	Somatic	<5%	PARP inhibitor	Olaparib (oral, not approved): metastatic[33]
NTRK1, -2, or *-3* gene fusion	Somatic	<1%	Inhibitor of TRKA,TRKB, and TRKC	Entrectinib, larotrectinib, and repotrectinib: metastatic disease with no alternative standard options available
Microsatellite instability–high or dMMR		<5%	Antibody immune checkpoint inhibitor	Pembrolizumab (IV) and dostarlimab (IV): metastatic disease with no alternative standard options available
High tumor mutational burden		<5%‡	Antibody immune checkpoint inhibitor	Pembrolizuamb (IV): metastatic disease with no alternative standard options available
RET gene fusion	Somatic	<1%	RET protein tyrosine kinase inhibitor	Selpercartinib (oral): metastatic disease with no alternative standard options available
HER2 (*ERBB2*) activating mutation	Somatic	<5%	HER2-targeted tyrosine kinase inhibitor	Neratinib (oral, not approved, combined with fulvestrant plus trastuzumab): metastatic[34] Tucatinib (oral, not approved, combined with trastuzumab with or without fulvestrant): metastatic[35]
FGFR1, -2, or *-3* mutation		<2%	Fibroblast growth factor receptor 1–4 tyrosine kinase inhibitor	Erdafitinib (oral, not approved): metastatic[36]

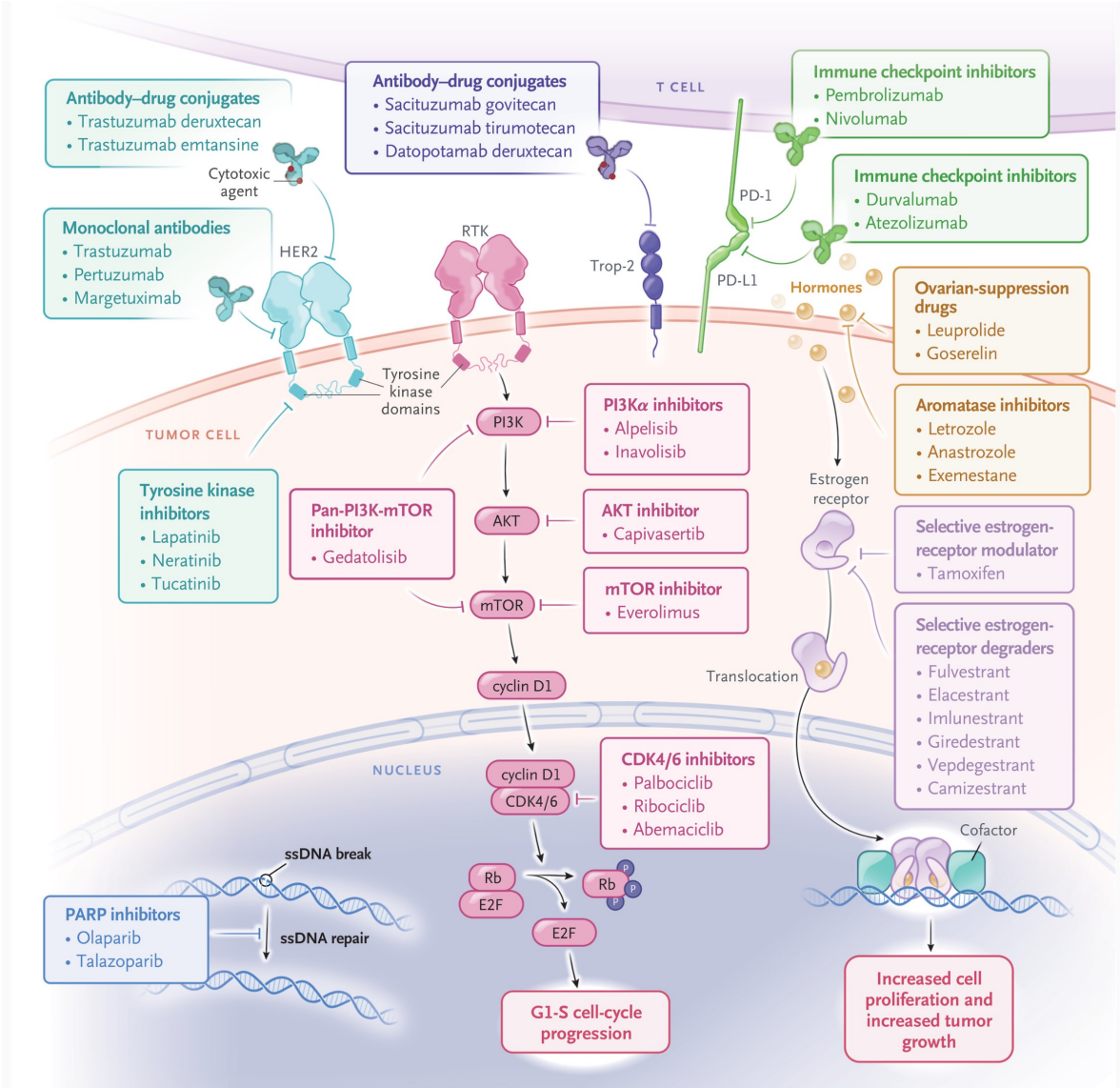

Mechanism of Action of Currently Available Targeted Therapies for Breast Cancer, Excluding Biosimilars and Reformulations.

Atezolizumab, durvalumab, giredestrant, nivolumab, and sacituzumab tirumotecan are not yet approved by the Food and Drug Administration. CDK4/6 denotes cyclin-dependent kinase 4 and 6, HER2 human epidermal growth factor receptor 2, mTOR mammalian target of rapamycin, PARP poly(ADP-ribose) polymerase, PD-1 programmed cell death protein 1, PD-L1 programmed death ligand 1, PI3K phosphatidylinositol 3-kinase, RTK receptor tyrosine kinase, ssDNA single-stranded DNA, and Trop-2 trophoblast cell-surface antigen 2.

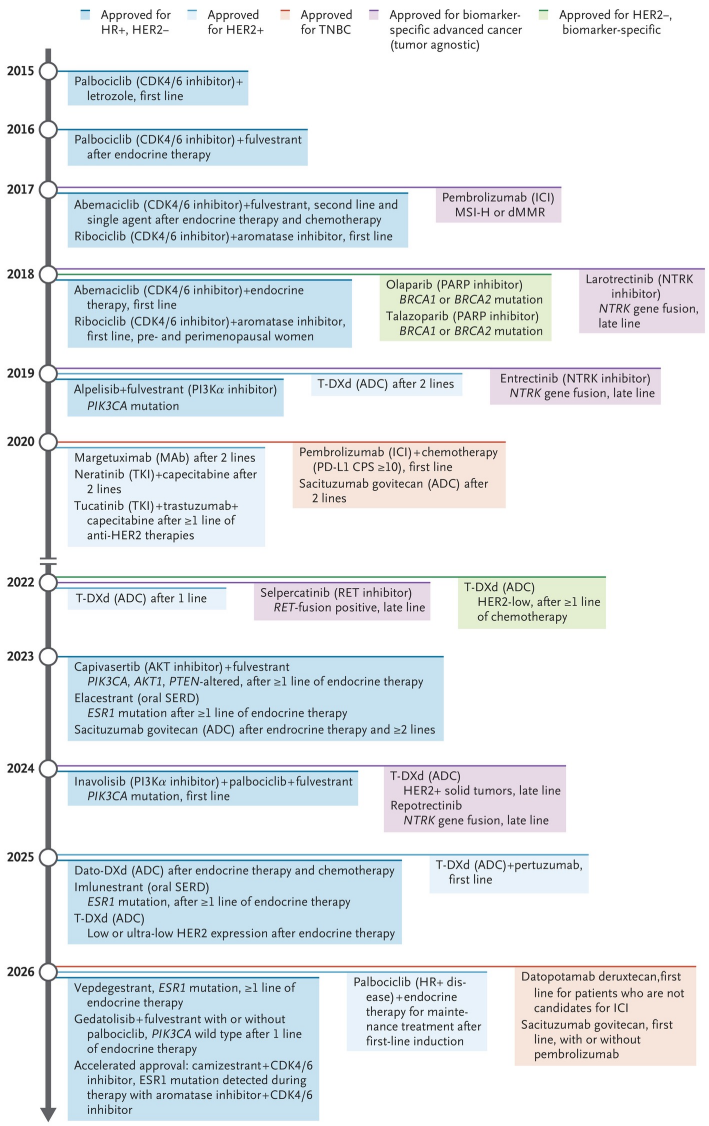

Timeline of Regulatory Approvals for Metastatic Breast Cancer since 2015.

ADC denotes antibody–drug conjugate, CPS combined positive score (the number of PD-L1–staining tumor cells, lymphocytes, and macrophages divided by the total number of viable tumor cells, multiplied by 100), Dato-DXd datopotamab deruxtecan, dMMR mismatch-repair–deficient, HR hormone receptor, ICI immune checkpoint inhibitor, MAb monoclonal antibody, MSI-H microsatellite-instability–high, SERD selective estrogen-receptor degrader, T-DXd trastuzumab deruxtecan, TKI tyrosine kinase inhibitor, and TNBC triple-negative breast cancer.

Timeline of Regulatory Approvals for Early Breast Cancer since 2015.

T-DM1 denotes trastuzumab emtansine.

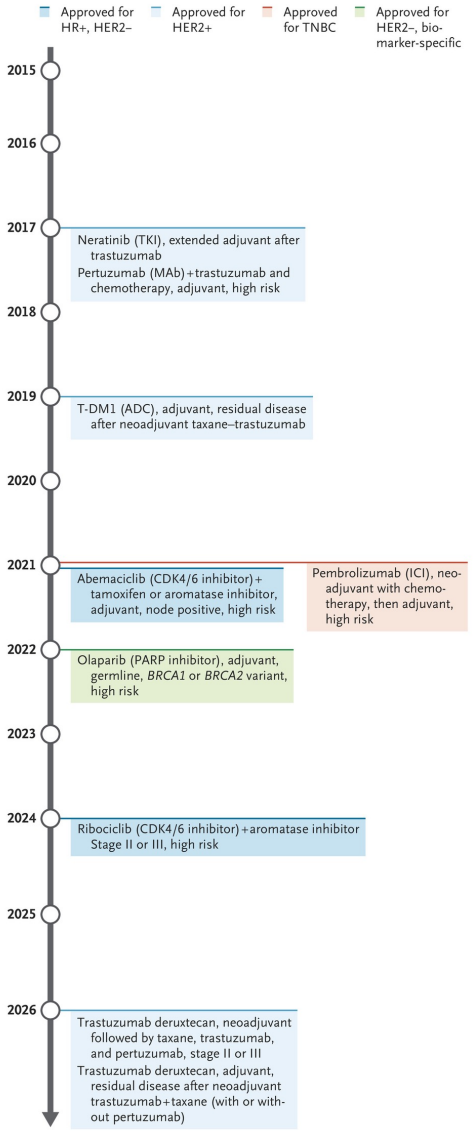

HR-Positive, HER2-Negative Breast Cancer Metastatic Disease

Approximately 70% of breast cancers are HR-positive, with normal expression of HER2 (HER2-negative). For many years, advances were incremental and largely limited to sequential endocrine therapies, including tamoxifen, aromatase inhibitors (anastrozole, letrozole, or exemestane), and fulvestrant, an intramuscularly delivered SERD. Although the approval of the mTOR inhibitor everolimus in combination with endocrine therapy marked a milestone event in 2012 for patients whose disease progressed after endocrine therapy, overall survival was not significantly improved, and patients were generally treated with chemotherapy by the third line.

KEY POINTS

Advances in Systemic Treatment of Breast Cancer

- Systemic therapy for breast cancer has advanced rapidly since 2020, with 17 targeted therapies approved or expanded across the major biologic subtypes.
- Integration of tumor molecular profiling and broader germline testing increasingly guides treatment selection and enables more personalized care.
- In hormone-receptor–positive disease, cyclin-dependent kinase 4 and 6 inhibitors remain foundational therapy, whereas phosphatidylinositol 3-kinase pathway inhibitors, oral selective estrogen-receptor degraders, and antibody–drug conjugates have expanded options after endocrine resistance.
- In human epidermal growth factor receptor 2–positive breast cancer, antibody–drug conjugates — particularly trastuzumab deruxtecan — have substantially improved outcomes and are being used earlier in treatment algorithms.
- In triple-negative breast cancer, immune checkpoint inhibitors have improved outcomes in early- and late-stage disease, whereas antibody–drug conjugates have improved survival in advanced disease but are still under investigation as a curative treatment.
- Ongoing challenges include improving the sequence of treatment, identifying predictive biomarkers, reducing disparities in access to standard therapies as well as newly approved and promising investigational therapies, and integrating emerging tools such as analysis of circulating tumor DNA into clinical decision making.

HER2-Positive Breast Cancer

Recognition of HER2 amplification — which is present in approximately 15 to 20% of breast cancers — as a key oncogenic driver, coupled with the development of HER2-targeted therapies, transformed a disease subtype with a historically poor prognosis into one with outcomes that are among the most favorable for breast cancer. Currently, eight HER2-targeted therapies are approved by the FDA (three monoclonal antibodies, three oral tyrosine kinase inhibitors, and two antibody–drug conjugates), with additional agents in advanced stages of clinical development.

Metastatic HER2-Positive Breast Cancer

Since the findings of the Clinical Evaluation of Pertuzumab and Trastuzumab (CLEOPATRA) trial in 2012, the THP regimen — induction taxane chemotherapy combined with the HER2-directed monoclonal antibodies trastuzumab and pertuzumab, followed by maintenance trastuzumab and pertuzumab until disease progression — has defined first-line therapy for HER2-positive metastatic breast cancer.

Triple-Negative Breast Cancer

Approximately 15% of all breast cancers lack expression of HRs and do not overexpress HER2, which defines triple-negative breast cancer — a subtype for which established targeted therapeutics are absent. Progress in managing this aggressive and molecularly heterogeneous subtype has historically been slow, and outcomes remain poorer than those observed in other breast cancer subtypes. During the past 5 years, however, glimmers of hope have emerged with respect to both metastatic disease and curative treatment.

Conclusion

The treatment of breast cancer has entered an era of unprecedented therapeutic expansion. Across all major subtypes, targeted therapies, antibody–drug conjugates, and immunotherapy have reshaped treatment algorithms and extended survival in the context of both metastatic disease and curative treatment. Increasingly, treatment decisions are guided not only by tumor subtype but also by molecular alterations and individual risk, which reflects a broader shift toward biologically informed, personalized care. As these advances continue to move earlier in the disease course, clinicians are increasingly tasked with balancing therapeutic intensity with considerations of long-term toxic effects, quality of life, and survivorship. The challenge ahead will be to translate this rapidly evolving evidence base into treatment strategies that are both effective and sustainable, ensuring that the expanding armamentarium of therapies meaningfully improves outcomes for patients across the spectrum of breast cancer.

Menkes Disease

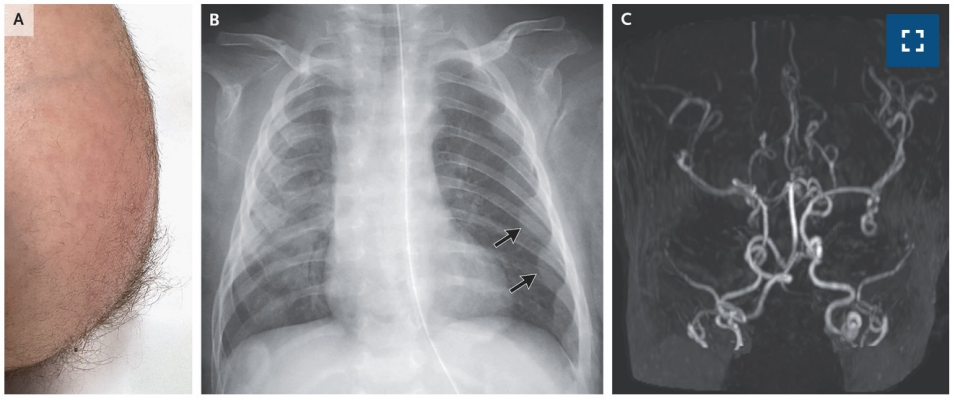

A 2-month-old boy who had been born late preterm was brought to the emergency department after a seizure. He had previously been hospitalized at 16 days of age for feeding difficulty, micrognathia, and hypotonia. Results of exome sequencing were pending at the time of discharge. There was no family history of genetic conditions. Physical examination during the current presentation was notable for decreased activity and shallow breathing. There was sparse, coarse, lightly pigmented hair on the scalp (Panel A). A chest radiograph showed flaring and expansion of the anterior rib ends (Panel B, arrows). Levels of serum copper and ceruloplasmin were markedly lower than normal. Magnetic resonance angiography of the brain revealed tortuosity and elongation of the intracranial and extracranial arteries (Panel C). Results of the previously ordered exome sequencing showed a hemizygous pathogenic variant in *ATP7A*. A diagnosis of Menkes disease was made. Menkes disease is an X-linked recessive neurodegenerative disorder of copper metabolism caused by deficiency or dysfunction of a copper-transporting ATPase. It manifests as developmental delay, seizures, kinky hair, bony abnormalities, and cerebral vessels that have a corkscrew appearance on imaging. Given the poor prognosis and lack of approved disease-specific therapy in Taiwan, the patient's family chose to pursue palliative care. The baby died at 5 months of age.

Syphilitic Chancre on the Nipple

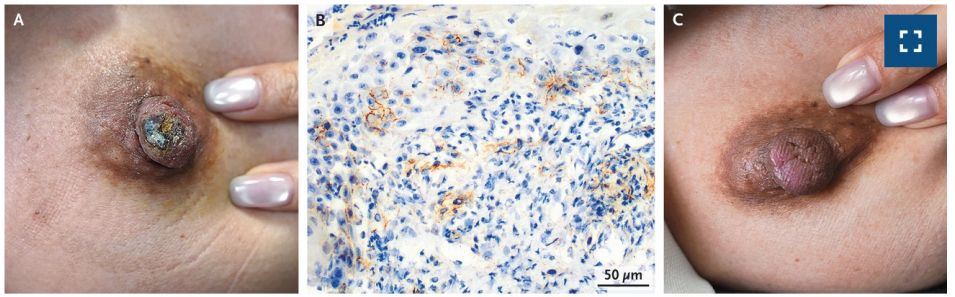

A 35-year-old woman presented to the hospital with a 20-day history of a painless nipple ulcer. On physical examination, there was ulceration, crusting, and a yellowish exudate on the right nipple (Panel A, which shows the patient's hand identifying the site). Erosive adenomatosis was initially suspected, and a skin biopsy was planned to establish the diagnosis and rule out cancer. As part of the hospital's routine preprocedural evaluation, testing for syphilis was performed. An assay for *Treponema pallidum* particle agglutination was positive, and the rapid plasma reagin titer was 1:8. The patient had no history of syphilis. Testing for human immunodeficiency virus infection was negative. Histopathological analysis of the nipple-biopsy specimen showed epidermal necrosis with an inflammatory exudate, dermal capillary proliferation, and dense perivascular lymphoplasmacytic infiltrates. Immunohistochemical analysis was positive for *T. pallidum* organisms (Panel B, shown at 400× magnification). A diagnosis of a syphilitic chancre of the nipple was made. Primary syphilitic chancres can occur at any site of inoculation (including extragenital erogenous locations) and should be considered in the differential diagnosis of an unexplained ulcerative lesion. Treatment with intramuscular benzathine penicillin G was given. At follow up 12 days after the initial diagnosis, the lesion had resolved (Panel C).

Die Kikuchi-Fujimoto-Krankheit (auch histiozytär nekrotisierende Lymphadenitis genannt) ist eine seltene, gutartige und meist selbstlimitierende Erkrankung, die durch schmerzhafte Lymphknotenschwellungen gekennzeichnet ist.

Symptome

- **Lymphknoten:** Schmerzhafte oder druckempfindliche Schwellungen am Hals (zervikal) in etwa 80 % der Fälle.
- **Allgemeinsymptome:** Leichtes Fieber, Müdigkeit (Fatigue), Nachtschweiß und Muskelschmerzen (Myalgien).
- **Selten:** Hautausschlag oder Gelenkschmerzen.

Ursachen

Die genaue Ursache ist bis heute **unbekannt**. Es wird vermutet, dass es sich um eine überschießende Immunreaktion des Körpers handelt. Als Auslöser werden virale Infektionen (wie Epstein-Barr-Virus) oder Autoimmunprozesse diskutiert. Die Erkrankung betrifft vor allem junge Erwachsene unter 40 Jahren, besonders Frauen.

Case 28-2026: A 19-Year-Old Woman with Fever, Cervical Lymphadenopathy, and Leukopenia

A 19-year-old woman presented to the pediatric emergency department of this hospital because of fever and tender cervical lymphadenopathy. The patient had been in her usual state of good health until 3 weeks before the current presentation, when painful cervical swelling developed on both sides of the neck, which was worse on the left. The swelling involved the anterior aspect of the neck, with pain referred to the left ear. The patient presented to her primary care pediatrician's office for evaluation of these symptoms. The temporal temperature was 36.8°C, and the other vital signs were normal. The tympanic membranes and external acoustic canals appeared normal, the posterior oropharynx showed no injection or exudates, and the tonsils were not enlarged. Tender, mobile posterior cervical lymphadenopathy was present on both sides, with the largest lymph node (approximately 2 cm by 1 cm) palpable over the left posterior cervical chain. The remainder of the physical examination was normal. Rapid antigen testing for *Streptococcus pyogenes* was negative, as was nucleic acid amplification testing of a posterior oropharyngeal specimen for influenza virus types A and B and severe acute respiratory syndrome coronavirus 2. A complete blood count showed a white-cell count of 2900 per microliter (reference range, 4000 to 11,000). The hemoglobin level and platelet count were normal. Serologic testing for Epstein–Barr virus (EBV) showed evidence of previous infection. Serologic testing for cytomegalovirus (CMV) was nonreactive. Additional laboratory test results are shown.

Variable	Reference Range, Adults, This Hospital†	3 Wk before Current Presentation, Outpatient Clinic	On Current Presentation, This Hospital
Blood			
Hemoglobin (g/dl)	12.0–16.0	13.5	11.5
Hematocrit (%)	36.0–46.0	41.4	34.5
White-cell count (per μl)	4000–11,000	2900	2710
Differential count (per μl)			
Neutrophils	1800–7700	1726	1450
Lymphocytes	720–4100	928	1030
Monocytes	160–1100	200	160
Eosinophils	0–500	41	40
Basophils	0–150	9	20
Immature granulocytes	0–90	0	0
Mean corpuscular volume (fl)	80–100	85	88
Platelet count (per μl)	150,000–450,000	285,000	221,000
Sodium (mmol/liter)	135–145	—	137
Potassium (mmol/liter)	3.4–5.0	—	3.9
Chloride (mmol/liter)	98–108	—	102
Carbon dioxide (mmol/liter)	23–32	—	25
Urea nitrogen (mg/dl)	8–25	—	12
Creatinine (mg/dl)	0.50–1.00	—	0.70
Calcium (mg/dl)	8.5–10.5	—	9.0
Glucose (mg/dl)	70–110	—	82
Aspartate aminotransferase (U/liter)	9–32	—	62
Alanine aminotransferase (U/liter)	7–33	—	57
Alkaline phosphatase (U/liter)	30–100	—	100
Total bilirubin (mg/dl)	0.0–1.0	—	0.2
Albumin (g/dl)	3.3–5.0	—	4.3
Total protein (g/dl)	6.0–8.3	—	7.0
Lactate dehydrogenase (U/liter)	110–210	—	732
Uric acid (mg/dl)	2.3–6.6	—	3.6
C3 (mg/dl)	81–157	—	138
C4 (mg/dl)	12–39	—	24
Ferritin (μg/liter)	110–210	—	172
Urine			
Color	Yellow	—	Yellow
Clarity	Clear	—	Clear
pH	5.0–9.0	—	6.0
Specific gravity	1.001–1.035	—	1.026
Blood	Negative	—	Negative
Leukocyte esterase	Negative	—	Negative
Ketones	Negative	—	Negative
Glucose	Negative	—	Negative
Protein	Negative	—	Negative
Nitrites	Negative	—	Negative
Urobilinogen	Negative	—	Negative

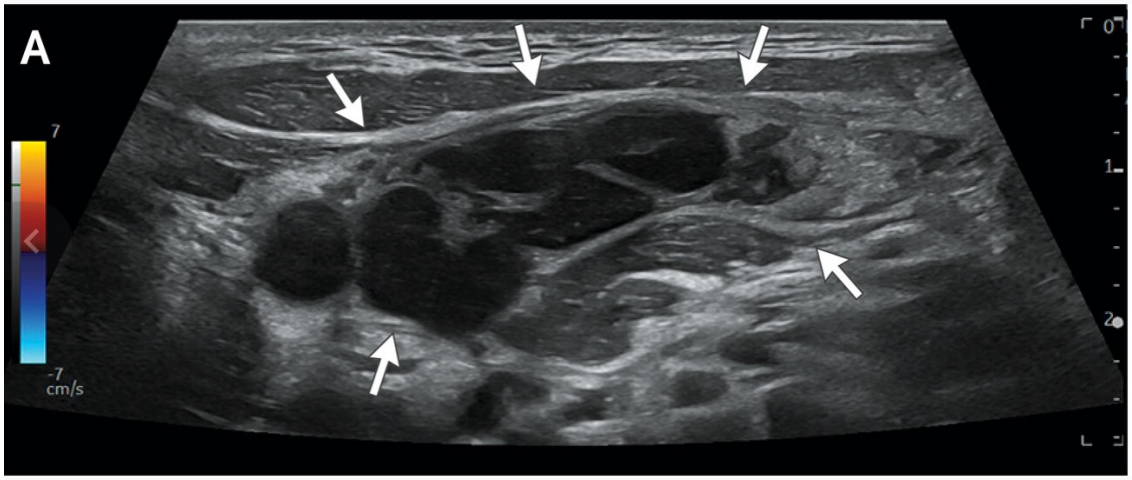

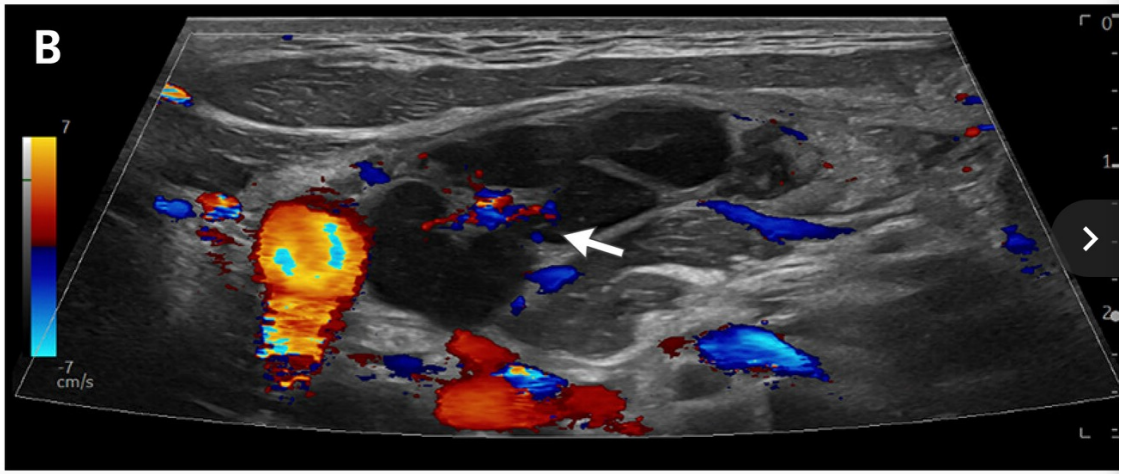

Soft-tissue ultrasonography of the left side of the neck showed mildly enlarged, oval-shaped lymph nodes with fatty hila and increased vascularity. In the left-lower jugular chain (level IV), the lymph nodes were clustered with indistinct margins and surrounding swelling of the perinodal fat. The right side of the neck showed nonenlarged, oval-shaped lymph nodes. No drainable fluid collection was identified.

Treatment with amoxicillin–clavulanate, ibuprofen, and acetaminophen was started, but the patient's symptoms persisted. Four days before the current presentation, fever with temperatures of up to 39.5°C occurred and were accompanied by drenching night sweats. During the next few days, she was unable to attend school because of debilitating exhaustion, which prompted her to present to the pediatric emergency department of this hospital for evaluation.

On arrival at the emergency department, the temperature was 38.3°C, and the heart rate was 71 beats per minute; the other vital signs were normal. The patient had shaking chills despite being covered with multiple blankets. Tender cervical lymphadenopathy was noted on palpation of the neck. The range of motion of the neck was normal. The white-cell count was 2710 per microliter, and the hemoglobin level was 11.5 g per deciliter (reference range, 12.0 to 16.0). The platelet count was normal.

Blood cultures were obtained, and treatment with vancomycin, ampicillin–sulbactam, and lactated Ringer's solution was initiated. The patient was admitted to the pediatrics service of this hospital for further evaluation.

On admission, the patient provided additional history. She reported persistent fever and fatigue, arthralgias involving the wrists and proximal interphalangeal joints without swelling, and tenderness over the left Achilles' tendon. A review of systems was negative for cough, coryza, myalgias, diarrhea, abdominal pain, dysuria, rash, oral and genital ulcers, dryness of the eyes and mouth, Raynaud's phenomenon, alopecia, anorexia, and weight loss. The medical history was notable for anxiety, which was being treated with sertraline. There were no known adverse reactions to medications.

On examination, the oral temperature was 38.4°C, the blood pressure 110/56 mm Hg, the heart rate 95 beats per minute, the respiratory rate 20 breaths per minute, and the oxygen saturation 100% while the patient was breathing ambient air. The weight was 48.3 kg, and the body-mass index (the weight in kilograms divided by the square of the height in meters) was 20.5. The patient appeared fatigued but was in no acute distress. No oropharyngeal injection or oral ulceration was present. The neck was supple, with free range of motion. Cervical, new submandibular, and supraclavicular lymph nodes were palpable on both sides but not fluctuant or suppurative. No axillary, epitrochlear, or inguinal lymphadenopathy was noted. Cardiopulmonary auscultation was unremarkable. The abdomen was soft and nontender. The wrists, proximal interphalangeal joints, and left Achilles' tendon were tender to palpation, without signs of synovitis. No rashes were noted.

The C-reactive protein level was 25.5 mg per deciliter (reference value, <8.0), and the erythrocyte sedimentation rate was 38 mm per hour (reference range, 0 to 19). Antinuclear antibodies (ANA), antineutrophil cytoplasmic antibodies, anti–cyclic citrullinated peptide antibodies, and rheumatoid factor were not detected. Blood cultures showed no growth, and screening tests for human immunodeficiency virus (HIV) antigen and antibody, *Treponema pallidum*, and hepatitis B and C viruses were negative, as was an interferon-γ release assay to detect previous infection with *Mycobacterium tuberculosis*.

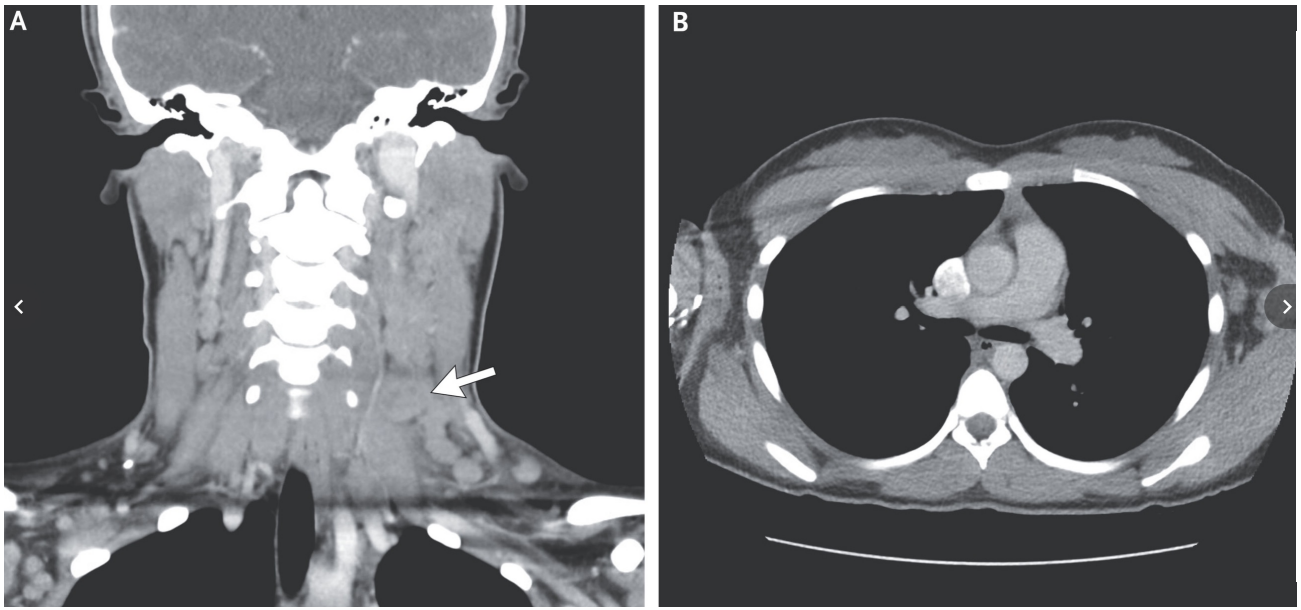

CT Images of the Neck and Chest.

CT images of the neck and chest were obtained after the administration of intravenous contrast material. A coronal view of the neck (Panel A) shows diffusely enlarged cervical lymph nodes on the left side with perinodal fat stranding, as well as a lymph node at the level of the lower jugular with internal heterogeneity (arrow). An axial view of the chest (Panel B) shows no radiologically significant axillary or mediastinal lymphadenopathy.

Computed tomography (CT) of the neck and chest, performed after the administration of intravenous contrast material, revealed diffuse left cervical and supraclavicular lymphadenopathy with perinodal fat stranding and internal nodal heterogeneity, findings suggestive of evolving necrosis. No radiologically significant axillary or mediastinal lymphadenopathy was present, and the lungs were clear

Differential Diagnosis

This 19-year-old woman presented with fever, cervical lymphadenopathy, and arthralgias involving the wrists, proximal interphalangeal joints, and left Achilles' tendon. Physical examination confirmed tenderness in these joints and palpable enlargement of the lymph nodes. These clinical findings suggest an inflammatory disorder characterized by lymphadenopathy, polyarthritis, and enthesitis. Laboratory evaluation revealed leukopenia with absolute neutropenia, as well as elevated levels of lactate dehydrogenase (LDH), aspartate aminotransferase (AST), alanine aminotransferase (ALT), and inflammatory markers. However, the ferritin level was normal, and microbiologic testing, including an interferon-γ release assay to detect previous infection with *Mycobacterium tuberculosis*, was also negative. CT of the neck was notable for perinodal fat stranding and lymphadenopathy, but the chest CT was unremarkable. Despite treatment with antimicrobial therapy, the patient's fever persisted.

Kikuchi–Fujimoto Disease

The clinical constellation of fever, neutropenia, and cervical lymphadenopathy in a young adult is the classic presentation for Kikuchi–Fujimoto disease. Also known as histiocytic necrotizing lymphadenitis, Kikuchi–Fujimoto disease is a rare, generally self-limited condition of unknown cause. Although its trigger is unknown, Kikuchi–Fujimoto disease is hypothesized to result from an exaggerated immune response to one of many possible viral infections, such as infection with human herpesvirus 6, human herpesvirus 8, EBV, or parvovirus B19. Kikuchi–Fujimoto disease is characterized by cervical lymphadenopathy that may or may not be painful. Although most cases involve the lymph nodes unilaterally, bilateral or generalized involvement can occur in a minority of patients. Associated symptoms include rigors, myalgias, arthralgias, night sweats, and weight loss. In some cases, the disease may have more severe features, such as aseptic meningitis, ataxia, or secondary hemophagocytic lymphohistiocytosis. Patients with secondary hemophagocytic lymphohistiocytosis usually present with a high ferritin level, which was not present in this patient.

Kikuchi–Fujimoto disease shares many features with SLE. Some experts propose that it may be a self-limited form of SLE or a precursor to autoimmune disease, a theory supported by the fact that certain monogenic diseases, such as complement component C1s deficiency, are associated with both Kikuchi–Fujimoto disease and SLE.

Diagnostic Testing

The first diagnostic procedure in this patient was a biopsy of a lymph node in the left side of the neck, with samples obtained by concurrent fine-needle aspiration and core-needle biopsy. At the time these samples were obtained, the differential diagnosis was broad with both infectious and noninfectious causes, including autoimmune, rheumatologic, and oncologic diseases, still under consideration. From an infectious disease standpoint, an extensive noninvasive evaluation for a wide range of pathogens was negative, including additional testing for the causative agents of tularemia, Lyme disease, bartonellosis, and toxoplasmosis.

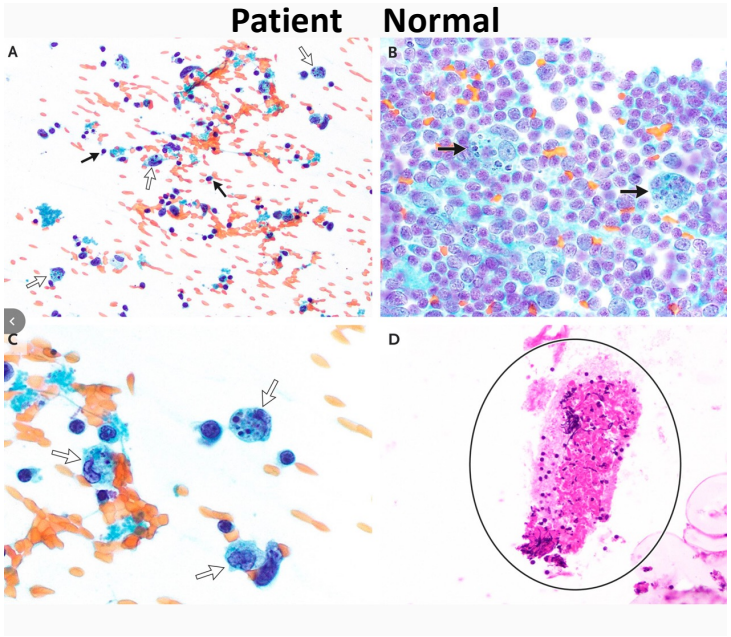

Fine-Needle Aspiration Specimen of a Cervical Lymph Node.

Papanicolaou (Pap) staining of the fine-needle aspiration specimen from the patient's abnormal lymph node (Panel A) shows scattered lymphocytes (black arrows) and histiocytes (white arrows) in a background of blood consistent with limited lymph-node sampling. For comparison, Pap staining of a normal reactive lymph node from a healthy patient (Panel B) shows tingible-body macrophages (arrows) with rounded nuclei and pinpoint nucleoli. In contrast, at higher magnification, Pap staining of the patient's lymph-node specimen (Panel C) shows abnormal histiocytes (arrows) with contorted nuclei that appear sharply angulated to crescent-shaped and have cytoplasmic debris that do not appear similar to normal tingible-body macrophages. Hematoxylin and eosin staining of a cell-block preparation of residual cytologic liquid material with scant yield (Panel D) shows a focal area suggestive of necrosis (circle).

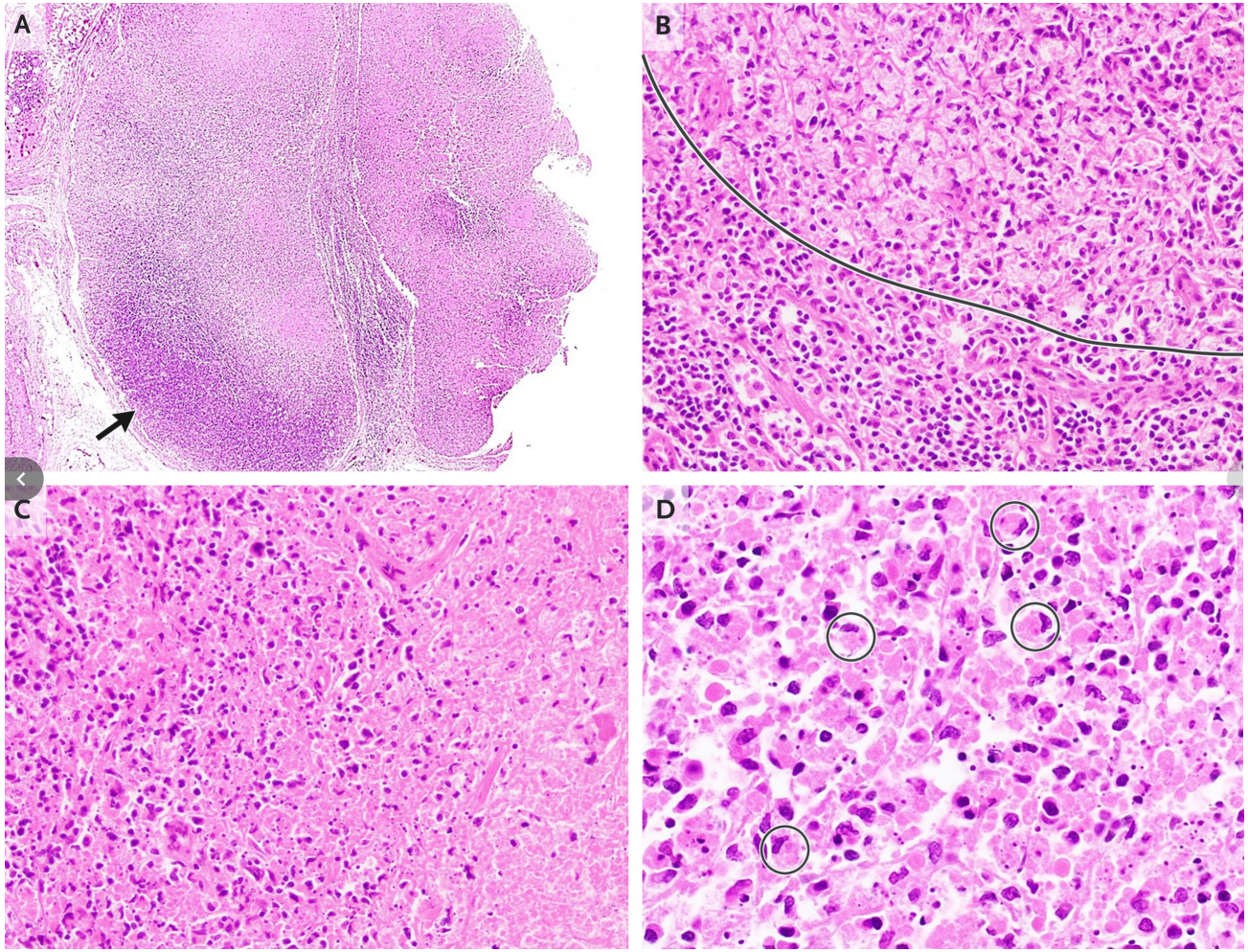

Excisional-Biopsy Specimen of a Cervical Lymph Node.

Hematoxylin and eosin staining of an excisional-biopsy specimen shows necrosis with only a thin rim of residual intact lymphoid tissue (arrow). At higher magnification (Panel B), at this interface (black line), lymphoid tissue (bottom of field) and histiocytes (top of field) are present. The central area shows necrosis with abundant karyorrhectic debris (Panel C, seen diffusely in this image). The histiocytes have contorted, angulated nuclei with ingested karyorrhectic debris (Panel D, circles), which are typical features of Kikuchi–Fujimoto disease.

Discussion of Rheumatology Management

Kikuchi–Fujimoto disease is most often a benign, self-limited illness with a duration of 1 to 4 months. Treatment is targeted toward controlling the initial symptoms while avoiding medications that may exacerbate other diseases that have not fully been ruled out. Typically, nonsteroidal anti-inflammatory drugs (NSAIDs) are used first to treat pain and fever, with glucocorticoid therapy reserved for patients with severe symptoms or in cases with insufficient symptom control once infection and cancer have been ruled out. The preferred duration of therapy has not been established, but the mean duration is 3 to 5 weeks.

After the lymph-node biopsy, a 2-week course of naproxen was initiated, and the patient was discharged from the hospital with plans for follow-up. Three days after discharge, she reported that the fever had resolved. After completing the course of naproxen, the patient remained fever-free and had no return of lymphadenopathy. At a follow-up visit in the rheumatology clinic 5 months after her initial presentation, the patient remained well, and repeat laboratory testing was negative for ANA. A follow-up visit in the rheumatology clinic was scheduled for 1 year later (17 months after symptom onset), with monitoring of autoantibodies to assess for early signs of SLE.

Final Diagnosis

Kikuchi–Fujimoto disease (Histeocytic necrotizing lymphadenitis).

THE LANCET

Retatrutid ist ein von Eli Lilly entwickelter, experimenteller Dreifach-Hormonrezeptoragonist (Triple-Agonist) zur Behandlung von Adipositas, Typ-2-Diabetes und Stoffwechselerkrankungen, der in der Europäischen Union (Stand 2026) **noch nicht zugelassen** ist.

Wirkmechanismus

Retatrutid kombiniert die Wirkung von drei verschiedenen Hormonen in einem Molekül:

- **GLP-1-Rezeptor:** Verzögert die Magenentleerung und dämpft den Appetit.
- **GIP-Rezeptor:** Unterstützt das Sättigungsgefühl und hilft bei der Blutzuckerregulation.
- **Glucagon-Rezeptor:** Steigert den Energieumsatz und kurbelt die Fettverbrennung (unter anderem in der Leber) an.

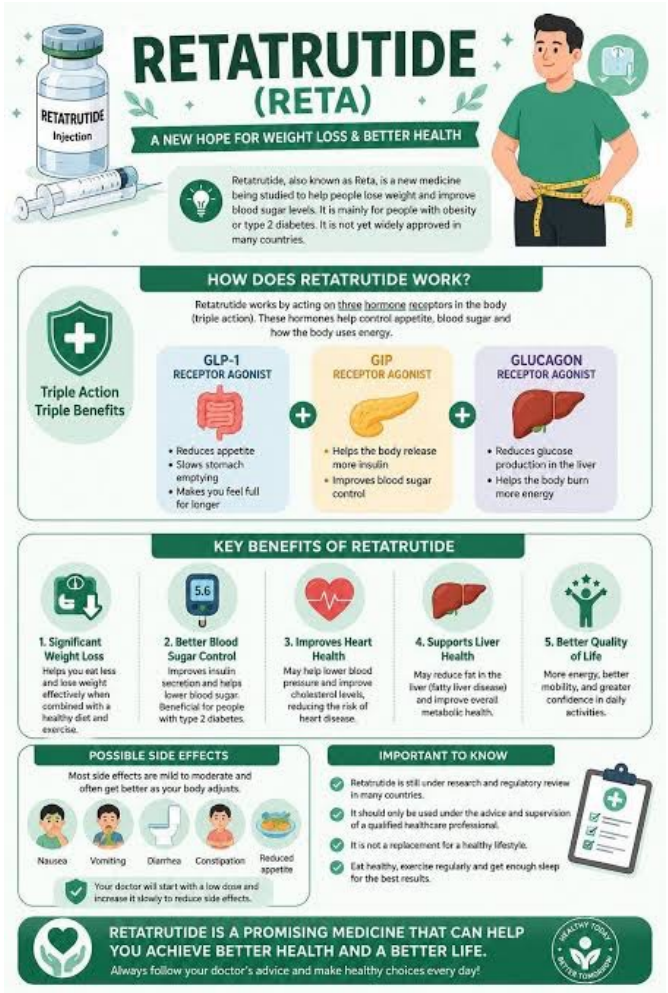

Retatrutide in adults with obesity and type 2 diabetes (TRIUMPH-2): a double-blind, parallel-group, randomised, placebo-controlled, phase 3 trial

Summary

Background Retatrutide is an agonist of GIP, GLP-1, and glucagon receptors, and is currently under investigation for the treatment of obesity, type 2 diabetes, and other comorbidities, including knee osteoarthritis and obstructive sleep apnoea. We aimed to assess the efficacy and safety of retatrutide in adults with obesity and type 2 diabetes.

Methods TRIUMPH-2 was a double-blind, parallel-group, randomised, placebo-controlled, phase 3 trial conducted at 92 medical and research centres and hospitals across eight countries. We enrolled adults (aged ≥18 years) with a BMI of 27 kg/m² or higher and type 2 diabetes (glycated haemoglobin [HbA_{1c}] 6·5–10·5%) on stable treatment for type 2 diabetes for at least 90 days before screening (diet or exercise alone, or up to three oral glucose-lowering medications), and a history of at least one self-reported unsuccessful dietary effort to reduce bodyweight. Participants were randomly assigned (1:1:1:1), using an interactive web-response system, to receive once-weekly subcutaneous injections (self-administered) of placebo or retatrutide 4 mg, 9 mg, or 12 mg. The primary endpoint was the percentage change from baseline to week 80 in bodyweight for the retatrutide 9 mg and 12 mg doses versus placebo, with 4 mg versus placebo a key secondary endpoint. Efficacy analyses included all randomly assigned participants, with missing data imputed with a primary multiple imputation strategy for the treatment regimen estimand. Safety analyses included all randomly assigned participants who received at least one dose of study drug. This trial is registered with ClinicalTrials.gov, NCT05929079 (completed).

Findings Between July 11, 2023, and Nov 1, 2024, 2047 participants were screened, and 1152 (mean age 55·1 years [SD 10·8], 554 [48%] females and 598 [52%] males, and 672 [58%] of White ethnicity) were randomly assigned to retatrutide 4 mg (n=292), 9 mg (n=284), or 12 mg (n=287), or placebo (n=289). At baseline, the mean BMI was 38·2 kg/m² (SD 7·4), mean HbA_{1c} was 7·71% (1·07), median duration of obesity was 21 years (IQR 11–31), and median duration of diabetes was 5·6 years (2·6–10·4). At baseline, 1055 (92%) of 1152 participants were on any oral glucose-lowering medication, including biguanides, SGLT2 inhibitors, sulfonylureas, and other oral glucose-lowering medications. Of 1152 participants, 965 (84%) completed the study drug. For the treatment regimen estimand, the mean percentage change from baseline in bodyweight at week 80 was –11·9% (SE 0·6) with retatrutide 4 mg, –16·8% (0·7) with retatrutide 9 mg, –18·8% (0·7) with retatrutide 12 mg, and –5·1% (0·7) with placebo. Estimated treatment differences compared with placebo for percentage change in bodyweight were –6·9% (95% CI –8·7 to –5·1) with retatrutide 4 mg, –11·8% (–13·7 to –9·8) with retatrutide 9 mg, and –13·8% (–15·8 to –11·8) with retatrutide 12 mg (p<0·0001 for all). The most frequently reported adverse events were gastrointestinal, which were more common in the retatrutide groups than in the placebo group (diarrhoea occurred in 80 [27%] of 292 participants in the 4 mg group, 95 [34%] of 284 in the 9 mg group, and 96 [34%] of 286 in the 12 mg group *vs* 38 [13%] of 287 in the placebo group, and nausea occurred in 40 [14%], 59 [21%], and 80 [28%] *vs* 23 [8%]). Hypotension and dysesthesia were more frequent with retatrutide than with placebo (four [1%] in the 4 mg group, 14 [5%] in the 9 mg group, and 18 (6%) in the 12 mg group *vs* one [<1%] in the placebo group with hypotension; 13 [4%], 16 [6%], and 21 [7%] *vs* two [1%] in the placebo group with dysesthesia). Permanent treatment discontinuation due to adverse events or death was more frequent in participants treated with retatrutide 9 mg (33 [12%]) and 12 mg (22 [8%]) compared with retatrutide 4 mg (11 [4%]) and placebo (14 [5%]). Two participants died in the retatrutide 4 mg group, three in the 9 mg group, one in the 12 mg group, and one in the placebo group; all deaths were deemed to be unrelated to the study intervention by the investigator.

Interpretation Treatment with retatrutide resulted in substantial improvements in bodyweight and was associated with improvements in glycaemic control in participants with obesity and type 2 diabetes, with a safety profile generally consistent with other molecules with GLP-1 receptor agonism. These results show that retatrutide might be effective for the treatment of obesity in people with type 2 diabetes.

Funding Eli Lilly and Company.

	Placebo group (n=289)	Retatrutide 4 mg group (n=292)	Retatrutide 9 mg group (n=284)	Retatrutide 12 mg group (n=287)	Overall (n=1152)
Age, years	56·0 (10·9)	54·4 (11·4)	55·3 (10·4)	54·9 (10·6)	55·1 (10·8)
Sex					
Female	138 (48%)	143 (49%)	135 (48%)	138 (48%)	554 (48%)
Male	151 (52%)	149 (51%)	149 (52%)	149 (52%)	598 (52%)
Race					
White	170 (59%)	165 (57%)	160 (56%)	177 (62%)	672 (58%)
American Indian or Alaska Native	59 (20%)	55 (19%)	54 (19%)	46 (16%)	214 (19%)
Black or African American	13 (4%)	12 (4%)	10 (4%)	10 (3%)	45 (4%)
Asian	36 (12%)	46 (16%)	47 (17%)	41 (14%)	170 (15%)
Multiple	5 (2%)	6 (2%)	8 (3%)	8 (3%)	27 (2%)
Native Hawaiian or other Pacific Islander	1 (<1%)	2 (1%)	0	0	3 (<1%)
Not reported	5 (2%)	6 (2%)	5 (2%)	5 (2%)	21 (2%)
Ethnicity					
Hispanic or Latino	142 (49%)	138 (47%)	131 (46%)	137 (48%)	548 (48%)
Not Hispanic or Latino	145 (50%)	151 (52%)	151 (53%)	149 (52%)	596 (52%)
Not reported	2 (1%)	3 (1%)	2 (1%)	1 (<1%)	8 (1%)
Bodyweight, kg	107·4 (24·9)	105·1 (24·8)	104·7 (22·8)	108·4 (26·7)	106·4 (24·9)
BMI, kg/m²	38·4 (7·4)	38·0 (7·2)	37·8 (7·2)	38·5 (7·7)	38·2 (7·4)
BMI categories					
<30 kg/m²	29 (10%)	33 (11%)	27 (10%)	41 (14%)	130 (11%)
30 to <35 kg/m²	86 (30%)	72 (25%)	81 (29%)	66 (23%)	305 (26%)
35 to <40 kg/m²	69 (24%)	86 (29%)	88 (31%)	76 (26%)	319 (28%)
40 to <50 kg/m²	82 (28%)	79 (27%)	66 (23%)	83 (29%)	310 (27%)
≥50 kg/m²	23 (8%)	22 (8%)	22 (8%)	21 (7%)	88 (8%)
Participants with BMI ≥35 kg/m²	174 (60%)	187 (64%)	176 (62%)	180 (63%)	717 (62%)
Duration of type 2 diabetes, years	6·6 (2·9–12·0)	5·6 (2·7–10·5)	5·2 (2·4–9·4)	5·1 (2·4–10·3)	5·6 (2·6–10·4)
Duration of obesity, years	22 (12–32)	19 (9–28)	20 (11–30)	22 (10–33)	21 (11–31)
HbA_{1c}, %	7·73% (1·17)	7·71% (0·97)	7·71% (1·06)	7·68% (1·08)	7·71% (1·07)
HbA_{1c}, mmol/mol	61·0 (12·7)	60·8 (10·6)	60·8 (11·6)	60·5 (11·9)	60·8 (11·7)
Participants with HbA_{1c} ≤8·5%	228 (79%)	231 (79%)	226 (80%)	230 (80%)	915 (79%)
Fasting serum glucose concentration, mg/dL	135·9 (42·3)	138·1 (39·7)	138·5 (37·6)	136·2 (38·3)	137·1 (39·5)
Waist circumference, cm	120·6 (15·4)	119·2 (15·4)	118·9 (14·6)	120·1 (16·4)	119·7 (15·4)
Waist-to-height ratio	0·72 (0·09)	0·72 (0·08)	0·72 (0·09)	0·72 (0·09)	0·72 (0·09)
Blood pressure, mm Hg					
Systolic	129·8 (13·7)	129·4 (13·7)	129·1 (13·9)	130·1 (13·5)	129·6 (13·7)
Diastolic	80·3 (8·87)	80·2 (9·13)	80·2 (9·23)	81·0 (8·61)	80·4 (8·96)

(Table 1 continues on next page)

(Continued from previous page)

	Placebo group (n=289)	Retatrutide 4 mg group (n=292)	Retatrutide 9 mg group (n=284)	Retatrutide 12 mg group (n=287)	Overall (n=1152)
Lipid parameters, mg/dL					
Total cholesterol	172·1 (148·1–196·4)	168·8 (142·3–192·2)	173·2 (148·1–203·4)	171·3 (140·4–202·2)	171·3 (145·4–199·1)
Triglycerides	145·3 (108·1–194·0)	139·1 (108·9–191·3)	152·3 (111·2–208·6)	149·7 (114·3–210·8)	146·1 (109·8–200·2)
VLDL cholesterol	29·0 (20·9–37·9)	28·2 (22·0–37·9)	30·2 (22·0–40·2)	30·2 (23·2–41·0)	29·0 (22·0–39·1)
Non-HDL cholesterol	128·2 (101·9–152·1)	123·9 (98·1–151·0)	128·2 (105·6–157·9)	125·9 (100·0–159·8)	125·9 (100·6–156·0)
HDL cholesterol	42·9 (36·0–51·0)	42·2 (35·2–50·3)	42·9 (36·0–50·3)	42·2 (35·2–49·1)	42·2 (35·2–50·3)
LDL cholesterol	95·1 (73·1–118·3)	94·5 (68.6–114.7)	97·1 (71·9–120·6)	94·0 (68.1–124·1)	95·1 (71·2–120·3)
eGFR*, mL/min per 1·73 m²	78·2 (20·6)	78·7 (20·4)	79·3 (19·5)	78·2 (20·6)	78·6 (20·3)
Participants with baseline eGFR <60 mL/min per 1·73 m²	59 (20%)	51 (17%)	45 (16%)	51 (18%)	206 (18%)
Fasting insulin, mU/L	21·1 (13·3–31·5)	21·5 (14·8–35·0)	21·6 (14·0–34·8)	23·5 (15·6–36·0)	21·9 (14·3–34·3)
High-sensitivity C-reactive protein, mg/L	3·4 (1·8–7·4)	4·0 (1·9–7·0)	3·9 (1·7–7·3)	3·2 (1·7–7·2)	3·7 (1·8–7·3)
Urine albumin-to-creatinine ratio, mg/g	10·3 (5·0–29·0)	10·0 (5·0–29·5)	11·0 (5·5–24·0)	10·5 (5·8–23·5)	10·5 (5·5–25·0)
Participants with baseline albumin-to-creatinine ratio <30 mg/g	215/286 (75%)	216/287 (75%)	222/278 (80%)	227/284 (80%)	880/1135 (78%)
Type of glucose-lowering medication used at randomisation					
Weight gain†	58 (20%)	56 (19%)	53 (19%)	65 (23%)	232 (20%)
Weight loss‡	55 (19%)	59 (20%)	50 (18%)	57 (20%)	221 (19%)
Weight neutral§	176 (61%)	177 (61%)	181 (64%)	165 (57%)	699 (61%)
Type of concomitant medication used at randomisation					
Glucose lowering¶	258 (89%)	275 (94%)	255 (90%)	267 (93%)	1055 (92%)
Antihypertensive	204 (71%)	198 (68%)	196 (69%)	198 (69%)	796 (69%)
Lipid lowering	182 (63%)	182 (62%)	173 (61%)	187 (65%)	724 (63%)

Data are mean (SD), n (%), or median (IQR). eGFR=estimated glomerular filtration rate. HbA_{1c}=glycated haemoglobin. *eGFR was calculated according to the cystatin C-based Chronic Kidney Disease Epidemiology Collaboration equation (2012). †Included use of an SGLT2 inhibitor alone or in combination with any other glucose-lowering agents except for a sulfonylurea or thiazolidinedione. ‡Use of a sulfonylurea alone or thiazolidinedione alone or in combination with any other glucose-lowering agents except for an SGLT2 inhibitor. §Included lifestyle management only (no background glucose-lowering agents); metformin monotherapy; SGLT2 inhibitor in combination with a sulfonylurea or thiazolidinedione, with or without other glucose-lowering agents; or all other monotherapy (such as glinides and alpha glucosidase inhibitors) or combination therapy that does not fall under weight loss or weight gain. ¶Participants were allowed to receive up to three oral glucose-lowering medications (excluding DPP-4 inhibitors, amylin analogues, GLP-1 receptor agonists, dual GIP and GLP-1 receptor agonists, or insulin).

Table 1: **Baseline demographics and clinical characteristics**

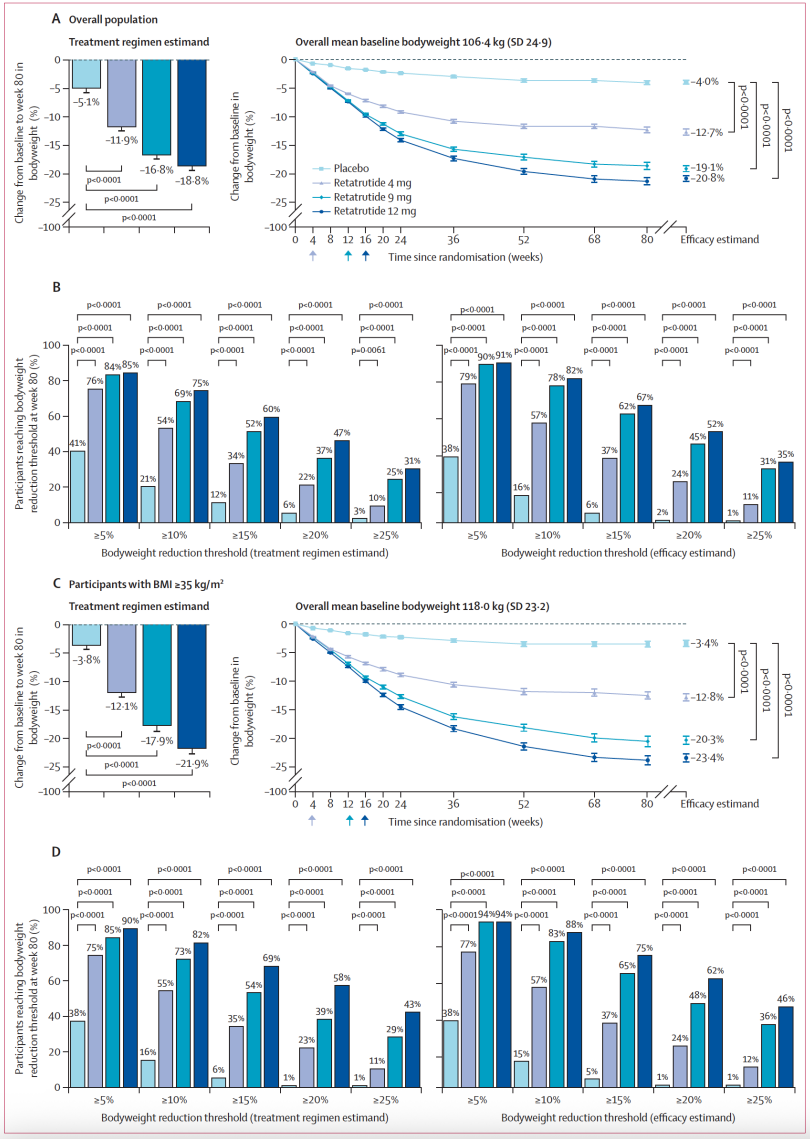

Figure 2: **Bodyweight and bodyweight reduction thresholds for the overall population and participants with BMI 35 kg/m² or higher**
Error bars indicate SEs. (A) Percentage change from baseline in bodyweight over time in the overall population. Data are observed mean (SE) for the efficacy analysis set, with week 80 data showing model-based estimate mean (SE) for the efficacy estimand and treatment regimen estimand. (B) Percentage of participants in the overall population who reached bodyweight reduction thresholds for the efficacy estimand and treatment regimen estimand. Data are model-based estimates. (C) Percentage change from baseline in bodyweight over time in participants with BMI ≥35 kg/m². Data are observed mean (SE) for the efficacy analysis set, with week 80 data showing model-based estimate mean (SE) for the efficacy estimand and treatment regimen estimand. (D) Percentage of participants who reached bodyweight reduction thresholds for the efficacy estimand and treatment regimen estimand in participants with BMI ≥35 kg/m². p values represent comparison with placebo. Data are model-based estimates.

	Placebo group (n=289)	Retatrutide 4 mg group (n=292)	Retatrutide 9 mg group (n=284)	Retatrutide 12 mg group (n=287)	Retatrutide 4 mg *vs* placebo	Retatrutide 9 mg *vs* placebo	Retatrutide 12 mg *vs* placebo
Primary endpoint at week 80							
Percentage change in bodyweight	−5·1% (0·7)	−11·9% (0·6)	−16·8% (0·7)	−18·8% (0·7)	ETD −6·9% (−8·7 to −5·1), p<0·0001	ETD −11·8% (−13·7 to −9·8), p<0·0001	ETD −13·8% (−15·8 to −11·8), p<0·0001
Key secondary endpoints for the overall population at week 80							
Participants with bodyweight reduction ≥5%*	119 (41%)	222 (76%)	237 (84%)	245 (85%)	RD 35·0 (26·9 to 43·2), p<0·0001	RD 43·2 (35·2 to 51·2), p<0·0001	RD 44·2 (36·4 to 52·0), p<0·0001
Participants with bodyweight reduction ≥10%*	62 (21%)	157 (54%)	194 (69%)	215 (75%)	RD 33·6 (25·6 to 41·5), p<0·0001	RD 48·0 (40·2 to 55·8), p<0·0001	RD 54·1 (46·9 to 61·4), p<0·0001
Participants with bodyweight reduction ≥15%*	36 (12%)	98 (34%)	146 (52%)	175 (60%)	RD 21·6 (14·6 to 28·7), p<0·0001	RD 39·5 (32·2 to 46·9), p<0·0001	RD 48·0 (40·9 to 55·0), p<0·0001
Participants with bodyweight reduction ≥20%*	18 (6%)	62 (22%)	103 (37%)	138 (47%)	RD 16·1 (10·2 to 22·0), p<0·0001	RD 31·1 (24·4 to 37·8), p<0·0001	RD 41·3 (34·7 to 48·0), p<0·0001
Participants with bodyweight reduction ≥25%*	10 (3%)	27 (10%)	69 (25%)	92 (31%)	RD 6·2 (1·8 to 10·6), p=0·0061	RD 21·8 (16·1 to 27·6), p<0·0001	RD 28·1 (22·1 to 34·0), p<0·0001
Change in waist circumference, cm	−4·9 (0·6)	−10·6 (0·6)	−14·3 (0·7)	−15·4 (0·7)	ETD −5·7 (−7·3 to −4·2), p<0·0001	ETD −9·5 (−11·2 to −7·8), p<0·0001	ETD −10·5 (−12·3 to −8·8), p<0·0001
Change in systolic blood pressure, mm Hg	−2·7 (0·9)	−5·0 (0·7)	−7·4 (0·8)	−9·7 (0·8)	ETD −2·3 (−4·5 to −0·1), p=0·039	ETD −4·6 (−6·9 to −2·4), p<0·0001	ETD −7·0 (−9·3 to −4·7), p<0·0001
Change in HbA_{1c}, %	−0·45% (0·08)	−1·38% (0·06)	−1·50% (0·07)	−1·45% (0·07)	ETD −0·92 (−1·12 to −0·73), p<0·0001	ETD −1·05 (−1·25 to −0·85), p<0·0001	ETD −1·00 (−1·21 to −0·80), p<0·0001
Participants with HbA_{1c} ≤6·5%*	86 (29%)	200 (68%)	201 (71%)	207 (72%)	RD 39·2 (30·5 to 47·8), p<0·0001	RD 41·4 (32·7 to 50·1), p<0·0001	RD 42·9 (34·2 to 51·5), p<0·0001
Change in fasting serum glucose, mg/dL	−8·2 (2·5)	−28·8 (2·0)	−31·6 (2·0)	−31·4 (2·3)	ETD −20·5 (−26·2 to −14·8), p<0·0001	ETD −23·3 (−29·0 to −17·6), p<0·0001	ETD −23·2 (−29·3 to −17·1), p<0·0001
Percentage change in triglycerides	−1·8% (2·7)	−23·7% (2·2)	−33·5% (1·9)	−35·6% (1·9)	ETD −22·3% (−28·0 to −16·2), p<0·0001	ETD −32·3% (−37·3 −27·0), p<0·0001	ETD −34·4% (−39·4 to −29·0), p<0·0001
Percentage change in non-HDL cholesterol	−4·7% (1·7)	−13·1% (1·6)	−15·0% (1·6)	−16·5% (1·5)	ETD −8·7% (−13·1 to −4·1), p=0·0003	ETD −10·8% (−15·0 to −6·4), p<0·0001	ETD −12·4% (−16·6 to −7·9), p<0·0001
Percentage change in high-sensitivity C-reactive protein	−16·8% (4·6)	−45·5% (3·4)	−54·9% (2·5)	−56·1% (2·5)	ETD −34·5% (−44·2 to −23·3), p<0·0001	ETD −45·8% (−53·3 to −37·2), p<0·0001	ETD −47·2% (−54·7 to −38·6), p<0·0001
Change in IWQOL-Lite-CT physical function composite score†	8·2 (1·4)	20·3 (1·2)	21·5 (1·3)	22·0 (1·2)	ETD 12·1 (8·6 to 15·7), p<0·0001	ETD 13·3 (9·5 to 17·1), p<0·0001	ETD 13·9 (10·3 to 17·4), p<0·0001
Key secondary endpoints for BMI ≥35 kg/m² subgroup at week 80							
Percentage change in bodyweight	−3·8% (0·6)	−12·1% (0·7)	−17·9% (0·9)	−21·9% (0·9)	ETD −8·3% (−10·1 to −6·6), p<0·0001	ETD −14·1% (−16·1 to −12·1), p<0·0001	ETD −18·1% (−20·2 to −16·0), p<0·0001
Participants with bodyweight reduction ≥5%*	66 (38%)	140 (75%)	150 (85%)	161 (90%)	RD 37·2 (27·3 to 47·2), p<0·0001	RD 47·4 (37·9 to 56·9), p<0·0001	RD 51·8 (42·9 to 60·8), p<0·0001
Participants with bodyweight reduction ≥10%*	29 (16%)	101 (55%)	127 (73%)	148 (82%)	RD 38·3 (29·1 to 47·5), p<0·0001	RD 56·6 (47·9 to 65·2), p<0·0001	RD 65·4 (57·2 to 73·5), p<0·0001
Participants with bodyweight reduction ≥15%*	10 (6%)	64 (35%)	95 (54%)	126 (69%)	RD 29·2 (21·6 to 36·8), p<0·0001	RD 48·3 (40·5 to 56·1), p<0·0001	RD 63·8 (56·4 to 71·3), p<0·0001
Participants with bodyweight reduction ≥20%*	3 (1%)	41 (23%)	69 (39%)	104 (58%)	RD 21·2 (15·1 to 27·3), p<0·0001	RD 37·7 (30·6 to 44·8), p<0·0001	RD 56·8 (49·5 to 64·1), p<0·0001
Participants with bodyweight reduction ≥25%*	2 (1%)	21 (11%)	52 (29%)	76 (43%)	RD 10·1 (5·4 to 14·8), p<0·0001	RD 27·9 (21·3 to 34·5), p<0·0001	RD 41·9 (34·8 to 49·0), p<0·0001

(Table 2 continues on next page)

Microsoft W

	Placebo group (n=289)	Retatrutide 4 mg group (n=292)	Retatrutide 9 mg group (n=284)	Retatrutide 12 mg group (n=287)	Retatrutide 4 mg *vs* placebo	Retatrutide 9 mg *vs* placebo	Retatrutide 12 mg *vs* placebo
(Continued from previous page)							
Other secondary endpoint at week 68							
Percentage change in bodyweight	−4·4% (0·6)	−11·8% (0·5)	−16·6% (0·6)	−19·0% (0·7)	ETD −7·4% (−9·0 to −5·9)	ETD −12·2% (−13·9 to −10·6)	ETD −14·7% (−16·4 to −12·9)
Other secondary endpoints at week 80							
Change in bodyweight, kg	−5·8 (0·9)	−12·9 (0·6)	−18·3 (0·8)	−20·7 (0·8)	ETD −7·2 (−9·2 to −5·1)	ETD −12·5 (−14·8 to −10·2)	ETD −15·0 (−17·2 to −12·7)
Participants with bodyweight reduction ≥30%*	5 (2%)	11 (4%)	40 (15%)	52 (18%)	RD 2·6 (−0·2 to 5·3)	RD 13·6 (9·3 to 18·0)	RD 16·2 (11·6 to 20·8)
Change in BMI, kg/m²	−1·8 (0·3)	−4·6 (0·2)	−6·6 (0·3)	−7·5 (0·3)	ETD −2·8 (−3·5 to −2·2)	ETD −4·8 (−5·5 to −4·0)	ETD −5·7 (−6·4 to −5·0)
Participants with BMI <30 kg/m²*	65 (22%)	102 (35%)	138 (47%)	149 (53%)	RD 13·2 (7·7 to 18·8)	RD 25·2 (18·8 to 31·7)	RD 31·1 (24·7 to 37·5)
Participants with BMI <27 kg/m²*	25 (9%)	53 (19%)	79 (28%)	88 (32%)	RD 10·4 (5·5 to 15·2)	RD 19·1 (13·4 to 24·8)	RD 23·0 (17·2 to 28·8)
Participants with BMI <25 kg/m²*	9 (4%)	17 (6%)	41 (14%)	52 (18%)	RD 2·4 (−0·9 to 5·7)	RD 10·4 (6·0 to 14·7)	RD 14·5 (10·0 to 19·1)
Participants with waist-to-height ratio <0·5*	2 (1%)	4 (1%)	10 (4%)	22 (8%)	RD 0·6 (−1·0 to 2·1)	RD 3·0 (0·7 to 5·2)	RD 6·9 (3·9 to 9·9)
Participants with waist-to-height ratio <0·53*	9 (3%)	10 (3%)	29 (10%)	42 (14%)	RD 0·3 (−2·5 to 3·0)	RD 7·2 (3·2 to 11·2)	RD 11·0 (6·8 to 15·1)
Participants with waist-to-height ratio <0·53 and BMI <27 kg/m²*	5 (2%)	6 (2%)	29 (10%)	39 (13%)	RD 0·4 (−1·4 to 2·2)	RD 8·3 (4·6 to 11·9)	RD 10·8 (7·0 to 14·6)
Change in diastolic blood pressure, mm Hg	−2·8 (0·5)	−2·8 (0·5)	−3·3 (0·5)	−4·3 (0·5)	ETD −0·1 (−1·4 to 1·3)	ETD −0·5 (−1·8 to 0·8)	ETD −1·5 (−2·9 to −0·2)
Participants with HbA_{1c} <7%*	124 (42%)	230 (78%)	225 (79%)	230 (81%)	RD 35·9 (26·7 to 45·1)	RD 37·2 (28·1 to 46·3)	RD 38·4 (28·9 to 47·9)
Participants with HbA_{1c} <5·7%*	15 (5%)	74 (26%)	97 (34%)	102 (35%)	RD 20·6 (14·7 to 26·6)	RD 28·8 (22·5 to 35·1)	RD 30·2 (24·0 to 36·4)
Participants with HbA_{1c} ≤6·5% and weight reduction ≥10%*	29 (10%)	128 (45%)	166 (59%)	184 (63%)	RD 35·1 (28·3 to 41·9)	RD 49·7 (42·9 to 56·5)	RD 53·7 (47·2 to 60·3)
Percentage change in urinary albumin-to-creatinine ratio	−2·8% (5·8)	−24·7% (4·0)	−17·6% (6·6)	−15·7 (4·9)	ETD −22·6 (−33·5 to −9·8)	ETD −15·3 (−29·5 to 1·8)	ETD −13·3 (−25·8 to 1·4)
Change in eGFR‡, mL/min per 1·73 m²	−0·1 (1·1)	3·0 (0·7)	5·0 (0·9)	5·5 (0·9)	ETD 3·0 (0·5 to 5·6)	ETD 5·1 (2·2 to 7·9)	ETD 5·6 (2·8 to 8·4)
Percentage change in fasting insulin	−10·5% (4·2)	−34·2% (2·4)	−40·7% (2·7)	−45·2% (2·2)	ETD −26·5% (−34·4 to −17·5)	ETD −33·7% (−41·5 to −24·9)	ETD −38·7% (−45·6 to −31·0)
Change in SF-36v2 acute form physical functioning domain score§	1·0 (0·5)	4·4 (0·4)	4·1 (0·5)	4·4 (0·4)	ETD 3·5 (2·2 to 4·7)	ETD 3·1 (1·8 to 4·4)	ETD 3·4 (2·1 to 4·7)

All changes are model-based estimated mean (SE) changes from baseline to week 80, unless otherwise specified, for all randomly assigned participants. eGFR=estimated glomerular filtration rate. ETD=estimated treatment difference. HbA_{1c}=glycated haemoglobin. IWQOL-Lite-CT=Impact of Weight on Quality of Life-Lite Clinical Trials Version. RD=risk difference. SF-36v2=Short Form 36-item Health Survey version 2. *Data are m (model-based estimated %), where m is calculated by the average number of participants achieving target across imputed datasets and then rounded to integer. Missing values were imputed using the primary multiple imputation method with the use of Rubin's rules. †Pooled dose comparison versus placebo: ETD 13·6 (95% CI 10·3–16·8), p<0·0001. ‡eGFR was calculated according to the cystatin C-based Chronic Kidney Disease Epidemiology Collaboration equation. §The SF-36v2 acute form physical functioning domain assessed limitations due to health "now". Each domain score was transformed to a 0–100 scale, with higher scores indicating better levels of function.

Table 2: **Primary and secondary endpoints (treatment regimen estimand)**

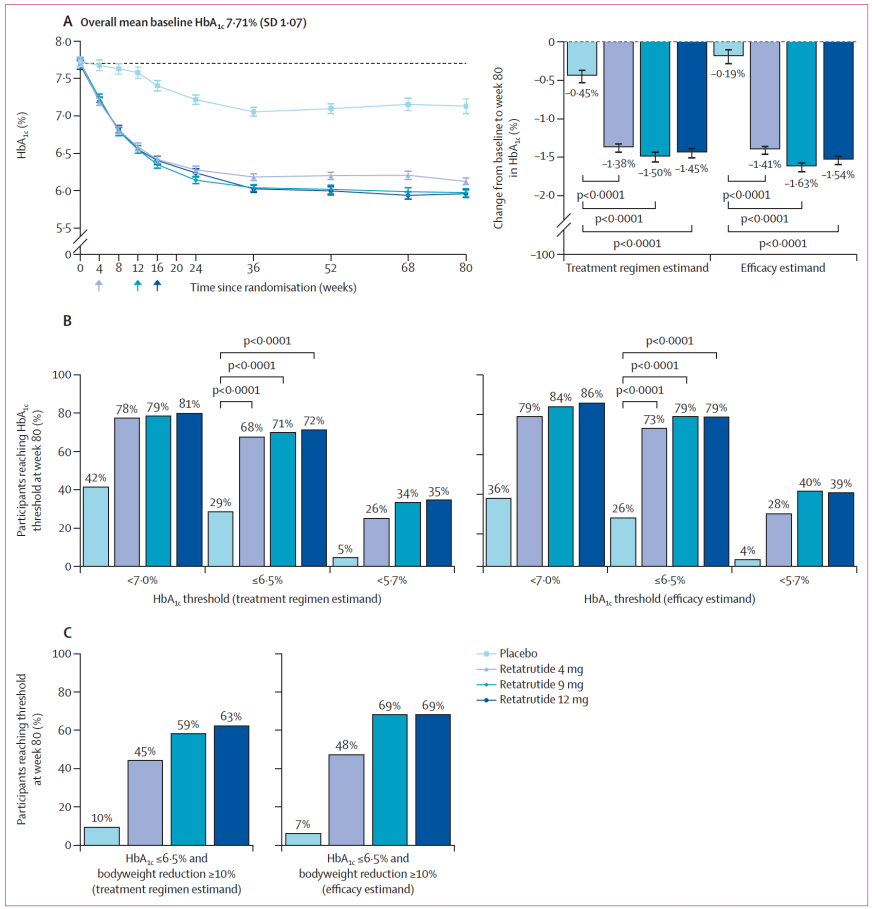

(Figure 3 continues on next page)

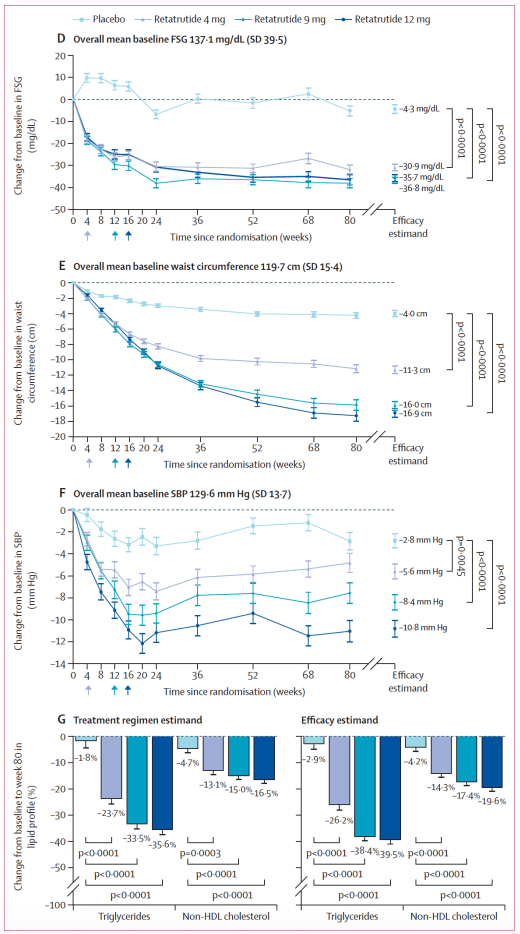

***Figure 3*: Association of retatrutide with changes in HbA_{1c}, FSG, waist circumference, SBP, and lipids**

Error bars indicate SEs. (A) HbA_{1c} (%) over time. Data are observed mean (SE), efficacy analysis set. Week 80 data shows change from baseline, model-based estimate mean (SE) for the efficacy estimand and treatment regimen estimand. (B) Percentage of participants who reached HbA_{1c} thresholds for the efficacy estimand and treatment regimen estimand at week 80. Thresholds of <7·0% and <5·7% are additional secondary endpoints and are not controlled for type I error. Data are model-based estimates. (C) Percentage of participants in the overall population who reached the composite endpoint of HbA_{1c} ≤6·5% and bodyweight reduction ≥10% for the efficacy estimand and treatment regimen estimand at week 80 (an additional secondary endpoint and is not controlled for type I error). Data are model-based estimates. (D) Change from baseline in FSG over time. Data are observed mean (SE), with week 80 data showing model-based estimate mean (SE) for the efficacy estimand. (E) Change from baseline in waist circumference over time. Data are observed mean (SE), with week 80 data showing model-based estimate mean (SE) for the efficacy estimand. (F) Change from baseline in SBP over time. Data are observed mean (SE), with week 80 data showing model-based estimate mean (SE) for the efficacy estimand. (G) Percentage change from baseline in multiplicity-controlled lipid levels. Data are model-based estimate mean (SE) for the efficacy estimand and treatment regimen estimand. p values represent comparison with placebo. FSG=fasting serum glucose. HbA_{1c}=glycated haemoglobin. SBP=systolic blood pressure.

	Placebo group (n=287)	Retatrutide 4 mg group (n=292)	Retatrutide 9 mg group (n=284)	Retatrutide 12 mg group (n=286)	Overall (n=1149)
Participants with ≥1 treatment-emergent adverse event	227 (79%)	231 (79%)	236 (83%)	242 (85%)	936 (81%)
Deaths*	1 (<1%)	2 (1%)	3 (1%)	1 (<1%)	7 (1%)
Adverse events by system organ class leading to study treatment discontinuation†	14 (5%)	11 (4%)	33 (12%)	22 (8%)	80 (7%)
Investigations	0	3 (1%)	7 (2%)	6 (2%)	16 (1%)
Gastrointestinal disorders	2 (1%)	0	6 (2%)	6 (2%)	14 (1%)
Neoplasm benign, malignant and unspecified (cysts and polyps included)	4 (1%)	4 (1%)	4 (1%)	1 (<1%)	13 (1%)
Treatment-emergent adverse events occurring in ≥5% of participants in any treatment group by preferred term					
Diarrhoea	38 (13%)	80 (27%)	95 (34%)	96 (34%)	309 (27%)
Nausea	23 (8%)	40 (14%)	59 (21%)	80 (28%)	202 (18%)
Constipation	27 (9%)	41 (14%)	46 (16%)	48 (17%)	162 (14%)
Decreased appetite	13 (5%)	17 (6%)	35 (12%)	49 (17%)	114 (10%)
Vomiting	12 (4%)	16 (6%)	29 (10%)	45 (16%)	102 (9%)
Hyperglycaemia	50 (17%)	22 (8%)	9 (3%)	11 (4%)	92 (8%)
Dyspepsia	12 (4%)	21 (7%)	20 (7%)	28 (10%)	81 (7%)
Nasopharyngitis	13 (5%)	24 (8%)	15 (5%)	23 (8%)	75 (7%)
Urinary tract infection (HLT)‡	19 (7%)	11 (4%)	18 (6%)	23 (8%)	71 (6%)
Abdominal distension	11 (4%)	13 (5%)	26 (9%)	20 (7%)	70 (6%)
Urinary tract infection	19 (7%)	10 (3%)	15 (5%)	23 (8%)	67 (6%)
Fatigue	8 (3%)	13 (5%)	19 (7%)	22 (8%)	62 (5%)
Eructation	2 (1%)	13 (5%)	25 (9%)	21 (7%)	61 (5%)
Arthralgia	15 (5%)	11 (4%)	17 (6%)	18 (6%)	61 (5%)
Upper respiratory tract infection	17 (6%)	17 (6%)	12 (4%)	14 (5%)	60 (5%)
Serious adverse events by system organ class occurring in ≥1% of overall participants	22 (8%)	24 (8%)	25 (9%)	27 (9%)	98 (9%)
Infections and infestations	7 (2%)	3 (1%)	3 (1%)	6 (2%)	19 (2%)
Cardiac disorders	4 (1%)	4 (1%)	7 (2%)	3 (1%)	18 (2%)
Neoplasms benign, malignant, and unspecified (cysts and polyps included)	5 (2%)	4 (1%)	4 (1%)	2 (1%)	15 (1%)
Gastrointestinal disorders	1 (<1%)	0	6 (2%)	4 (1%)	11 (1%)

(Table 3 continues on next page)

(Continued from previous page)

	Placebo group (n=287)	Retatrutide 4 mg group (n=292)	Retatrutide 9 mg group (n=284)	Retatrutide 12 mg group (n=286)	Overall (n=1149)
Adverse events of special interest					
Diabetic retinopathy, diabetic macular oedema, and related complications	26 (9%)	14 (5%)	14 (5%)	11 (4%)	65 (6%)
Dysesthesia (skin burning sensation and related adverse events)	2 (1%)	13 (4%)	16 (6%)	21 (7%)	52 (5%)
Hypotension, orthostatic hypotension, and blood pressure decreased	1 (<1%)	4 (1%)	14 (5%)	18 (6%)	37 (3%)
Injection-site reactions	2 (1%)	7 (2%)	10 (4%)	13 (5%)	32 (3%)
Severe or serious gastrointestinal adverse events	4 (1%)	3 (1%)	16 (6%)	8 (3%)	31 (3%)
Malignancies	7 (2%)	8 (3%)	5 (2%)	4 (1%)	24 (2%)
Level 2 or level 3 hypoglycaemia§	5 (2%)	2 (1%)	4 (1%)	9 (3%)	20 (2%)
Adjudication-confirmed major adverse cardiovascular event	4 (1%)	3 (1%)	4 (1%)	4 (1%)	15 (1%)
Severe or serious arrhythmias and cardiac conduction disorders	1 (<1%)	2 (1%)	7 (2%)	2 (1%)	12 (1%)
Severe or serious gallbladder and biliary tract disorders	1 (<1%)	3 (1%)	1 (<1%)	1 (<1%)	6 (1%)
Potential non-immediate severe or serious hypersensitivity reactions	0	1 (<1%)	1 (<1%)	1 (<1%)	3 (<1%)
Severe or serious acute renal events	0	1 (<1%)	1 (<1%)	1 (<1%)	3 (<1%)
Adjudication-confirmed pancreatitis	0	0	1 (<1%)	2 (1%)	3 (<1%)
Severe or serious hepatic disorders	1 (<1%)	1 (<1%)	0	0	2 (<1%)
Severe or serious malnutrition	1 (<1%)	0	0	1 (<1%)	2 (<1%)
Severe or serious depression and suicidal ideation or behaviour	0	1 (<1%)	0	0	1 (<1%)
Medullary thyroid carcinoma, papillary carcinoma, and C-cell hyperplasia	0	1 (<1%)	0	0	1 (<1%)
Severe or serious starvation ketoacidosis, euglycaemic diabetic ketoacidosis, and diabetic ketoacidosis	0	1 (<1%)	0	0	1 (<1%)
Potential immediate severe or serious hypersensitivity reactions	0	0	0	0	0

Data are n (%). CEC=clinical endpoint committee. HLT=high-level term. *Deaths were adjudicated by an independent CEC that determined whether the death was cardiovascular related. Causes of death were: septic shock in the placebo group; thermal burn and hepatic cirrhosis in the retatrutide 4 mg group; one case of brain herniation (CEC-adjudicated cardiovascular death), one of upper gastrointestinal haemorrhage, and one with cardiac arrest (CEC-adjudicated cardiovascular death) in the retatrutide 9 mg group; and one participant with acute myocardial infarction (CEC-adjudicated cardiovascular death; see appendix p 55 for further details) in the retatrutide 12 mg group. †Adverse events by system organ class leading to treatment discontinuation is reported for those occurring in ≥1% of overall participants. ‡HLT refers to a specific level in the Medical Dictionary for Regulatory Activities hierarchy used to group related preferred terms describing medical conditions in clinical trials. §Occurring at any timepoint post baseline on treatment and excluding events occurring after initiation of new glucose-lowering medication.

Table 3: **Adverse events and safety**

Research in context

Evidence before this study

On July 29, 2026, we searched PubMed using the terms "obesity or overweight" OR "type 2 diabetes" AND "glucagon-like peptide 1 receptor agonist (GLP-1)" OR "glucose-dependent insulinotropic polypeptide (GIP)" OR "glucagon" with no date or study duration restrictions. The results of our search showed that treatment with GLP-1 and dual GLP-1 and GIP receptor agonists results in robust reductions in bodyweight and glycated haemoglobin (HbA_{1c}) in participants with obesity and type 2 diabetes. Weight reduction has been challenging and less pronounced in people living with obesity when they also have type 2 diabetes. The highest efficacy has been observed with the dual GIP and GLP-1 receptor agonist tirzepatide, amylin and GLP-1 receptor co-agonist cagrilintide–semaglutide, and the GIP, GLP-1, and glucagon triple receptor agonist retatrutide. In a phase 3 trial in participants with type 2 diabetes, retatrutide has shown weight reduction beyond that observed with GLP-1 and dual GIP and GLP-1 receptor agonists.

Added value of this study

TRIUMPH-2 was an 80-week phase 3 trial assessing the efficacy and safety of retatrutide (4 mg, 9 mg, or 12 mg) as an adjunct to lifestyle modification in adults with a BMI of 27 kg/m^2 or higher and type 2 diabetes. The primary objective focused on changes in bodyweight. Treatment with retatrutide resulted in significant bodyweight reductions beyond those previously observed in this population with GLP-1 and dual GIP and GLP-1 receptor agonists. In a subgroup of participants with baseline BMI of 35 kg/m^2 or higher, bodyweight reduction was even more pronounced. Additionally, retatrutide treatment was associated with reductions in HbA_{1c}, as well as improvements in cardiometabolic risk factors and quality of life in both populations. The safety profile was generally similar to other GLP-1 and dual GIP and GLP-1 receptor agonists, with the most commonly reported adverse events being gastrointestinal events with retatrutide treatment. TRIUMPH-2 demonstrated that retatrutide could deliver clinically meaningful and significant weight reduction, along with associated improvements in glycaemic control, cardiometabolic risk factors, and quality of life for people with obesity and type 2 diabetes.

Implications of all the available evidence

Findings from TRIUMPH-2 suggest that retatrutide might advance the treatment of people with obesity and type 2 diabetes, a population in which weight reduction has been challenging. Retatrutide showed substantial reduction in bodyweight alongside improvements in glycaemic control and cardiometabolic risk factors, with a safety profile generally similar to other molecules with GLP-1 receptor agonist activity. These findings support obesity treatment as a strategy for people with obesity and type 2 diabetes. Further studies are required to determine whether these benefits translate to improvements in other obesity-related complications.

An **atypical meningioma** is a WHO Grade 2 brain and spinal cord tumor. It represents an intermediate level of aggressiveness between slow-growing (benign, Grade 1) meningiomas and fast-growing (malignant, Grade 3) anaplastic meningiomas.

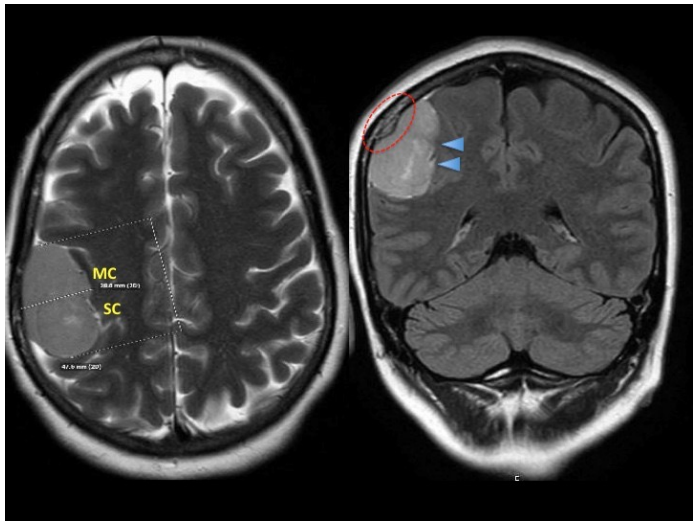

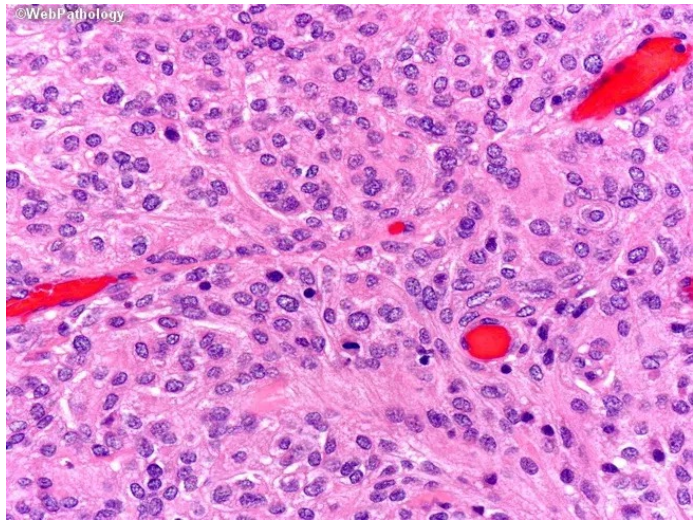

Key Characteristics

- **Prevalence:** They make up roughly **5% to 20%** of all diagnosed meningiomas.
- **Growth and Behavior:** They grow faster than Grade 1 tumors, are more locally aggressive, and have a higher likelihood of invading nearby brain tissue or bone.
- **Recurrence Risk:** They recur more frequently—with a 5-year recurrence rate of roughly **29% to 52%** compared to about 12% for Grade 1 tumors.

Radiotherapy versus observation following surgical resection of WHO grade 2 atypical meningioma (ROAM/EORTC-1308): an international, multicentre, open-label, phase 3, randomised controlled trial

Summary

Background WHO grade 2 atypical meningioma is a primary brain tumour with a high risk of recurrence even after complete surgical resection. The role of adjuvant radiotherapy remains uncertain. We aimed to assess whether adjuvant radiotherapy reduces recurrence compared with observation in patients with a newly diagnosed atypical meningioma who have undergone complete surgical resection.

Methods ROAM/EORTC-1308 was an international, multicentre, open-label, phase 3, randomised controlled trial, conducted at 58 hospitals and academic centres in 11 countries. Eligible sites had appropriate multidisciplinary expertise, neurosurgery, and radiotherapy facilities. Patients aged 16 years or older who had undergone a surgeon-assessed complete surgical resection of newly diagnosed atypical meningioma were randomly assigned (1:1) to adjuvant radiotherapy or observation. Randomisation was done using a web-based interface using random variable blocks of sizes two and four, stratified by location (UK or non-UK). Participants assigned to the radiotherapy group received fractionated external-beam intensity-modulated radiotherapy at a total dose of 60 Gy in 30 fractions over 6 weeks. Participants were followed up for a minimum of 4 years. The primary outcome was disease-free survival, defined as time from surgery to MRI-confirmed recurrence or death due to any cause, analysed in all randomly assigned participants in their assigned treatment group. Harms analysis was done in the as-treated population. The trial was registered with ISRCTN, ISRCTN71502099, and has completed.

Findings Between April 28, 2016, and May 21, 2021, 990 patients were assessed for eligibility, 157 of whom were randomly assigned to radiotherapy (n=78) or observation (n=79). Median age was 57·40 years (IQR 49·09–66·93); 84 (54%) participants were female and 73 (46%) were male. At a median follow-up of 64 months (IQR 50–75), meningioma recurrence occurred in 11 (14%) of 78 participants in the radiotherapy group and 24 (30%) of 79 in the observation group. 5-year disease-free survival was 79·9% (95% CI 67·6–87·9) in the radiotherapy group and 64·3% (51·9–74·2) in the observation group (absolute difference 15·6% percentage points [95% CI 0·6–30·5]). Disease-free survival was improved in the radiotherapy group compared with the observation group (hazard ratio 0·51 [95% CI 0·27–0·97]; p=0·0396). Grade 2 or 3 radiation-related serious adverse events occurred in five (8%) of 66 participants in the radiotherapy group, with no treatment-related deaths.

Interpretation Our findings suggest that adjuvant radiotherapy should be considered in patients with atypical meningioma after complete surgical resection of atypical meningioma when the prevention of recurrence is valued higher than the potential delayed adverse effects of radiotherapy. This practice will benefit patients by reducing meningioma recurrence. Decisions should be based on individual discussion with the patient.

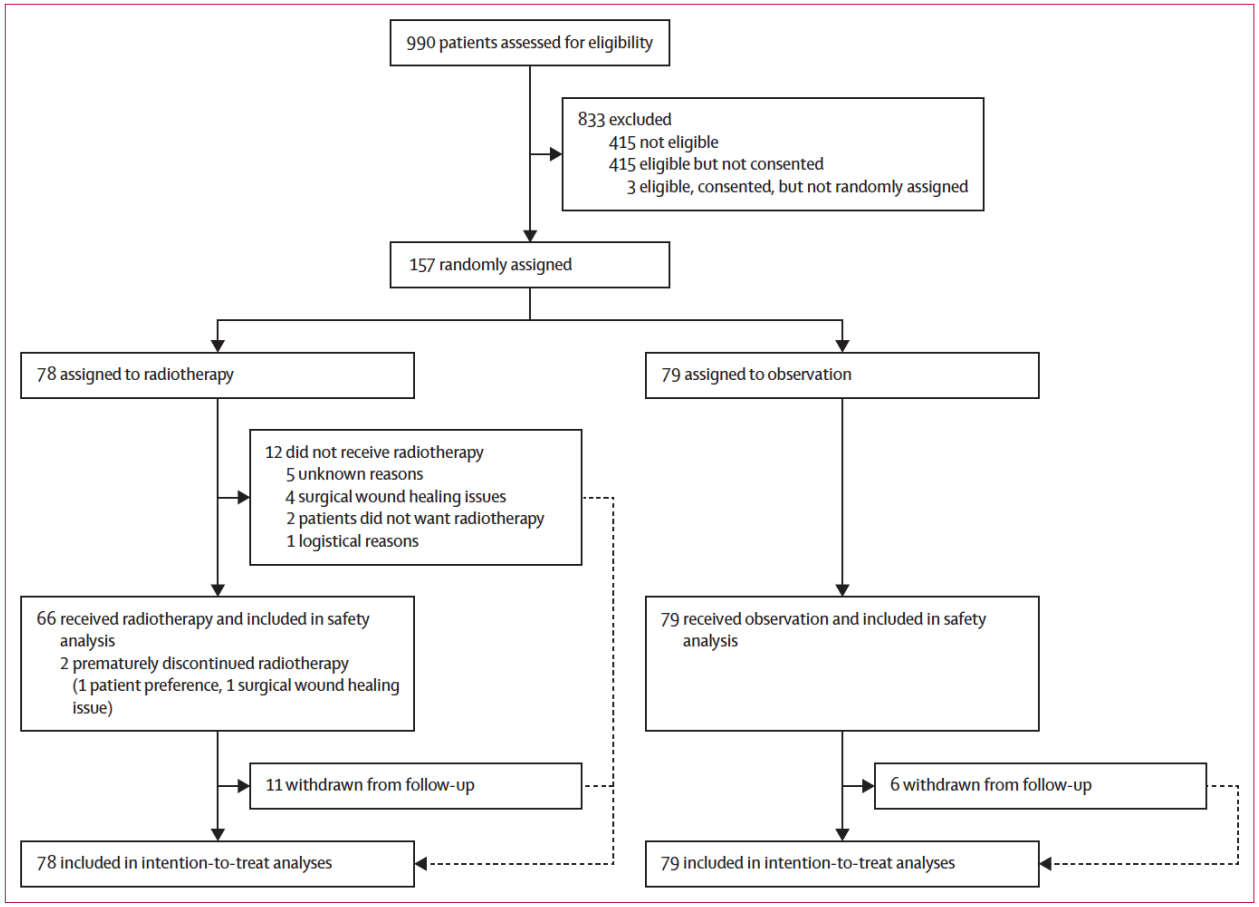

Figure 1: **Trial profile**

	Radiotherapy group (n=78)	Observation group (n=79)
Sex		
Female	41 (53%)	43 (54%)
Male	37 (47%)	36 (46%)
Age, years		
Median (IQR)	56·94 (49·29–64·38)	59·44 (48·01–68·92)
Range	33·36–77·40	26·44–77·06
WHO performance status		
0	42 (54%)	40 (51%)
1	31 (40%)	34 (43%)
2	5 (6%)	5 (6%)
Simpson grade		
Grade I	33 (42%)	39 (49%)
Grade II	37 (47%)	37 (47%)
Grade III	8 (10%)	3 (4%)
Tumour location		
N	70	75
Anterior cranial fossa	13 (19%)	7 (9%)
Convexity	23 (33%)	34 (45%)
Falcine or parasagittal	24 (34%)	16 (21%)
Posterior fossa	3 (4%)	4 (5%)
Sphenoid wing	5 (7%)	8 (11%)
Tentorial	2 (3%)	0
Other	0	6 (8%)
Missing	8	4
Seizures at presentation		
N	74	79
Yes	16 (22%)	18 (23%)
No	58 (78%)	61 (77%)
Missing	4	0

Data are n (%), unless otherwise specified.

Table 1: **Characteristics of the intention-to-treat population at baseline**

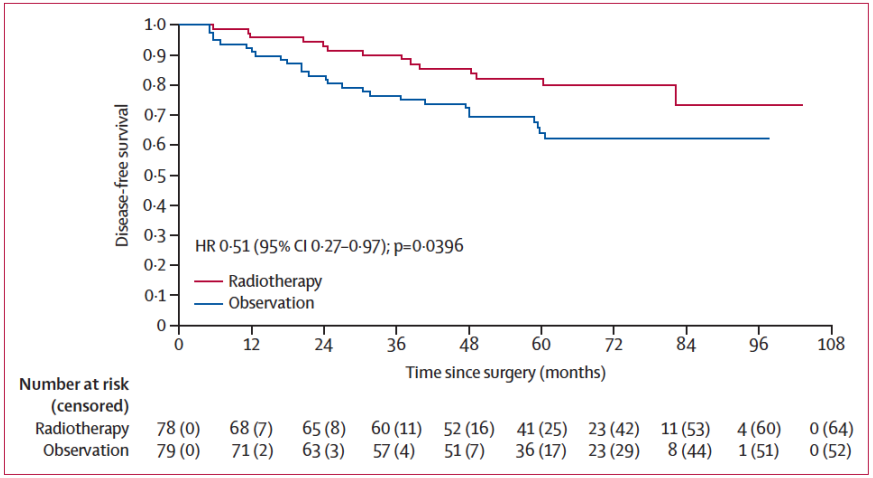

Figure 2: **Kaplan–Meier estimates of disease-free survival by treatment group in the intention-to-treat population**

Median follow-up was 64 months (IQR 50–75). HR=hazard ratio.

	Radiotherapy group (n=66)										Observation group (n=91)									
	Grade 1		Grade 2		Grade 3		Grade 4		Overall		Grade 1		Grade 2		Grade 3		Grade 4		Overall	
	Events	Patients	Events	Patients	Events	Patients	Events	Patients	Events	Patients	Events	Patients	Events	Patients	Events	Patients	Events	Patients	Events	Patients
Early adverse events within 90 days																				
Alopecia	8	8 (12%)	7	7 (11%)	0	0	0	0	15	14 (21%)	0	0	0	0	0	0	0	0	0	0
Fatigue	16	14 (21%)	9	9 (14%)	0	0	0	0	25	20 (30%)	0	0	0	0	0	0	0	0	0	0
Headache	8	7 (11%)	5	5 (8%)	0	0	0	0	13	11 (17%)	2	2 (2%)	1	1 (1%)	0	0	0	0	3	2 (2%)
Other (not related to study treatment)	27	16 (24%)	9	6 (9%)	0	0	0	0	36	20 (30%)	2	2 (2%)	0	0	0	0	0	0	3	3 (3%)
Scalp erythema	11	10 (15%)	1	1 (2%)	0	0	0	0	12	10 (15%)	0	0	0	0	0	0	0	0	0	0
Seizures	0	0	3	3 (5%)	1	1 (2%)	0	0	4	4 (6%)	1	1 (1%)	0	0	1	1 (1%)	0	0	2	2 (2%)
Transient neurological symptoms	15	13 (20%)	1	1 (2%)	1	1 (2%)	0	0	17	14 (21%)	4	3 (3%)	2	1 (1%)	0	0	0	0	6	3 (3%)
Late adverse events after 90 days																				
Cognitive decline	7	5 (8%)	1	1 (2%)	0	0	0	0	8	6 (9%)	6	5 (5%)	2	1 (1%)	0	0	0	0	8	5 (6%)
Leukoencephalopathy	1	1 (2%)	1	1 (2%)	0	0	0	0	2	2 (3%)	0	0	0	0	0	0	0	0	0	0
Other (not related to study treatment)*	56	22 (33%)	19	13 (20%)	3	1 (2%)	0	0	80	27 (41%)	49	23 (25%)	26	16 (18%)	10	9 (10%)	1	1 (1%)	87	34 (37%)
Seizures and epilepsy	3	2 (3%)	6	5 (8%)	2	2 (3%)	0	0	11	7 (11%)	6	5 (5%)	7	6 (7%)	0	0	0	0	13	10 (11%)

Data are number of events or n (%). Adverse events were graded according to Common Terminology Criteria for Adverse Events. There were five adverse events in the radiotherapy group and six adverse events in the observation group for which the treatment starting date or the adverse event onset date was missing, so they could not be categorised as early (within 90 days) or late (after 90 days) adverse events and are not included in this table. *There were two events in the radiotherapy group and one in the observation group for which the grade was missing; they have been included only in the overall column.

Table 2: **Early and late adverse events in the as-treated population**

	Radiotherapy group (n=60)	Observation group (n=72)
Methylation class		
Benign	41 (68%)	41 (57%)
Intermediate	18 (30%)	29 (40%)
Malignant	1 (2%)	2 (3%)
Integrated score		
Low	24 (40%)	26 (36%)
Intermediate	30 (50%)	40 (56%)
High	6 (10%)	6 (8%)
1p loss*		
Yes	28 (47%)	37 (51%)
No	32 (53%)	35 (49%)
***CDKN2A/B* deletion†**		
Yes	5 (8%)	5 (7%)
No	55 (92%)	67 (93%)
***TERT* promoter mutation**		
Yes	0	1 (1%)
No	60 (100%)	71 (99%)

Data are n (%). *Whole-arm loss for nine (15%) participants in the radiotherapy group and 16 (22%) in the observation group; segmental loss for 19 (32%) participants in the radiotherapy group and 21 (29%) in the observation group. †Homozygous deletion for two (3%) participants in the radiotherapy group and two (3%) in the observation group; heterozygous loss for three (5%) participants in the radiotherapy group and three (4%) in the observation group.

***Table 3*: Molecular characteristics of the subgroup with tissue available for analysis**

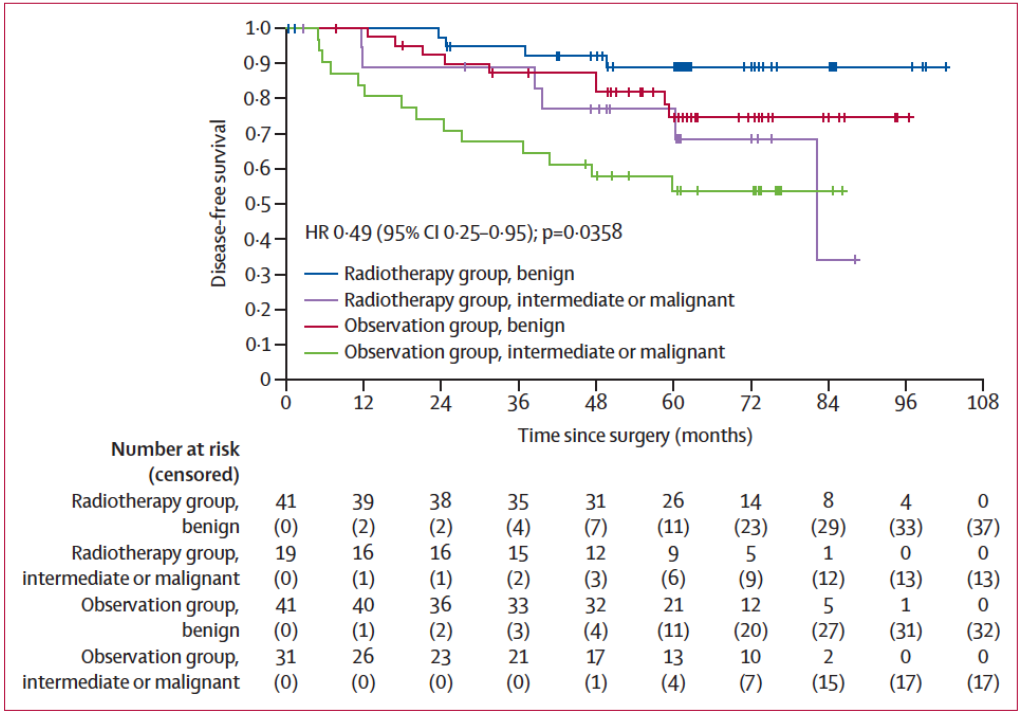

***Figure 3*: Exploratory post-hoc analysis of Kaplan–Meier estimates of disease-free survival stratified by treatment group and methylation class**

Post-hoc analysis included a molecular subset of 132 participants (radiotherapy group n=60; observation group n=72). Methylation class was categorised as benign versus intermediate or malignant. HR=hazard ratio.

Research in context

Evidence before this study

The management of completely resected WHO grade 2 atypical meningiomas has remained controversial because treatment recommendations and guidelines have relied almost entirely on retrospective studies. These tumours are rare, but changes to the WHO classification in 2000 and 2007 led to an increase in diagnosis of atypical meningiomas from 5% to 20–25% of all meningiomas. When this study was conceived in 2011, there was no randomised trial evidence and the literature comprised multiple, single institution, retrospective studies of between ten and 114 patients. Some studies reported a reduced recurrence rate with adjuvant radiotherapy, whereas others reported that radiotherapy did not reduce recurrence rate. A 2014 systematic review of 398 patients from ten retrospective studies reported a 5-year progression-free survival of 38–100% for those receiving radiotherapy, and 44–77% in those undergoing surgery alone. A PubMed search from database inception to Aug 26, 2026, for the terms "atypical meningioma" and "radiotherapy" in the title or abstract, with article filters set to "clinical trial" and all languages, yielded 15 articles. There was one randomised controlled trial protocol (ROAM/EORTC-1308). There were two prospective, non-randomised, phase 2 trials of adjuvant radiotherapy. The remaining 13 were non-randomised studies of systemic therapy, radiosurgery, radionucleotide therapy, carbon ion irradiation, and boron neutron capture therapy. These findings highlight the need for a randomised controlled trial to inform clinical practice, guidelines, and health-care policy.

Added value of this study

To our knowledge, ROAM/EORTC-1308 is the first randomised controlled trial evaluating the role of adjuvant fractionated radiotherapy for reducing the risk of recurrence in patients who have undergone complete resection of an atypical meningioma. Compared with observation, adjuvant fractionated radiotherapy significantly improved disease-free survival. There were no between-group differences in health-related quality of life or neurocognitive function and there was minimal radiation toxicity.

Implications of all the available evidence

From both the patient's and clinician's perspectives, efforts should be made to reduce the risk of meningioma recurrence. Salvage treatment often requires repeat surgery or radiotherapy, or both, which affects health-related quality of life. Having shown a marked reduction in recurrence, the ROAM/EORTC-1308 trial has provided the best available evidence to support the use of adjuvant fractionated radiotherapy in patients who have undergone complete surgical resection of atypical meningioma. The trial will inform national and international guidelines.

Adolescents living with HIV (ALHIV) face unique global health, developmental, and treatment challenges compared to adults.

Key Global Statistics & Demographics

- **Population Size:** There are approximately 1.57 million to 2.4 million children and adolescents (ages 10–19) living with HIV globally.
- **New Infections:** Adolescents account for roughly 11% to 12% of all new HIV infections, with young women and girls disproportionately affected (representing roughly 70% to 90% of new adolescent infections in sub-Saharan Africa).
- **Treatment Coverage:** Antiretroviral therapy (ART) coverage for adolescents (around 64–65%) lags behind adult coverage rates (roughly 77%).

Switch to injectable cabotegravir–rilpivirine given every 8 weeks in adolescents living with HIV with virological suppression in sub-Saharan Africa (LATA): a randomised, open-label, multicentre, 96-week non-inferiority trial

Summary

Background Adolescents living with HIV have poorer treatment outcomes than other age groups and might benefit from long-acting-injectable (LAI) antiretroviral therapy (ART). We evaluated efficacy and safety of LAI cabotegravir–rilpivirine compared with daily oral ART in adolescents living with HIV with virological suppression in Africa.

Methods LATA, a randomised, open-label, multicentre, non-inferiority trial, recruited adolescents with HIV aged from 12 years to younger than 20 years from five clinics in Kenya, South Africa, Uganda, and Zimbabwe. Participants had to have virological suppression (HIV-1 viral load <50 copies per mL) for more than 12 months and no previous treatment failure. Participants were randomly assigned (1:1) to receive either LAI cabotegravir–rilpivirine (LAI group) or daily oral dolutegravir–lamivudine–tenofovir disoproxil fumarate (TLD; control group). Randomisation was stratified by clinical centre and mode of infection (vertical *vs* horizontal or other). Participants, clinical staff, and researchers were unmasked to treatment allocation, whereas laboratory staff measuring viral loads were masked. Participants in the LAI group were assigned to receive cabotegravir (600 mg)–rilpivirine (900 mg) intramuscular injections at weeks 4, 8, 16, and every 8 weeks thereafter. Participants in the control group were assigned to receive the oral fixed-dose combination, dolutegravir (50 mg)–lamivudine (300 mg)–tenofovir disoproxil fumarate (300 mg), every day. Viral loads were measured every 24 weeks. The primary outcome was the proportion of participants with two consecutive (confirmed) viral load measurements equal to or higher than 50 copies per mL by week 96, estimated using adjusted Kaplan–Meier methods, by intention to treat. The non-inferiority margin and confidence level depended on the control event rate (8·9% margin, 99% CI, for 6% event rate). If non-inferiority was demonstrated, superiority was assessed at the α=5% level. This trial is completed and registered with ClinicalTrials.gov, NCT05154747.

Findings Between June 22, 2023, and April 15, 2024, 476 of 560 screened adolescents with HIV were enrolled in LATA and randomly assigned to either the LAI group (n=235) or the control group (n=241). Of the 476 randomised participants, 466 (98%) had acquired HIV vertically, and 200 (42%) were recruited from Uganda, 128 (27%) from Zimbabwe, 77 (16%) from Kenya, and 71 (15%) from South Africa. Median age was 16·5 years (IQR 14·8–18·1), 256 (54%) participants were female, 220 (46%) were male, 474 (>99%) were Black, and median duration of previous ART was 11·7 years (IQR 8·5–14·1). Median follow-up was 120 weeks (IQR 104–128). Two participants in the LAI group had confirmed viral load of 50 copies per mL or higher by week 96 (Kaplan–Meier estimated proportion 0·9%, 95% CI 0·0 to 2·2) versus 15 participants (6·4%, 3·7 to 9·8) in the control group (estimated difference –5·5%, 99% CI –10·3 to –1·5). LAI met the non-inferiority criterion and demonstrated superiority over control (p=0·0013). By the end of follow-up, seven participants permanently discontinued LAI (one confirmed viral load ≥200 copies per mL, two LAI-related adverse events [serious hypersensitivity reaction; non-serious drug eruption], one incident tuberculosis, two planning pregnancy, and one participant choice). There were 14 serious adverse events (in 14 participants) in the LAI group, including one homicide, compared with 18 (in 12 participants) in the control group, including one death from metastatic osteosarcoma (hazard ratio [HR] 1·16, 95% CI 0·54 to 2·51; p=0·71). The only treatment-related serious adverse event was hypersensitivity reaction. There were 31 adverse events of grade 3 or higher (in 27 participants) in the LAI group and 34 (in 26 participants) in the control group (HR 1·07, 0·62 to 1·83; 0·81). These events included four injection-site reactions (in the LAI group); otherwise, adverse event profiles were similar between trial groups.

Interpretation In adolescents with HIV with virological suppression, LAI cabotegravir–rilpivirine was superior to TLD for maintaining virological suppression, with no new safety concerns observed. These findings support LAI cabotegravir–rilpivirine as a maintenance treatment option for this population.

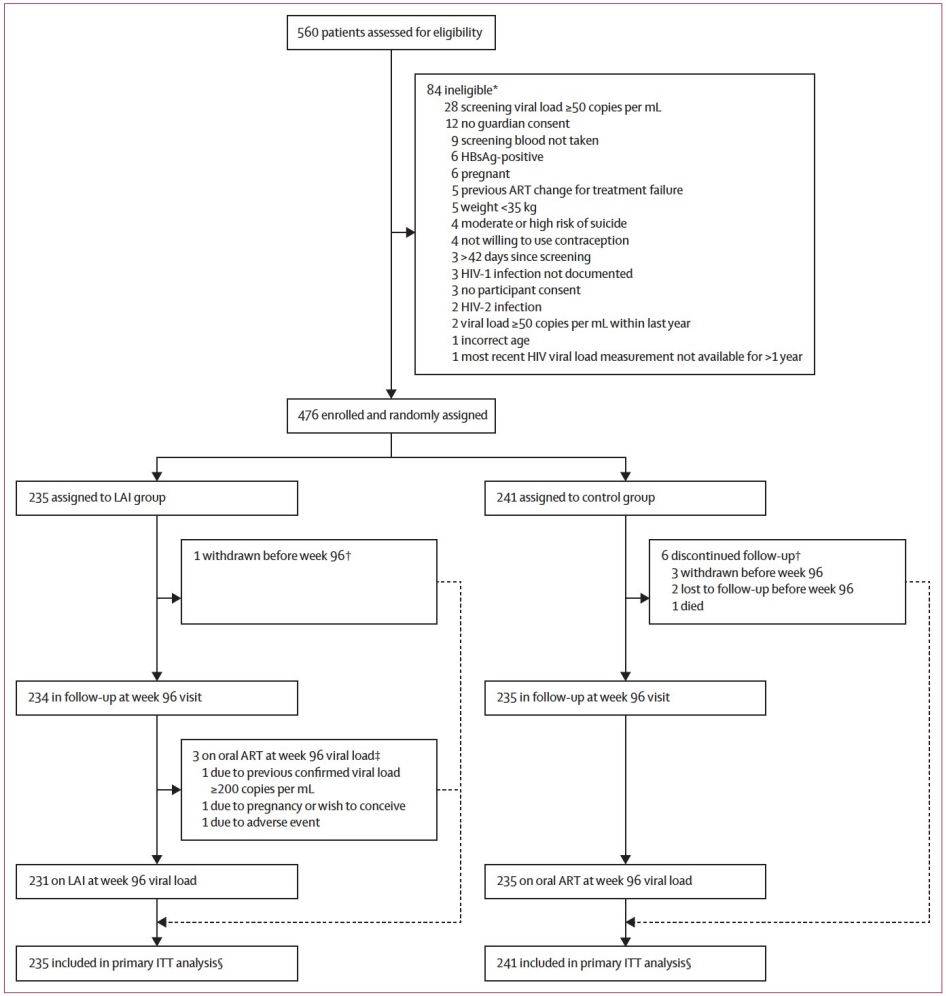

Figure 1: **Trial profile**
Participants in LAI group were allocated to receive cabotegravir–rilpivirine intramuscular injections and participants in the control group were allocated to receive a daily oral fixed-dose combination of dolutegravir–lamivudine–tenofovir disoproxil fumarate. ART=antiretroviral therapy. HBsAg=hepatitis B surface antigen. ITT=intention-to-treat. LAI=long-acting injectable. *Reasons for ineligibility not mutually exclusive. †No participants who died, withdrew, or were lost to follow-up had met the primary endpoint. ‡Two participants were on LAI at week 96 viral load measurement but returned to oral ART at this visit. §All randomised participants contributed up to meeting the primary endpoint or censoring.

	LAI group (n=235)	Control group (n=241)	Total (n=476)
Age, years	16·5 (14·8–18·3)	16·4 (14·7–17·8)	16·5 (14·8–18·1)
Sex			
Male	97 (41%)	123 (51%)	220 (46%)
Female	138 (59%)	118 (49%)	256 (54%)
Country			
Kenya	39 (17%)	38 (16%)	77 (16%)
South Africa	35 (15%)	36 (15%)	71 (15%)
Uganda	98 (42%)	102 (42%)	200 (42%)
Zimbabwe	63 (27%)	65 (27%)	128 (27%)
Ethnicity			
Asian	2 (1%)	0	2 (<1%)
Black	233 (99%)	241 (100%)	474 (100%)
Mode of HIV acquisition			
Vertical	232 (99%)	234 (97%)	466 (98%)
Other*	1 (<1%)	4 (2%)	5 (1%)
Unknown	2 (1%)	3 (1%)	5 (1%)
Weight, kg	50·2 (44·6–56·6)	49·4 (44·2–55·4)	50·0 (44·3–55·9)
BMI, kg/m²	19·8 (18·1–21·7)	19·4 (18·0–21·6)	19·6 (18·0–21·6)
Total cholesterol, mmol/L	3·3 (2·9–3·9)	3·2 (2·7–3·8)	3·3 (2·8–3·8)
Estimated glomerular filtration rate, mL/min	115 (101–133)	115 (100–135)	115 (101–134)
CD4 T-cell count, cells per µL	823 (652–1007)	848 (658–1042)	832 (653–1034)
CD8 T-cell count, cells per µL	652 (505–803)	665 (518–824)	659 (516–814)
Time since HIV diagnosis, years	12·8 (10·2–15·5)	12·5 (9·7–15·1)	12·6 (10·0–15·3)
Time spent on antiretroviral therapy, years	11·8 (9·2–14·2)	11·6 (7·9–13·9)	11·7 (8·5–14·1)
Previous use of dolutegravir	235 (100%)	239 (99%)	474 (100%)
Time spent on dolutegravir, years	3·5 (2·8–4·1)	3·5 (2·8–4·2)	3·5 (2·8–4·2)
Previous use of NNRTIs	201 (86%)	193 (80%)	394 (83%)
Time spent on NNRTIs, years	7·0 (2·8–9·9)	6·1 (2·4–9·3)	6·4 (2·7–9·7)
Previously received full HBV vaccine course	193 (82%)	205 (86%)	398 (84%)

Data are median (IQR) or n (%). Data for ethnicity and race were collected at enrolment by investigators according to the following categories: Asian, Black, Hispanic or Latinx, White, and other. Three participants were missing data for baseline total cholesterol, two were missing data for baseline estimated glomerular filtration rate, three were missing data for baseline CD4 cell count, and three were missing data for baseline CD8 cell count. Two participants in the control group had missing HBV vaccination status and are excluded from the denominator for percentages. 68 (89%) of 76 participants who had not previously received a full HBV vaccination course received the full course during the trial. Those with no previous use of dolutegravir or NNRTIs contribute 0 years to the summary of time on dolutegravir–NNRTIs. All 474 participants with previous use of dolutegravir were on dolutegravir immediately before randomisation (473 participants were on tenofovir disoproxil fumarate–lamivudine–dolutegravir). HBV=hepatitis B virus. LAI=long-acting injectables. NNRTI=non-nucleoside reverse transcriptase inhibitor. *Other mode of HIV transmission included four participants (one in the LAI group, three in the control group) with sexually acquired HIV and one (in control group) with HIV acquired through suspected malicious infection via blood. In error, one participant with vertically acquired HIV was randomly assigned in the stratum for horizontal or other mode of infection, and one participant with HIV acquired through sexual contact was randomly assigned in the stratum for vertical mode of infection.

Table 1: **Baseline characteristics of study participants**

	LAI group (n=235)		Control group (n=241)		Risk difference, LAI *vs* control (CI)	p value
	Number of participants	Estimated proportion, % (95% CI)	Number of participants	Estimated proportion, % (95% CI)		
Primary outcome						
Confirmed HIV-1 RNA ≥50 copies per mL by week 96	2	0·9% (0·0 to 2·2)	15	6·4% (3·7 to 9·8)	−5·5% (99% CI −10·3 to −1·5)*	0·0013
Secondary outcomes						
HIV-1 RNA ≥50 copies per mL at week 48 using modified FDA snapshot	1	0·4% (0·0 to 2·3)	3	1·2% (0·3 to 3·6)	−0·8% (−2·4 to 0·8)	0·32
HIV-1 RNA ≥50 copies per mL at week 96 using modified FDA snapshot	1	0·4% (0·0 to 2·3)	8	3·3% (1·4 to 6·4)	−2·8% (−5·2 to −0·5)	0·018
HIV-1 RNA <50 copies per mL at week 24	231/235	98·3% (96·6 to 100·0)	229/239	95·8% (93·3 to 98·4)	2·4% (−0·5 to 5·4)	0·11
HIV-1 RNA <50 copies per mL at week 48	232/235	98·7% (97·3 to 100·0)	224/234	95·7% (93·1 to 98·3)	2·9% (0·0 to 5·8)	0·049
HIV-1 RNA <50 copies per mL at week 96	233/234	99·6% (98·7 to 100·0)	222/234	94·9% (92·0 to 97·7)	4·6% (1·7 to 7·5)	0·0019
Confirmed HIV-1 RNA ≥200 copies per mL by week 96	2	0·9% (0·0 to 2·6)	6	2·5% (0·8 to 5·1)	−1·7% (−4·3 to 0·5)	0·18
Confirmed HIV-1 RNA ≥1000 copies per mL by week 96	2	0·9% (0·0 to 2·6)	2	0·8% (0·0 to 2·2)	0·0% (−1·3 to 1·7)	0·98
Major resistance mutations following confirmed HIV-1 RNA ≥50 copies per mL by week 96						
INSTI-resistant	1/2	50% (1 to 99)	0/8	0% (0 to 37)	..	..
NRTI-resistant	0/2	0% (0 to 84)	1/8	12% (0 to 53)	..	..
NNRTI-resistant	1/2	50% (1 to 99)	2/8	25% (3 to 65)	..	..
PI-resistant	0/2	0% (0 to 84)	0/8	0% (0 to 37)	..	..

Data are n, n/N or % (95% CI), unless otherwise indicated. Participants in LAI group were allocated to receive cabotegravir–rilpivirine intramuscular injections and participants in the control group were allocated to receive a daily oral fixed-dose combination of dolutegravir–lamivudine–tenofovir disoproxil fumarate. Proportions for the primary analysis and confirmed HIV-1 RNA (viral load) ≥1000 copies per mL and ≥200 copies per mL are based on adjusted Kaplan–Meier estimates. CIs (calculated with bias-corrected percentiles) and p values are based on at least 1000 bootstrap samples (10 000 for the primary analysis and 1000 otherwise, adjusted for site). p values and CIs for viral loads <50 copies per mL at each week are based on adjusted logistic regression. Proportions as well as CIs and p values for the modified FDA snapshot algorithm are based on the Cochran–Mantel–Haenszel test stratified by region (eastern or southern Africa). Results from unadjusted test of proportions for the primary outcome: two of 235 participants in the LAI group *vs* 15 of 241 participants in the control group, difference −5·4% (95% CI −8·6 to −2·1, 99% CI −9·7 to −1·1; p=0·002). All participants contributed to the analyses of confirmed viral loads of ≥50, 200, and 1000 copies per mL, and to analysis of the FDA snapshot. The modified FDA snapshot algorithm uses the latest viral load within the respective visit window for participants who were on randomised treatment allocation (including those who had used oral bridging previously in the LAI group, provided the viral load before bridging was <50 copies per mL). Participants who had switched from allocated treatment or exited the trial are assigned either as viral load ≥50 copies per mL if their latest on-treatment viral load ≥50 copies per mL, or as no virological data if their latest on-treatment viral load <50 copies per mL or they had no viral load data within the visit window (appendix 1 p 51). Resistance testing was not possible for four participants due to insufficient viraemia (all in the control group), and no results were available for a further three participants for whom the sample failed to amplify (all in the control group). FDA=US Food and Drug Administration. INSTI=integrase strand transfer inhibitor. LAI=long-acting injectables. NNRTI=non-nucleoside reverse transcriptase inhibitor. NRTI=nucleoside reverse transcriptase inhibitor. PI=protease inhibitor. *99% CI used for estimated proportion with confirmed viral load of ≥50 copies per mL for the LAI group *vs* control group according to the Smooth Away From Expected (SAFE) non-inferiority framework; 95% CI is −9·1 to −2·4. 95% CIs are presented in all other cases.

Table 2: **Efficacy outcomes**

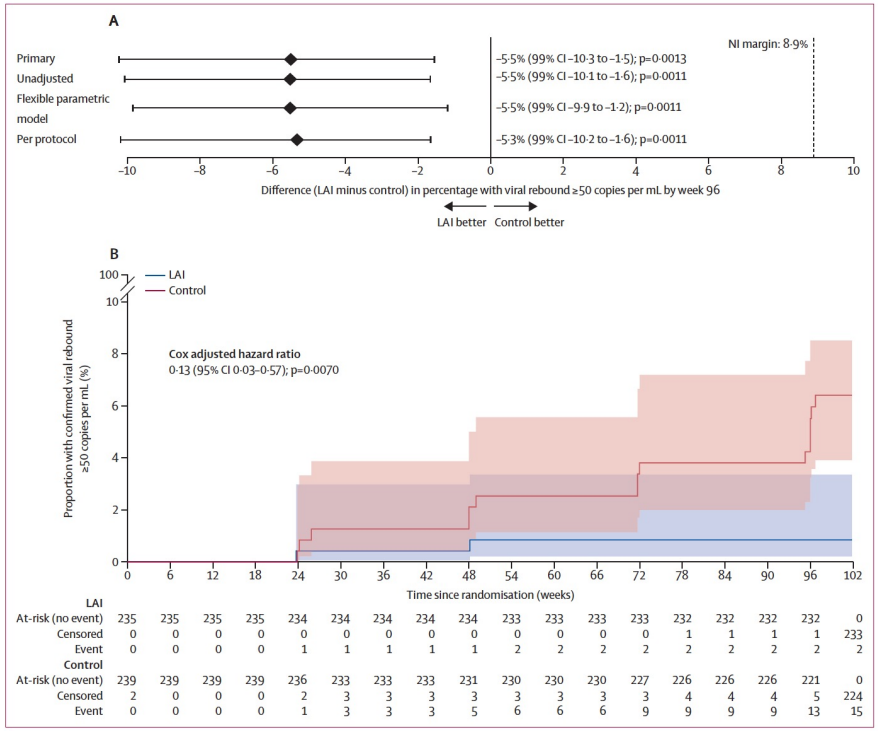

Figure 2: **Primary outcome findings**

(A) The difference between trial groups (LAI minus control) in the proportion of participants with confirmed viral rebound. (B) Kaplan–Meier estimate of the proportion of participants with confirmed viral rebound (first of two consecutive viral load measurements of ≥50 copies per mL) in the LAI and control groups. End of week 96 window is week 102 minus 1 day, events and follow-up are captured to this point. The risk table presented differs to that proposed initially by Morris and colleagues[21] as part of KMunicate. Here, "At-risk (no event)" includes those observed without the event up to and including time t; "Censored" includes those censored before time t; and "Event" includes those with an event up to and including time t. Using this approach, we assumed that the outcome was known before censoring where both occur on same day. The Cox-adjusted hazard ratio was a secondary analysis of the treatment effect and should be interpreted as supportive of the primary analysis, given the small number of events (two in the LAI group). Please note the y-axis ranges from 0 to 10%, for a representation of this graph with a y-axis ranging from 0 to 100% see appendix 3 (p 18). Participants in the LAI group were allocated to receive cabotegravir–rilpivirine intramuscular injections and participants in the control group were allocated to receive a daily oral fixed-dose combination of dolutegravir–lamivudine–tenofovir disoproxil fumarate. LAI=long-acting injectables. NI=non-inferiority.

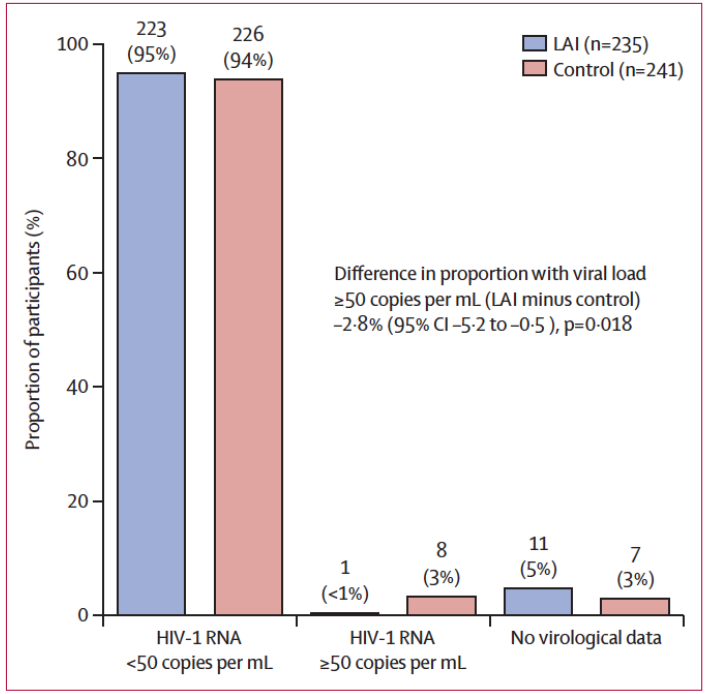

Figure 3: **Modified FDA snapshot algorithm**

The modified FDA snapshot algorithm uses the latest viral load within the respective visit window for participants who were on randomised treatment allocation (including those who had used oral bridging previously in the LAI group, provided the viral load before bridging was <50 copies per mL). Participants who had switched from allocated treatment or exited the trial were assigned either as viral load of at least 50 copies per mL if their latest on-treatment viral load was at least 50 copies per mL, or as no virological data if their latest on-treatment viral load was less than 50 copies per mL or if they had no viral load within the visit window (appendix 1 p 51). Participants in the LAI group were allocated to receive cabotegravir–rilpivirine intramuscular injections and participants in the control group were allocated to receive a daily oral fixed-dose combination of dolutegravir–lamivudine–tenofovir disoproxil fumarate. FDA=US Food and Drug Administration. LAI=long-acting injectables.

	LAI group (n=235)	Control group (n=241)	LAI *vs* control*	p value
Adverse events during follow-up				
WHO stage 3–4 events or deaths	3 events (3 participants)	2 events (2 participants)	1·50 (0·25 to 8·99)	0·66
Serious adverse events	14 events (14 participants)	18 events (12 participants)	1·16 (0·54 to 2·51)	0·71
Grade ≥3 clinical and laboratory adverse events	31 events (27 participants)	34 events (26 participants)	1·07 (0·62 to 1·83)	0·81
ART-modifying events†	5 events (5 participants)	1 event (1 participants)	5·17 (0·60 to 44·25)	0·13
Participants with change in assigned ART regimen‡	13 (5·5%)	0	5·5% (2·6 to 8·5)	0·0002
Safety laboratory measures, estimated mean change from baseline§				
Total cholesterol at week 96, mmol/L	0·60 (0·53 to 0·67)	0·10 (0·03 to 0·18)	0·49 (0·39 to 0·59)	<0·0001
Total-to-HDL cholesterol ratio at week 96	0·00 (−0·08 to 0·08)	0·00 (−0·08 to 0·08)	0·00 (−0·11 to 0·11)	0·98
eGFR at week 96, mL/min	10·60 (8·10 to 13·11)	−2·81 (−5·30 to −0·31)	13·41 (9·87 to 16·94)	<0·0001
CD4 T-cell count at week 48, cells per µL	−28·9 (−53·6 to −4·3)	−17·6 (−42·1 to 7·0)	−11·3 (−46·1 to 23·4)	0·52
CD4 T-cell count at week 96, cells per µL	−55·5 (−80·1 to −30·8)	−39·8 (−64·4 to −15·2)	−15·7 (−50·5 to 19·2)	0·38
CD4/CD8 ratio at week 48	0·02 (−0·01 to 0·06)	−0·04 (−0·08 to −0·00)	0·07 (0·01 to 0·12)	0·014
CD4/CD8 ratio at week 96	0·04 (−0·00 to 0·07)	−0·05 (−0·09 to −0·01)	0·08 (0·03 to 0·14)	0·0022
Anthropometric measures, estimated mean change from baseline§				
Bodyweight at week 48, kg	3·17 (2·72 to 3·63)	2·34 (1·88 to 2·80)	0·84 (0·19 to 1·49)	0·012
Bodyweight at week 96, kg	5·29 (4·82 to 5·75)	4·20 (3·74 to 4·66)	1·09 (0·43 to 1·74)	0·0011
BMI at week 48, kg/m²	0·74 (0·58 to 0·90)	0·34 (0·18 to 0·51)	0·40 (0·17 to 0·63)	0·0007
BMI at week 96, kg/m²	1·22 (1·05 to 1·38)	0·63 (0·47 to 0·80)	0·59 (0·35 to 0·82)	<0·0001

Data are number of events (number of participants), number of participants (%), or mean change (95% CI), unless otherwise indicated. Participants in LAI group were allocated to receive cabotegravir–rilpivirine intramuscular injections and participants in the control group were allocated to receive a daily oral fixed-dose combination of dolutegravir–lamivudine–tenofovir disoproxil fumarate. ART=antiretroviral therapy. eGFR=estimated glomerular filtration rate. LAI=long-acting injectables. *LAI versus control data represent HRs (95% CIs) for adverse events until close-out, difference in proportion for change in assigned ART regimen, and the differences in change from baseline for safety laboratory and anthropometric measures. HRs are based on time to first event, adjusted for site. All changes from baseline estimates are based on a linear random effects model on the original scale, adjusted for site and baseline value, with measurements truncated at the 1st and 99th percentile; conclusions were unchanged compared with those obtained using log-transformed outcomes or untruncated measures. †ART-modifying event was defined as any adverse event that led to a change in assigned ART, defined as a change to any component of the allocated regimen (excluding switches between tenofovir disoproxil fumarate and tenofovir alafenamide and between lamivudine and emtricitabine and use of oral ART for bridging in the injectables group) or change to ART dose. In the LAI group, one case of hypersensitivity reaction possibly related to LAI cabotegravir–rilpivirine led to permanent discontinuation, one case of drug eruption probably related to LAI cabotegravir–rilpivirine led to permanent discontinuation, one case of malaria that was initially considered to be oral rilpivirine-related anaemia led to discontinuation of oral lead-in but participant subsequently initiated LAI, one case of pulmonary tuberculosis unrelated to ART led to interruption to LAI cabotegravir–rilpivirine, and one case of lymph node tuberculosis unrelated to ART led to permanent discontinuation of LAI cabotegravir–rilpivirine. In the control group, one case of pulmonary tuberculosis considered unrelated to ART led to increase in dolutegravir dosing. ‡Change in assigned ART regimen defined as a change to any component of the allocated regimen, excluding switches between tenofovir disoproxil fumarate and tenofovir alafenamide and between lamivudine and emtricitabine, dose modification for tuberculosis, and use of oral ART for bridging in the Injectables groups. Seven of 13 participants discontinued injectables permanently, including three of seven discontinuations due to adverse events (hypersensitivity reaction, drug eruption, and lymph node tuberculosis described above). Six of 13 participants did not permanently discontinue injectables, including two of six interruptions due to adverse events (malaria and pulmonary tuberculosis described above). §Estimates presented are mean change from baseline values: total cholesterol 3·36 mmol/L, total-to-HDL cholesterol 3·23, eGFR 120·21 mL/min, CD4 T-cells 865 cells per µL, CD4/CD8 ratio 1·41, bodyweight 50·5 kg, BMI 20·1 kg/m². Number of participants contributing to each measure at each timepoint (LAI group and control group): total cholesterol 232 and 234, total-to-HDL cholesterol 232 and 234, eGFR 232 and 234, CD4 233 and 235 at week 48 and 232 and 233 at week 96, CD4/CD8 ratio 233 and 235 at week 48 and 232 and 233 at week 96, bodyweight 231 and 230 at week 48 and 224 and 225 at week 96, BMI 231 and 230 at week 48 and 224 and 225 at week 96. One participant in the control group diagnosed with metastatic osteosarcoma contributed six serious adverse events or adverse events grade ≥3 (one new event for each hospitalisation and death).

Table 3: **Safety outcomes**

Research in context

Evidence before this study

Long-acting injectable (LAI) cabotegravir–rilpivirine provides a potential solution for the adherence challenges of daily medication faced by adolescents living with HIV. We searched PubMed and Embase for articles published from Jan 1, 2000, to June 1, 2026, using the terms "cabotegravir", "rilpivirine", and "trial". We focused on randomised trials of LAI cabotegravir–rilpivirine given every 4 or 8 weeks compared with oral 3-drug antiretroviral therapy (ART) in adults or adolescents without known adherence challenges and single-arm trials in adolescents with virological suppression who switch to LAI cabotegravir–rilpivirine. Two trials evaluated early switch to LAI cabotegravir–rilpivirine in previously ART-naive adults aged 18 years or older who achieved virological suppression after 20 weeks of oral ART. LATTE-2 compared LAI cabotegravir–rilpivirine given every 4 weeks and every 8 weeks with oral cabotegravir plus abacavir–lamivudine taken daily, reporting non-inferior maintenance of viral suppression in the LAI groups through 96 weeks. FLAIR compared 4-weekly LAI cabotegravir–rilpivirine given every 4 weeks with oral abacavir–dolutegravir–lamivudine taken daily and also demonstrated non-inferiority, with 3% of participants in each trial group having HIV-1 RNA of 50 copies per mL or higher at week 96. Three trials investigated LAI cabotegravir–rilpivirine in treatment-experienced adults (aged ≥18 years) with virological suppression. ATLAS compared monthly LAI cabotegravir–rilpivirine with continued oral ART taken daily, and SOLAR compared every-2-month LAI cabotegravir–rilpivirine with continued oral bictegravir–emtricitabine–tenofovir alafenamide taken daily; both demonstrated non-inferiority of LAI at approximately 1 year. CARES, conducted in Uganda, Kenya, and South Africa, included 58% women (median age 42 years [IQR 35–51]) and evaluated switch to LAI cabotegravir–rilpivirine given every 8 weeks compared with continued daily oral ART with viral load monitoring every 24 weeks. At 96 weeks, 97% of participants in each group had viral load lower than 50 copies per mL. Although adults (aged ≥18 years) could be enrolled into these trials, few participants younger than 20 years were likely recruited, and median ages ranged from 34 to 42 years. IMPAACT 2017/MOCHA trial was a phase 1–2, multicentre, open-label, single-arm study in Botswana, South Africa, Thailand, Uganda, and USA. 144 adolescents (aged ≥12 to <18 years, weight ≥35 kg) who were treatment-experienced and had virological suppression were enrolled and switched to LAI cabotegravir–rilpivirine given every 8 weeks. There were no virological failures through week 96. These trials consistently demonstrated excellent safety and tolerability and strong patient preference for LAI cabotegravir–rilpivirine over daily ART, in addition to virological efficacy.

Added value of this study

The LATA trial is a large (n=476) randomised trial of LAI cabotegravir–rilpivirine in adolescents (aged 12–<20 years) with HIV with virological suppression and enrolled entirely in sub-Saharan Africa. LATA demonstrated superior virological efficacy of LAI cabotegravir–rilpivirine every 8 weeks compared with daily oral standard-of-care dolutegravir–lamivudine–tenofovir disoproxil fumarate in adolescents over 96 weeks, alongside reassuring safety, tolerability data, and strong patient preference. This provides clear evidence for the potential benefit of this treatment strategy with viral load monitoring every 24 weeks for adolescents with HIV with virological suppression.

Implications of all the available evidence

The results of the LATA trial, together with other phase 1–2 data in adolescents, extensive phase 3 adult trial data across multiple settings, and accumulating real-world evidence, provide strong evidence supporting LAI cabotegravir–rilpivirine as a maintenance treatment option for adolescents with HIV with virological suppression. While international guidelines now recommend LAI cabotegravir–rilpivirine for adolescents with virological suppression, significant barriers to delivery of this option remain for those who would benefit the most. Further evidence is required to explore its potential role for adolescents with non-suppressed HIV.

The arts as a global health resource: key priorities for future research

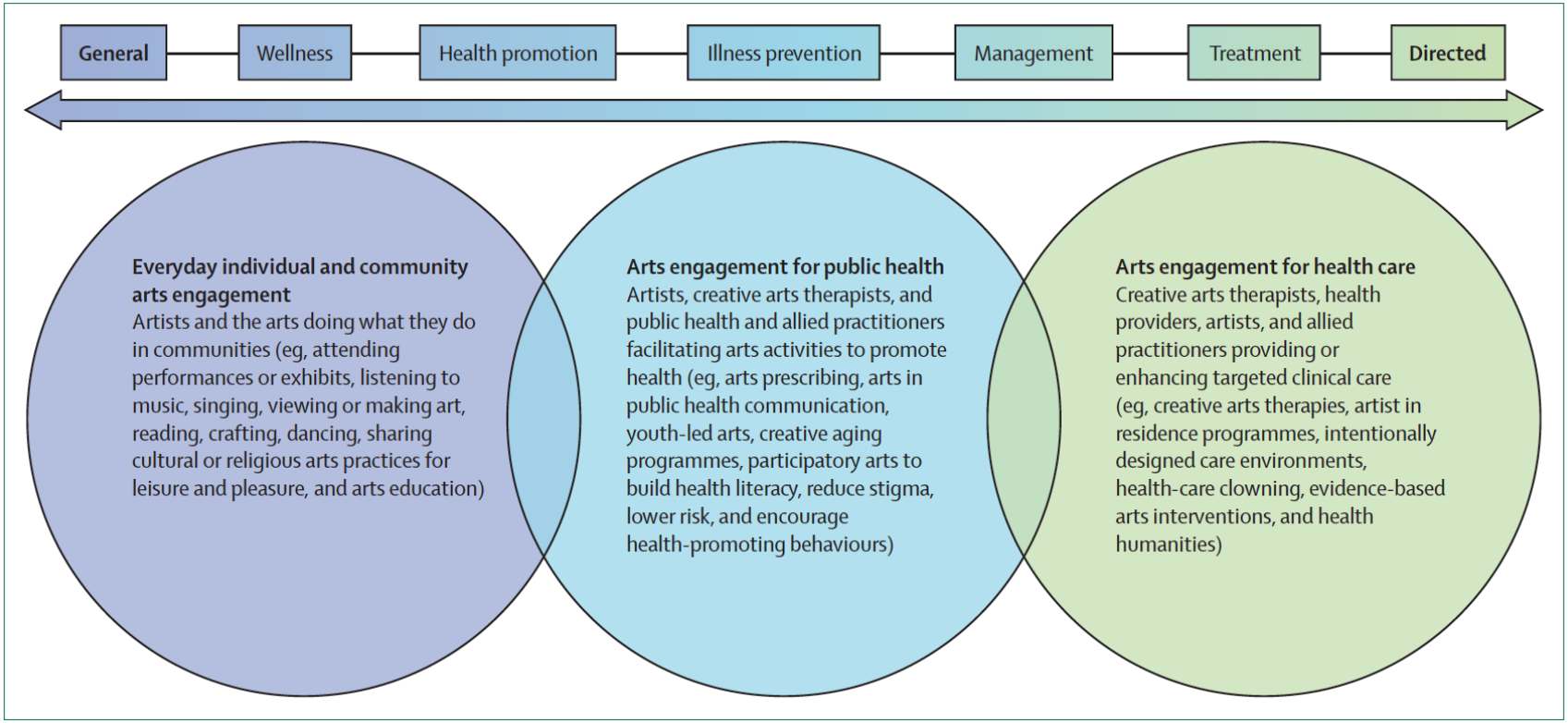

Figure: **Arts engagement across a continuum from health promotion and prevention to the management and treatment of health conditions in homes, schools, workplaces, and spiritual, community, and clinical settings, spanning universal arts exposure, to targeted public health initiatives, and more individualised health-care practices**

Developing roadmaps for advancing practice, research, and policy in the arts and health

Despite arts engagement being a ubiquitous human behaviour across human history, research and awareness on the health benefits of engagement are still emerging, accelerating over the past decade. Building on the evidence and research challenges outlined in the first paper of this *Lancet* collection, this Review puts forward a series of roadmaps for advancing research, policy, and practice to enable appropriate and effective integration of the arts into health and wellbeing systems globally. First and foremost, we advocate for the fundamental principle that all individuals, regardless of their characteristics and location, should have regular opportunities to engage in the arts, proposing policy and research steps to monitor and achieve this goal. Second, we emphasise the importance of implementing population-level strategies that use the arts as part of broader portfolios of approaches to help address the fundamental determinants of health inequities. Third, we underscore the necessity of developing and embedding across society diverse public-health pathways that connect individuals living with or at risk of health challenges to the arts within communities. Fourth, we argue for more clinical innovation in integrating bespoke evidence-based arts and creative arts therapies programmes into clinical care across the care pathway. Finally, we stress the crucial need for enhanced cross-sectoral stakeholder engagement and more strategic investment and research to facilitate the development and dissemination of the necessary tools, training, and evidence to achieve these objectives.

Key messages

- This paper makes a series of propositions (roadmaps) intended as a flexible template for how the mainstreaming of arts and health work could progress.
- Arts engagement is a health-enhancing behaviour that can advance equity by modifying structural and intermediary determinants of health across the life course, the continuum of care (from prevention and health promotion to management and treatment of illness), and diverse settings.
- Overall, implementation strategies should be context specific: there is no single global model, so roadmaps should be locally coproduced and adapted to health-system designs and cultural practices.
- Research to support implementation requires plural methods: rigorous quantitative evaluation and culturally grounded qualitative or creative inquiry should be recognised as complementary, not competing. International cross-sector funding, policy integration, and equity-focused monitoring are essential, especially in low-income and middle-income countries where research models must fit local realities.
- Ways of working are important: we need to build competencies across clinicians, creative arts therapists, artists, and community organisers; embed education across sectors; and ensure all work is underpinned by coproduction and public involvement to ensure relevance, legitimacy, and sustainability.

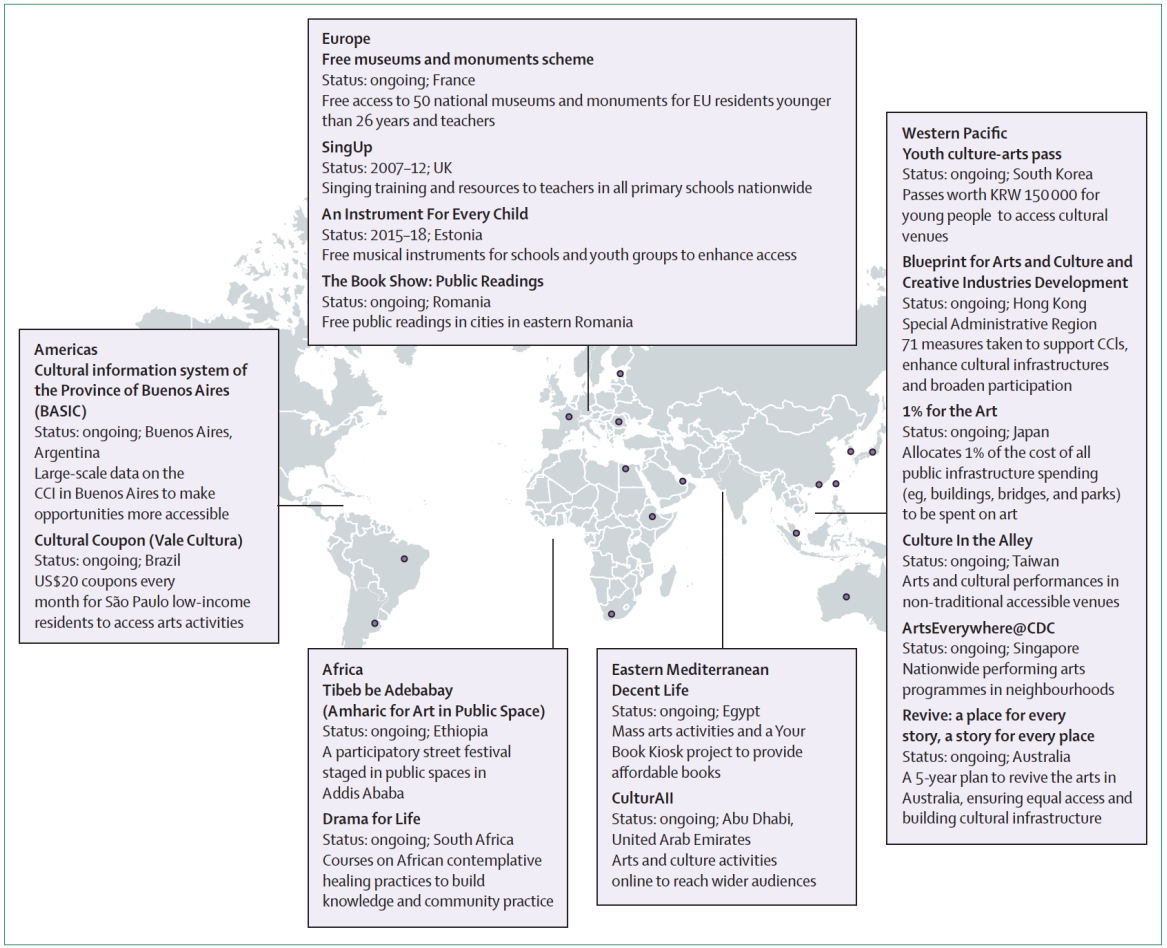

Figure 1: **Case studies of large-scale initiatives to democratise arts engagement**
CCI=creative and cultural industries.

Panel 1: Policy actions required to embed and monitor the arts as health behaviours

- The integration of health and wellbeing within cultural policies and, reciprocally, arts and culture within public health policies, recognising the intrinsic health and wellbeing benefits that arts engagement brings and the consequent importance of ensuring equal access
- The setting of both incremental national targets for arts participation and individual-level behavioural guidance via large-scale public health campaigns (akin to 30 minutes of exercise or five-a-day fruit and vegetables but based on epidemiological and experimental evidence pertaining to the arts)
- Investment in tangible and intangible assets that underpin engagement in the arts as part of government spending reviews (eg, buildings and spaces, training and education courses, and working conditions for arts professionals), acknowledging (and working to quantify further) the health economic value these bring
- The establishment of equity taskforces responsible for the comprehensive mapping and removal of barriers to arts access that currently result in inequitable patterns of engagement, aiming to increase rates of engagement in the arts
- The development and embedding of large-scale interventions that follow the principals of proportionate universalism (ie, focusing on increasing arts engagement among populations with low levels of engagement, aiming to increase equity in access to the arts
- The development and continued investment in monitoring of arts engagement rates and patterns at local and national levels to enable clear assessments of progress, including distribution-sensitive indicators and routine data disaggregation by relevant demographic and socioeconomic factors
- The continued development and integration of sensitive, culturally relevant, and pluralistic questions on arts engagement as part of national and international cohorts and surveys, to enable continued assessment of how arts engagement relates to population health outcomes

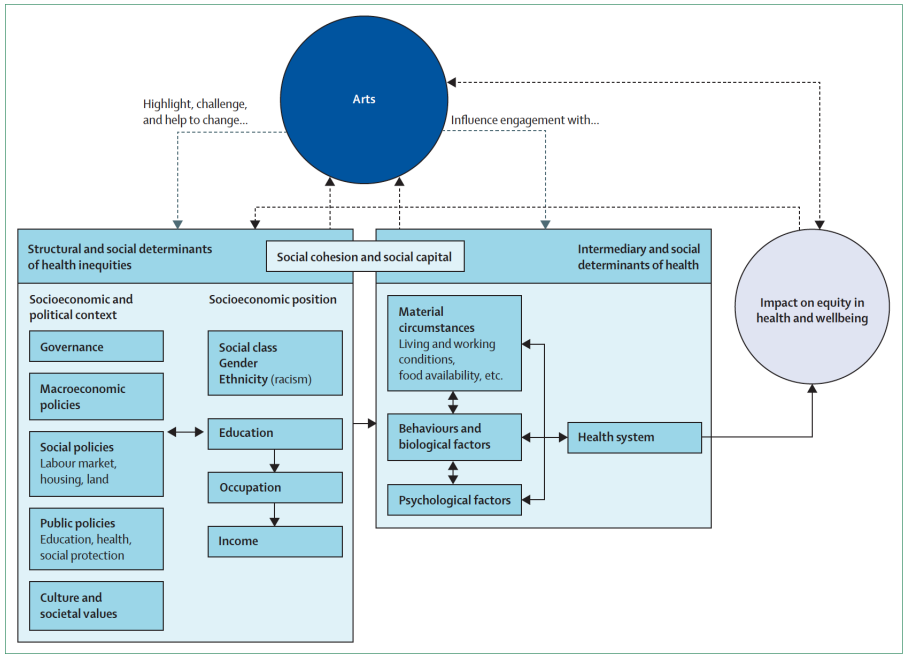

Figure 2: Opportunities for the arts to be integrated into efforts to address structural drivers of health inequities

***Panel 2*: Examples of arts-based interventions for addressing structural social determinants of health from the past 50 years**

Mexico: television drama to improve adult literacy rates
Ven Conmigo (Come with Me) was launched in 1975 as a television programme targeted at improving adult literacy rates. The storyline focused on a teacher who travelled into the countryside to teach adult reading classes, getting involved in a national distribution centre providing free literacy booklets. Following the airing of the series, new enrolments in adult literacy programmes across Mexico increased nine-fold, with 25 000 people visiting the specific national distribution centre the show mentioned for their free booklet the day after the related episode aired.[45]

Tanzania: radio series to improve family planning
Twende na Wakati (Let's Go with the Time) was launched in 1993 as a radio series targeted at improving family planning. It was broadcast in six regions of Tanzania, where it was listened to by 55% of the country's population. Data from the Tanzania Demographic and Health Survey comparing fertility rates in the country before and after the series was broadcast showed declines from 6·3 children to 5·8 children. National Ministry of Health data showed that nearly half of the people who started using family planning methods in that time directly attributed their decision to the radio drama. Comparison data collected from a region in Tanzania that received a comparison music programme for the first 2 years rather than the radio show showed no such improvements.[46]

Brazil: theatre to challenge social stigma, exclusion, and advance legislation
Theatre of the Oppressed was devised initially in the 1970s in Rio de Janeiro with the goal of tackling major social and political issues in society by making power imbalances, oppression, and domination visible through theatre. Performances and improvisations, often in public spaces, were used to highlight key problems within society, understanding and addressing stigma and discrimination about health issues, including domestic violence and mental health disorders. There was also a particular focus on understanding the challenges that less advantaged people in the city were facing. Members of the public were then invited to participate by enacting solutions to the problems. The ideas became the basis of actual legislation that director Augusto Boal then put forward in his role as city councillor.[47] Development of the work since has focused on the role of the bystanders who are aware of inequities but feel unable to act.

Columbia: arts as part of urban regeneration programmes
The arts have been part of major urban transformation in Medellín, Columbia. Major investment in cultural spaces, music schools, visual and fine arts laboratories, and performing arts and dance spaces was undertaken with the aim of building values and collective consciousness, connecting citizens to one another and their social, political, and historical contexts. The programme is credited with increasing a sense of belonging and empowering citizens to be agents of change, with the arts providing opportunities for reflecting on and expressing social and political issues. Cultural regeneration has occurred alongside other important social, education and urban programmes and led to decreases in crime rates and improvements in education, health, and quality of life.[48,49]

The USA: transmedia approaches to address racial inequalities in health
East Los High was launched as a TV series in 2013 by Population Media Center in the USA to try and reduce health inequalities among Latinx teenagers living in Los Angeles. The sixty-episode multi-award-winning drama followed the lives of adolescents at a fictional high school, featuring storylines on family planning, adolescent reproductive rights, women's rights, domestic violence, HIV/AIDS, substance abuse, nutrition, education, voting rights, undocumented immigration, and health care. The series featured educational storylines cocreated with non-profit organisations specialising in the issues raised, as well as taking a transmedia approach, providing additional online newsletters, videos, vlogs, blogs, chats, and widgets to signpost and connect viewers to supportive resources. The series led to high use of the resources and changes in specific knowledge and behaviours among the target audience, such as correct use of contraception.

UK: theatre to challenge and change legal practices around sexual assault
First premiered in Sydney in 2019 and since performed in nearly 50 countries, the play *Prima Facie* by playwright Suzie Miller exposes how legal systems treat victims and survivors of sexual crimes, particularly examining the impact of rape myths in criminal cases. *Prima Facie* has not only led to increased public conversation but also sparked substantial debate among legal professionals. In the UK, it led to a group of barristers in the UK forming The Examination of Serious Sexual Assault (TESSA; named after the lead character in the play) to re-evaluate the statutory definitions of rape, consent and sexual assault in the Sexual Offences Act 2003.[50] Events led by TESSA and other groups included public debates around legislation involving barristers, ministers, Miller, and lead actress Jodie Comer discussing the issues exposed in the play. In late 2025, a range of legal reforms were announced for Rape and Serious Sexual Offences cases, some reflecting key issues brought up in the play. In addition, the direction read out by judges to the jury in the UK was rewritten in what has been dubbed the Prima Facie direction, including specific lines from the play, and a video of the play is now used in Northern Ireland as training material for judges.[51,52]

Panel 3: How social prescribing works in practice

Social prescribing is a powerful public-health approach as it is both strengths based (supporting patients to draw on their strengths to improve their outcomes) and asset based (mobilising often underused community assets to support health), and has a quadruple aim: enhancing patient experience, improving population health, reducing health-care costs, and improving the work life of health-care professionals.[74-76] As a goal-directed approach, individuals are encouraged to identify specific needs they wish to address with the programme, such as reducing loneliness or isolation; improving mental health and wellbeing; engaging in more physical activity or other health behaviours; and gaining skills, advice, or support that will improve their quality of life. Prescriptions involve individual choice of a range of activities, enabling participants to exercise self-determination and select activities that match their social identity.[77] The arts are one of the activities most commonly prescribed as part of social-prescribing schemes; some schemes even focus exclusively on the arts (sometimes known as arts on prescription schemes).

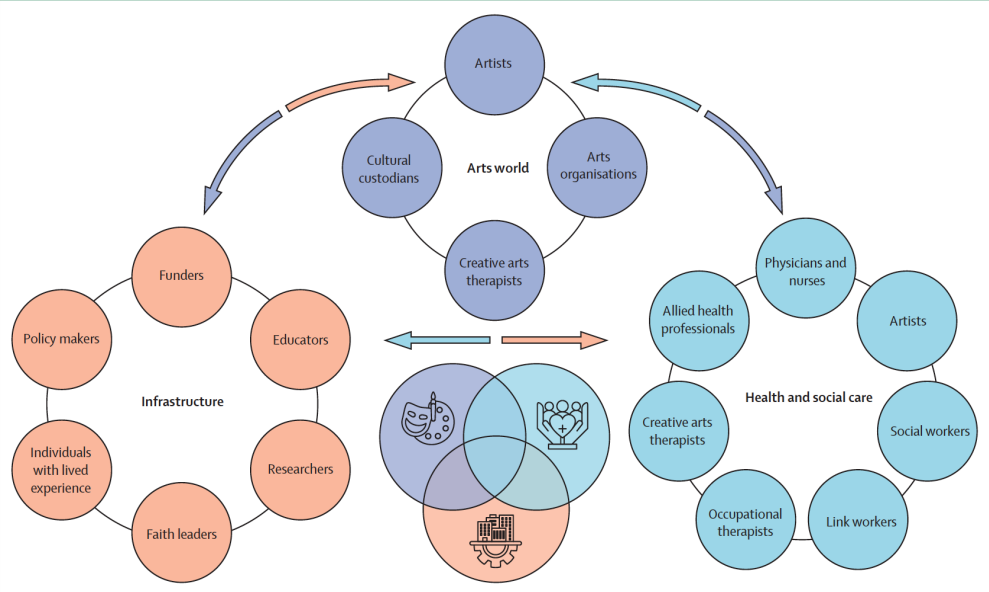

Figure 3: The ecosystem of stakeholders involved in arts and health

The priorities outlined here include ambitious targets that present major opportunities for impact. They align with sustainable development goals relating to good health and wellbeing, as well as broader social determinants of health and align with recognised priorities around prevention within public health, and there is already some evidence of this being acknowledged in international policy from decision-making bodies, such as WHO, UNESCO, and the EU.[136–138] As we look ahead, there are clear opportunities to further this work. For instance, the UN Inter-Agency Platform on Culture for Sustainable Development launched in 2021 continues to lack any meaningful discussion about health, especially when compared with the equivalent UN Inter-Agency Group on Sports for Development and Peace, which has articulated the impact of sports on health from its very inception in 2002.[139] Most of all, we call for the continued acceleration of global engagement with this field and hope that this Review supports increased dialogue moving forwards. Arts engagement is ubiquitous across every human society; opportunities to engage in the arts to support health and wellbeing must be too.

The human gut microbiome primes fever after vaccination

INTRODUCTION: Vaccination is a critical tool for global public health, but wide variability in human vaccine responses influences vaccine effectiveness. Vaccine adverse reactions, including common side effects such as fever and flu-like symptoms, are a factor in vaccine hesitancy, and these reactions are currently challenging to predict. Vaccine hesitancy is considered a top-10 global health threat by the World Health Organization as a result of its impact on vaccine-preventable diseases such as measles, cervical cancer, and COVID-19.

RATIONALE: People differ markedly in their adverse responses to vaccination, but this variation is not well understood. The gut microbiome has been implicated in adaptive immune responses to vaccination; we hypothesized that interactions between commensal gut microbes and the immune system may influence the risk of adverse inflammatory vaccine reactions.

RESULTS: The µHEAT (Microbial-Human Ecology and Temperature) Study longitudinally tracked 171 healthy young adults receiving severe acute respiratory syndrome coronavirus 2 mRNA vaccines. Thrice-daily oral temperature records were used to quantify fever, and fecal and serum samples were collected for microbiome and immune profiling. We found that fever had very little effect on the microbiome; by contrast, fever-positive participants displayed chronic low-grade intestinal inflammation and a microbiome characterized by high expression of bacterial flagellins, both pre- and postvaccination. Microbiomes from fever-positive participants induced heightened inflammatory responses in human colonic organoids and exacerbated acute vaccine responses when transplanted into gnotobiotic mice, and this was dependent on sensing of bacterial flagellin through host innate immune receptors. Moreover, microbial flagellin production was modifiable by diet: Dietary additives increased bacterial flagellin production in vitro, and a Western-style diet exacerbated vaccine reactions in mice. Consistent with this, fever was associated with dietary and metabolic markers in humans. Although interventional human studies are needed to establish causality, this suggests that diet modification could be a viable strategy to influence microbiome-dependent vaccine responses.

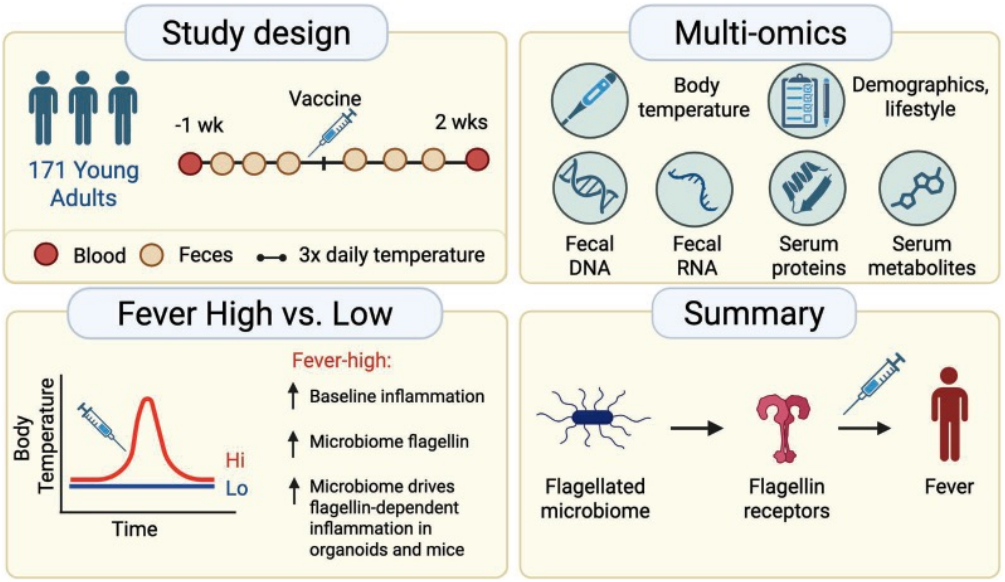

The µHEAT (Microbial-Human Ecology and Temperature) Study indicates that flagellated human gut microbes prime fever after vaccination.

CONCLUSION: These data suggest that chronic production of flagellin within the human gut microbiome sets the immune tone to drive inflammatory vaccine responses. The ability to predict and control the risk of vaccine-induced adverse reactions is a crucial factor in vaccine hesitancy and global public health; our findings establish the possibility that microbiome-targeted strategies could mitigate vaccine side effect risk in humans. The identified microbiomeimmune axis may also have implications for other inflammatory processes beyond vaccination.

Scientists uncover a clue that could hint at why we regain weight after diets

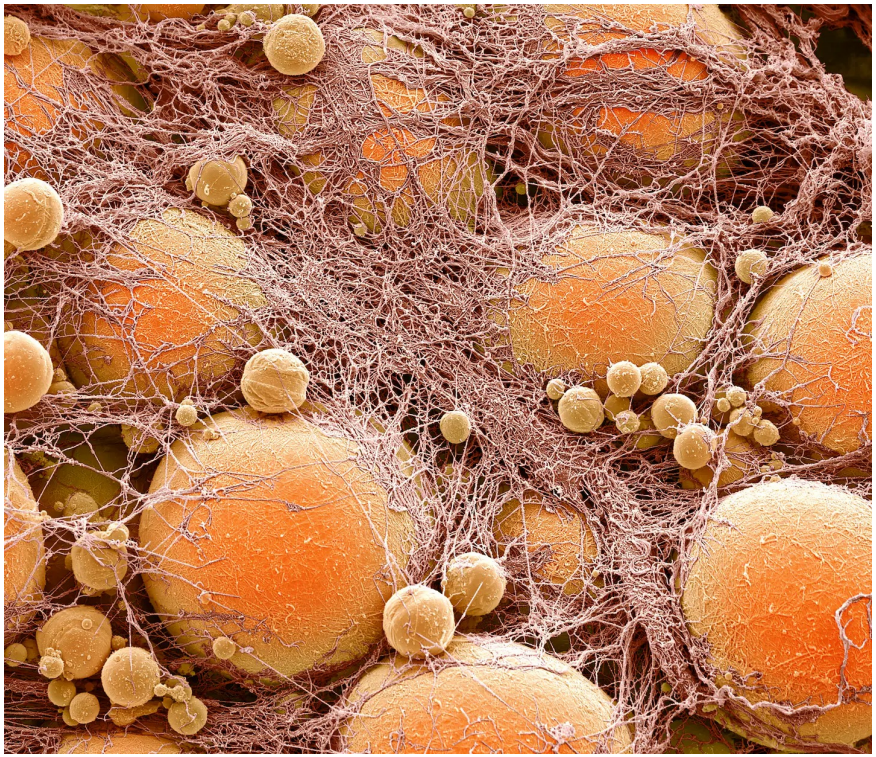

Researchers have long puzzled over why people who diet or take weight-loss drugs are quick to regain weight after they stop. A new study has proposed a potential clue: a chemical mechanism that may encourage fat cells to continue making a hormone that makes us hungry and create a “memory” of obesity even after weight loss.

Scientists caution that the study’s evidence involves mice and is not proof of the mechanisms that explains weight regain. But it’s a step forward in a growing understanding of the cellular functions and changes underlying obesity, experts said. Recent studies have challenged the idea that inactivity is the main cause of obesity and identified other genetic factors, such as impaired GLP-1 production, associated with some types of obesity.

As weight-loss drugs become more popular, understanding why their effects can wear off so quickly once people stop taking the medications is becoming more important, the study's authors said. Beyond losing weight, the researchers said, treating obesity could require tackling a "biological memory" in our cells.

"If we understand where that memory is coming from, maybe eventually we'll have some way to stop that," said Seth Field, a professor of medicine in endocrinology at Case Western Reserve University and an author of the study published September in Cell Reports.

The idea that cells can carry a memory of obesity is not new but researchers are still trying to understand the mechanisms of how it influences weight regain. Through epigenetics, scientists are examining how external factors can affect how our cells behave by altering chemical markers which can turn genes — and certain cellular functions — on and off.

A study in 2024 examined how obesity can cause epigenetic changes. It suggested that fat cells in both humans and mice retain lasting epigenetic changes after weight loss.

Mice with these cellular differences quickly regained weight, but researchers did not have a definitive answer to explain why.

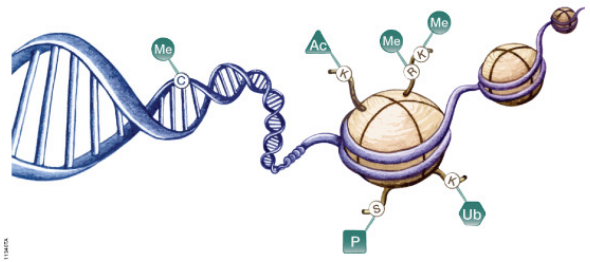

Adipose tissue retains an epigenetic memory of obesity after weight loss

Reducing body weight to improve metabolic health and related comorbidities is a primary goal in treating obesity[1,2]. However, maintaining weight loss is a considerable challenge, especially as the body seems to retain an obesogenic memory that defends against body weight changes[3,4]. Overcoming this barrier for long-term treatment success is difficult because the molecular mechanisms underpinning this phenomenon remain largely unknown. Here, by using single-nucleus RNA sequencing, we show that both human and mouse adipose tissues retain cellular transcriptional changes after appreciable weight loss. Furthermore, we find persistent obesity-induced alterations in the epigenome of mouse adipocytes that negatively affect their function and response to metabolic stimuli. Mice carrying this obesogenic memory show accelerated rebound weight gain, and the epigenetic memory can explain future transcriptional deregulation in adipocytes in response to further high-fat diet feeding. In summary, our findings indicate the existence of an obesogenic memory, largely on the basis of stable epigenetic changes, in mouse adipocytes and probably other cell types. These changes seem to prime cells for pathological responses in an obesogenic environment, contributing to the problematic 'yo-yo' effect often seen with dieting. Targeting these changes in the future could improve long-term weight management and health outcomes.

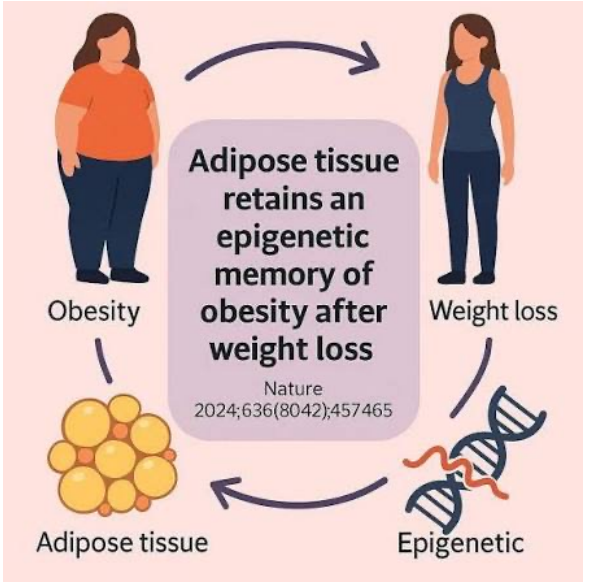

Nature 2026